ARABIDOPSIS ECERIFERUM2-LIKE PROTEINS ARE COMPONENTS OF THE FATTY ACID ELONGATION MACHINERY REQUIRED FOR THE PRODUCTION OF CUTICULAR WAXES

by

Tegan M. Haslam

B.Sc., The University of Calgary, 2009

A THESIS SUBMITTED IN PARTIAL FULFILLMENT OF
THE REQUIREMENTS FOR THE DEGREE OF

DOCTOR OF PHILOSOPHY
in
THE FACULTY OF GRADUATE AND POSTDOCTORAL STUDIES
(BOTANY)

THE UNIVERSITY OF BRITISH COLUMBIA
(Vancouver)

April 2017

© Tegan Haslam, 2017

Abstract

Very-long-chain fatty acids (VLCFAs) are essential molecules produced by all plant cells, and are precursors of diverse primary and specialized metabolites. VLCFAs are elongated by a fatty acid elongation (FAE) complex of four core enzymes located on the endoplasmic reticulum, which sequentially adds two carbon units to a growing acyl-CoA chain. Identification and characterization of FAE enzymes in *Arabidopsis thaliana* has revealed that three of the four enzymes act as generalists, contributing to all metabolic pathways that require VLCFAs. A fourth component, the condensing enzyme, provides substrate specificity and determines the chain length of product synthesized by the entire complex. Chain length is important because it defines what downstream pathway a VLCFA can be used for.

In Arabidopsis, characterized condensing enzymes can only elongate VLCFAs up to 28 carbons in length, despite the predominance of 29- and 31-carbon components in plant cuticular wax. This suggests that elongation beyond 28 carbons is unique and requires different protein components. The wax-deficient mutant *eceriferum2* (*cer2*) of Arabidopsis lacks waxes longer than 28 carbons, suggesting that CER2 is specifically required for VLCFA extension past this threshold length. Molecular characterization of the *CER2* gene, both *in planta* and by heterologous expression in *Saccharomyces cerevisiae*, demonstrates that CER2 is a component of the elongation machinery required to synthesize 30-carbon cuticular wax precursors (Chapter 3). Five homologous *CER2-LIKE* genes were identified in Arabidopsis; these *CER2-LIKE*s have similar metabolic functions to CER2, but different expression patterns and substrate specificities (Chapter 4). *CER2-LIKE*s form a distinct clade of the BAHD acyltransferase superfamily. However, structural predictions and site-directed mutagenesis reveal fundamental differences in the mechanism of activity of *CER2-LIKE*s relative to characterized BAHDs (Chapter 5). My results suggest that CER2-LIKEs enable condensing enzymes to accept longer VLCFA substrates. I suggest several mechanisms to explain the activity of CER2-LIKEs. This peculiarity of elongation is unique to land plants, and to the production of cuticular wax precursors. Because the acquisition of cuticles as barriers to transpirational water loss was key to plant colonization of land, CER2-LIKE activity is an important specialization of plant lipid metabolism.

Preface

A version of Chapter 1 has been published as a review article: Haslam, T.M., and Kunst, L. (2013) Extending the story of very-long-chain fatty acid elongation. *Plant Sci.* **210**: 93-107. Tegan Haslam wrote the manuscript with the assistance of Ljerka Kunst.

A version of Chapter 3 has been published as: Haslam, T.M., Mañas-Fernández, A., Zhao, L., and Kunst, L. (2012) Arabidopsis ECERIFERUM2 is a component of the fatty acid elongation machinery required for fatty acid extension to exceptional lengths. *Plant Physiol*. **160**: 1164-1174. Aurora Mañas-Fernández, Ljerka Kunst, and Tegan Haslam designed the research experiments, Tegan Haslam performed all experiments except for SEM of stem wax, which was carried out by Lifang Zhao. Tegan Haslam wrote the manuscript with the assistance of Ljerka Kunst.

A portion of Chapter 4 has been published as: Haslam, T.M., Haslam, R., Thoraval, D., Pascal, S., Delude, C., Domergue, F., Mañas Fernández, A., Beaudoin, F, Napier, J.A., Kunst, L., and Joubès, J. (2015) ECERIFERUM2-LIKE proteins have unique biochemical and physiological functions in very-long-chain fatty acid elongation. *Plant Physiol.* **167**: 682-692. Ljerka Kunst, Aurora Mañas-Fernández, Jérôme Joubès, and Tegan Haslam contributed ideas for this project. Data for the peer-reviewed article were contributed by the Kunst, Napier, and Joubès labs, however the data presented in this thesis was produced by Tegan Haslam, with the following exceptions: Aurora Mañas-Fernández constructed plasmids for complementation tests with *CER2-LIKE1*, and Jérôme Joubès' lab carried out the expression profiling of *CER2-LIKE2* in flowers, and tested the activity of *CER2-LIKEs* with the KCSs specified in the manuscript. Tegan Haslam wrote the manuscript with the assistance of Ljerka Kunst and Jérôme Joubès.

A version of Chapter 5 will be submitted as a research article for peer-review. The project was conceived and interpreted by Ljerka Kunst and Tegan Haslam, and Tegan Haslam carried out the experiments.

Table of Contents

List of Tables

List of Figures

List of Symbols and Abbreviations

35S	promoter from the *35S* RNA from the cauliflower mosaic virus
ACA2	calcium ATPase (Arabidopsis gene)
ACP	acyl carrier protein
ATP	adenosine triphosphate
BAHD	BEAT (benzylalcohol *O*-acetyltransferase)
	AHCT (anthocyanin *O*-hydroxycinnamoyltransferase)
	HCBT (*N*-hydroxycinnamoyl/benzoyltransferase)
	DAT (deacetylvindoline 4-*O*-acetyltransferase)
CAPS	cleaved amplified polymorphic sequences
CAS9	CRISPR-associated protein 9
cDNA	complementary DNA
CER	ecer iferum genes identified in Arabidopsis based on glossy, wax-deficient mutant phenotypes
CoA	Coenzyme A
CRISPR	clustered regularly-interspaced short palindromic repeats
CSG	calcium-sensitive growth (genes identified in *Saccharomyces*)
DNA	deoxyribonucleic acid
ECR	enoyl-CoA reductase
ELO	elongation-defective (genes identified in *Saccharomyces*)
EMS	ethyl methanesulfonate
En/Spm	enhancer/suppressor-mutator (transposable element system)
ER	endoplasmic reticulum
EW	epicuticular wax (Arabidopsis genes)
FAE	fatty acid elongase
FAE1	fatty acid elongation 1 (Arabidopsis gene)
FAME	fatty acid methyl ester
FAR	fatty acyl reductase
FAS	fatty acid synthase
FID	flame ionization detection
FTA	flinders technology associates
GAL1/GAL10	bidirectional, galactose-inducible promoter from *Saccharomyces cerevisiae*

GAPC	glyceraldehyde-3-phosphate dehydrogenase C subunit (Arabidopsis gene)
GC	gas chromatography
GFP	green fluorescent protein
GLOSSY	genes identified in maize based on wax-deficient mutant phenotypes
GPD	glyceraldehyde-3-phosphate dehydrogenase (yeast gene)
HA	human influenza hemagglutinin
HCD	3-hydroxyacyl-CoA dehydratase
HMG1	3-hydroxy-3-methylglutaryl CoA reductase 1 (Arabidopsis gene)
HCT	hydroxycinnamoyltransferase
HXXXD	catalytic motif of BAHD acyltransferases; histidine, any three amino acids, aspartic acid
KAS	ketoacyl-ACP synthase
KCR	ketoacyl-CoA reductase
KCS	ketoacyl-CoA synthase
LC	liquid chromatography
LUC	luciferase gene from firefly (*Photinus pyralis*)
MES	2-(*N*-morpholino)ethanesulfonic acid (buffer)
MS	mass spectrometry
MS	Murashige and Skoog (medium)
MRM	multiple reaction monitoring
MYC/C-MYC	avian myelocytomatosis viral oncogene homolog
NADH	nicotinamide adenine dinucleotide
NADPH	nicotinamide adenine dinucleotide phosphate
OD	optical density
PAM	protospacer adjacent motif
PAS	pasticcino genes identified in Arabidopsis in a screen for hypertrophic growth in response to cytokinins
PCR	polymerase chain reaction
PHS1	*PTPLA* homolog involved in sphingolipid biosynthesis 1 (Arabidopsis gene)
PI	protease inhibitor
PKS	polyketide synthase
PMSF	phenylmethane sulfonyl fluoride

PTPLA	protein tyrosine phosphatase-like
qPCR	quantitative polymerase chain reaction
QTL	quantitative trait locus
QTRAP	quadrupole-linear ion trap
RNA	ribonucleic acid
RT	room temperature
RT-PCR	reverse-transcription polymerase chain reaction
SC	synthetic complete
SD	standard deviation
SEM	scanning electron microscopy
SML	sucrose monolaurate
T-DNA	transfer DNA
Ti	tumour-inducing
TSC	temperature-sensitive *csg2*Δ (genes identified in *Saccharomyces*)
VLCFA	very-long-chain fatty acid
WSD	bifunctional wax ester synthase/diacylglycerol acyltransferase
YPAD	yeast extract-peptone-adenine-dextrose medium

Acknowledgements

Many people have contributed to this research project, and I feel immensely fortunate and thankful for the scientific and personal support I have received throughout my degree.

Dr. Ljerka Kunst, your encouragement, advice, and kindness are at the heart of this thesis. Thank you so much for training me. I cannot articulate my gratitude for the countless opportunities you have given me to succeed.

To my all-star committee, thank you for making yourselves available, and for always being helpful and constructive. Dr. George Haughn, thank you for your logical insight, your criticism, and for teaching me how to present my work. Thank you Dr. Lacey Samuels for your enthusiasm for this project, and for the many ways you've supported and encouraged me. I would have liked to thank Dr. Carl Douglas for the patience and wisdom he shared with me and with everyone in our department.

The Haughn and Kunst lab has been a wonderful place to work; without exception, I'm grateful for everyone I've met here. I'd like to give special thanks to Dr. Aurora Mañas-Fernández for her patient mentorship, and for teaching me to persevere and work hard regardless of whether I feel that everything or nothing is working at the lab bench. I'd also like to thank Dr. Gill Dean for technical advice, and for having the absolute best attitude out of everyone I've ever met. Thank you to Amy Harrington, who worked in our lab under my supervision for one summer. Although Amy's work mapping the *eceriferum19* mutant isn't included in this thesis, I'm grateful to have had such a bright and industrious student to work with.

I could not have asked for a more professional and knowledgeable group of collaborators than my colleagues at Rothamsted. Thank you Dr. Fred Beaudoin, Dr. Richard Haslam, and Dr. Johnathan Napier for working with me on this project, and for being such terrific hosts. Thank you Dr. Jérôme Joubès for having the resolve to turn our race into a collaboration; I'm pleased that we had the opportunity to work together.

Funding for this project was provided in the form of a UBC Four-Year Fellowship, an NSERC Canada Graduate Scholarship, a Killam Doctoral Scholarship, and a UBC International Research Mobility Grant.

Thank you to my parents, Dan and Susan, and my sister Bronwyn for patience and support. Thank you Val, Jesse, Kiko, Susan, Alex, Billy, Chad, and Nick for friendship, kindness, and for great times.

Thank you K. Adrian Yip for your love, companionship, and for having faith in me.

For my undergraduate mentors, Drs. Ed Yeung and Dae-Kyun Ro:
Thank you for fostering my interest in plant biology, and for giving me the confidence to pursue a career in science.

Chapter 1: Introduction

1.1 Very-long-chain fatty acids and the plant cuticle

Lipid barriers are essential across all domains of life. Glycerolipid membranes serve as barriers that enable the organization and regulation of cellular processes. On a larger scale, lipids can form barriers that protect and seal specific tissues and organs. One such barrier is the cuticle, which coats the primary aerial surfaces of land plants. The cuticle consists of two lipidic components, cutin and cuticular waxes. Cutin is a polymer of oxidized fatty acid derivatives and glycerol, linked by ester bonds. Cutin forms a continuous matrix across the plant surface that provides resistance to pathogens and herbivores, and prevents the fusion of epidermal cells. Cutin is embedded and overlaid with cuticular waxes, which are a mixture of very-long-chain fatty acids (VLCFAs) and their derivatives, generally 26-34 carbons in length. Cuticular waxes restrict transpiration, allowing plants to retain water and thrive in terrestrial environments. Waxes often form unique structures and textures on the surface of the cuticle, which can affect the refraction of light on the plant surface, and facilitate or impede insect movement on the plant.

There are many tools for studying cuticular wax biosynthesis, secretion, and the regulation of wax production. Our understanding of all of these processes has been greatly improved by the characterization of wax-deficient "*eceriferum*" ("*cer*") mutants in the model plant *Arabidopsis thaliana* (Koornneef et al., 1989, and Hannoufa et al., 1993), and by reverse genetic approaches. Investigations of wax metabolism in Arabidopsis have benefitted not only from the wealth of genetic tools available in this model organism, but also from the ease of screening for wax-deficient mutants. Wax-deficient Arabidopsis stems are glossy and green in comparison to the glaucous wild type. Further, mutations affecting cuticular wax metabolism do not affect plant viability or fitness unless they have pleiotropic effects. The analysis of wax load and composition is also a relatively simple process; deposited on the outermost surface of the plant, waxes can be extracted by dipping the plant in an organic solvent. Finally, the study of cuticular wax biosynthesis has benefitted greatly from the use of *Saccharomyces cerevisiae* (*S. cerevisiae*, or yeast) as a host for heterologous gene expression to test biochemical activities. Given this toolkit, considerable progress has been made in our field in recent years. This progress has in many instances laid the groundwork for further progress in related, or broader, fields of biology.

1.2 Cuticular wax metabolism in Arabidopsis stems

Wax synthesis begins in the epidermis with the elongation of long-chain fatty acids to very-long-chain fatty acids by a fatty acid elongase (FAE) complex. The process of VLCFA elongation is shared with other metabolic pathways in plants; VLCFAs are also used for the synthesis of sphingolipids, suberin, tryphine, and in some plant species, seed oil. However, chain lengths in excess of 26 carbons are used exclusively for cuticular waxes (and tryphine, which is similar to wax in both its composition and its biosynthesis; discussed in Chapter 4). As such, elongation is the committed step in wax biosynthesis. A small fraction of VLCFAs are secreted to the cuticle directly, but these make up only 1-3% of the total stem wax load in Arabidopsis. Most fatty acids are processed by either an acyl reduction or alkane-forming pathway prior to secretion to the cuticle.

The acyl reduction pathway produces primary alcohols and wax esters, which together make up 10-25% of the total wax load of Arabidopsis stems and leaves. VLCFAs are reduced to primary alcohols by the reductase CER4, which uses 24-30-carbon acyl-CoAs as substrates (Rowland et al., 2006). CER4 is a member of the fatty acyl reductase (FAR) family, which catalyze thioester cleavage of either acyl-ACP or acyl-CoA, as well as the subsequent reduction of the carboxylic acid product to an alcohol. There are eight FARs in Arabidopsis, which contribute to the synthesis of wax, tryphine, sporopollenin, cutin, suberin, and suberin-associated waxes (Rowland and Domergue, 2012). The identity of CER4/FAR3 as the reductase required for the synthesis of cuticular wax primary alcohols was determined based on crude mapping of the glossy *cer4* mutant, comparison of the rough chromosomal location of the *cer4* lesion with the established positions of the *FAR* genes, and confirmation of the predicted *CER4/FAR3* gene identity by complementation of the *cer4* mutant phenotype (Rowland et al., 2006).

While most primary alcohols are exported directly to the cuticle in Arabidopsis, some are esterified to long-chain fatty acids (LCFAs, 16-18 carbons in length) to make wax esters. In wild-type Arabidopsis, wax esters 42, 44, and 46 carbons in length are largely made by esterification of a 16-carbon acyl group to 26-, 28-, or 30-carbon primary alcohol (Lai et al., 2007). The Arabidopsis wax ester synthase was identified using a reverse genetic approach (Li et al., 2008). Sequences of wax ester synthases (WSs) from mammals, jojoba, and bifunctional wax ester synthase/diacylglycerol acyltransferase (WS/DGATs) from *Acinetobacter calcoaceticus* were used to search the Arabidopsis genome for candidate genes. One particular *WS/DGAT*, named *WSD1*, was selected for study based on its high expression in elongating stem epidermal cells (Suh et al., 2005). The function of *WSD1* in the synthesis of cuticular wax esters

was demonstrated by mutant analysis, and its biochemical function was confirmed by activity assays in *Escherichia coli* (*E. coli*) and *S. cerevisiae* (Li et al, 2008).

75-90% of stem and leaf waxes of Arabidopsis are derived from the alkane-forming pathway, which generates aldehydes, alkanes, secondary alcohols, and ketones. Early biochemical work by Cheesbrough and Kolattukudy (1984) and Dennis and Kolattukudy (1992) demonstrated that alkanes are synthesized by reduction of acyl-CoAs to fatty aldehydes, followed by removal of the carbonyl group to form alkanes. Two co-expressed Arabidopsis genes, *CER1* and *CER3*, were identified in forward genetic screens for glossy, cuticular wax-deficient *eceriferum* mutants (Koornneef et al, 1989; Hannoufa et al, 1993). *cer1* and *cer3* mutants both have dramatically reduced alkane, secondary alcohol, and ketone loads, providing evidence that these proteins are involved in alkane formation (Koornneef et al, 1989; Hannoufa et al, 1993; Jenks et al, 1995). However, phenotypes of the *cer1* and *cer3* mutants are not identical, as *cer1* accumulates twice as much 30-carbon aldehyde as the wild type, while *cer3* accumulates only trace amounts of aldehydes of all chain lengths. This suggests that CER3 may function as an acyl-CoA reductase, and CER1 as an enzyme responsible for aldehyde conversion to alkanes. Both genes encode integral membrane proteins of unknown function whose N-terminal domains contain eight conserved histidines in a tripartite motif (HX_3H, HX_2HH, HX_2HH) (Aarts et al., 1995; Chen et al., 2003). In desaturases and related enzymes, this motif forms a di-iron binding site essential for redox catalytic activity. Biochemical confirmation of the roles of CER1 and CER3 in alkane formation was provided by reconstitution of the plant alkane biosynthetic pathway in yeast (Bernard et al., 2012). Heterologous expression of CER1 and CER3 in VLCFA-producing yeast cells demonstrated that these two genes are necessary and sufficient for alkane production. Alkanes were not produced when either gene was expressed alone, and aldehydes were not detected when either gene was expressed alone nor when both genes were co-expressed. This study also demonstrated that the yield of alkanes produced by CER1 and CER3 in yeast could be increased two-fold by co-expression of cytochrome B5 reductases. The authors proposed that CER1, CER3, and cytochrome B5 reductases form a complex that catalyzes the two-step conversion of acyl-CoAs to alkanes in a redox-dependent manner.

A portion of alkanes synthesized by the CER3/CER1 complex is further modified to secondary alcohols and ketones by the mid-chain alkane hydroxylase MAH1, a cytochrome P450 (Greer et al., 2007). MAH1 was identified using a reverse-genetic approach, selecting for P450s predicted to use fatty acid-derived substrates, and with heightened expression in stem epidermal cells. A simplified model of wax biosynthesis is presented in Figure 1-1.

Though the focus of this thesis will be genetic studies in Arabidopsis, there has also been rapid progress in the identification and characterization of genes required for the synthesis of cuticular waxes in maize, barley, rice, tomato, and many other plants in the past decade. As cuticular wax composition varies among plant species, these studies have been important in uncovering the breadth of metabolic pathways that synthesize the acyl-lipid components of wax, as well as triterpenoids and phenolics that may also accumulate in the cuticle. Such diversity underlines the fact that different cuticular waxes confer different properties to the plant surface. Further, that cuticular wax composition is consistently heterogeneous suggests that having a diversity of wax components on a given plant surface is advantageous. However, deciphering what specific physical properties and physiological advantages different chain lengths and functional groups confer is very much a work in progress. It is also of interest to note that waxy surface layers are not unique to the plant kingdom. Animals also have surface lipids that vary immensely in composition, from insect cuticles that primarily consist of hydrocarbons (Golebiowski et al., 2011), to lipids of human skin that include triacylglycerols, wax esters, and squalene (Pappas, 2014). Some prokaryotes also secrete oily capsules that can be considered a type of cuticle. Among the best studied is the mycolic acid capsule of the cell wall of *Mycobacterium tuberculosis*, which plays an important role in pathogenesis (Asselineau et al., 2002).

One feature of cuticular wax composition that is consistent across flowering plant phyla is the exceptionally long chain length of wax components; most waxes are derived from fatty acids 28-34 carbons in length. Other metabolic pathways that incorporate VLCFAs, such as sphingolipid and suberin synthesis, use shorter acyl chain lengths. The regulation of elongation is therefore of substantial developmental and physiological importance. The present work will describe how extension of fatty acids from 28 to 34 carbons is also biochemically distinct from elongation to shorter chain lengths. Aside from the core elongation machinery involved in the synthesis of all VLCFAs, an additional protein family, CER2-LIKEs, is uniquely required to generate VLCFA precursors of cuticular waxes. The following introduction will present the core components of the elongase with the aim of setting a context for the discovery and characterization of CER2-LIKEs.

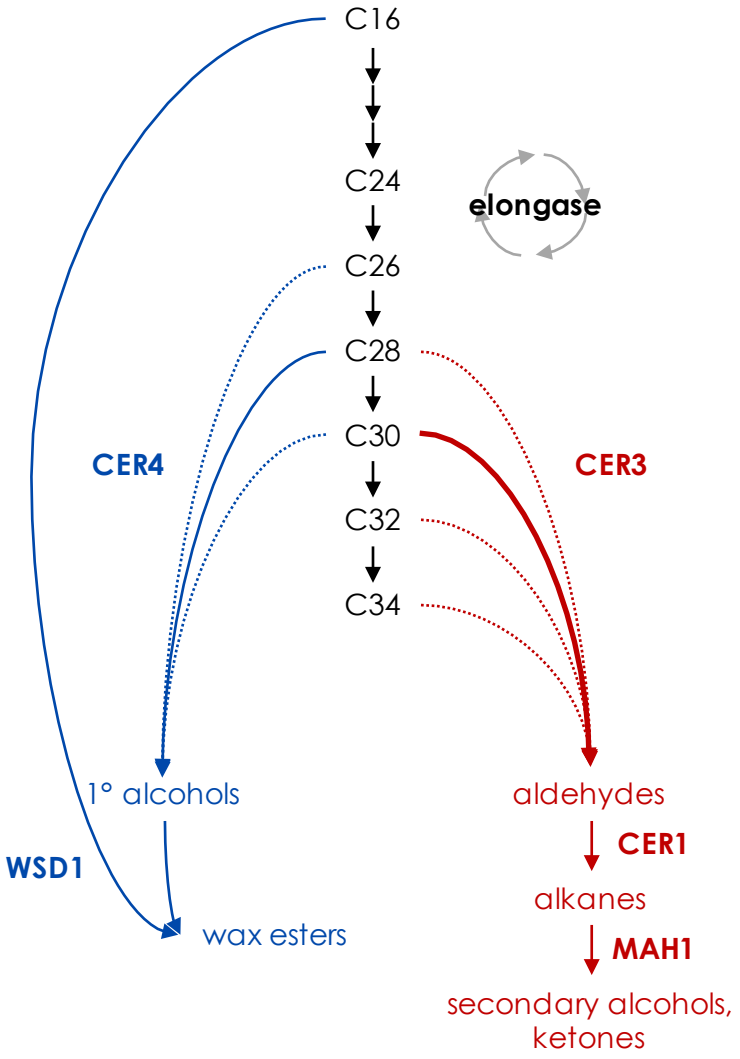

Figure 1-1 Schematic representation of wax biosynthesis

VLCFAs are lengthened in two-carbon increments (**black**), and derivatized by one of two pathways. The acyl reduction pathway produces primary alcohols, a portion of which is esterified to fatty acids to make wax esters (**blue**). The alkane-forming pathway produces aldehyde intermediates, from which a carbonyl group is lost to form an alkane; alkanes may subsequently undergo mid-chain oxidation to produce secondary alcohols and ketones (**red**). CER, ECERIFERUM; WSD, bifunctional wax ester synthase/diacylglycerol acyltransferase; MAH1, mid-chain alkane hydroxylase.

1.3 Discovery of plant elongase complexes

The *de novo* synthesis and elongation of fatty acids share a basic mechanism across domains of life. This consists of a sequence of four core reactions that add two carbon units to an acyl substrate. First, either a starter molecule or a growing acyl chain is condensed with malonate, both of which are activated by conjugation to either acyl carrier protein (ACP) or coenzyme A (CoA). This condensation reaction produces an activated β-ketoacyl that is two carbons longer than the initial acyl chain. Subsequently, the β-keto group is reduced to an alcohol, dehydrated to an enoyl, and reduced again to form an n+2 acyl product. Beyond this core sequence of reactions, there is variation in the form of substrate activation, the localization of biosynthetic enzymes, the mechanisms determining substrate and product specificity, and in the enzymes involved in both *de novo* synthesis and elongation.

Fatty acid synthases (FAS) are enzymes or enzyme complexes that catalyze the *de novo* synthesis of fatty acids; they can generally be grouped according to whether their catalytic activities reside on a single, multifunctional protein, referred to as a type I fatty acid synthase, or whether the activities are associated with four separate, monofunctional proteins, making up a type II fatty acid synthase. Plants have soluble, plastid-localized type II fatty acid synthases, which elongate fatty acyl groups esterified to ACP up to 18 carbons in length. Plant fatty acid synthases are essential for the production of membrane lipids and the long-chain precursors of VLCFAs (Harwood, 2005).

Early work aimed at isolating enzymes required for the production of VLCFAs in plants revealed that fatty acid elongation differs markedly from the *de novo* synthesis of fatty acids catalyzed by the FAS. Extensive biochemical studies using cuticular wax-producing leek (*Allium porrum*) epidermal cells as a model revealed that elongation activity is present predominantly in a microsomal cell fraction (Cassagne and Lessire, 1978), that the elongase uses malonyl-CoA and acyl-CoA as substrates and nicotinamide adenine dinucleotide phosphate (NADPH) as a reductant (Agrawal et al., 1984), and that elongation products are released from the elongase as CoA thioesters (Lessire et al., 1985a). Use of chemical inhibitors in this system demonstrated varied effects of chemicals on elongase activity, suggesting the existence of multiple elongases (Lessire et al., 1985b). Biochemical approaches were also crucial for our early understanding of the nature of the elongase enzyme(s); purification of the leek elongase resulted in enrichment of at least three proteins, suggesting that the elongase is not a single multifunctional protein unit, but rather consists of multiple protein components (Bessoule et al., 1989). Additionally, genetic analysis of cuticular wax production in barley demonstrated that several elongase systems must exist in a given plant, as mutagenesis or treatment of tissues with chemical inhibitors or

exposure to different environmental conditions had varied effects on the distribution of cuticular wax component chain lengths (von Wettstein-Knowles, 1982). Together, biochemical and genetic evidence suggested a model where multiple heteromeric fatty acid elongase complexes carry out VLCFA elongation in the endoplasmic reticulum, with different elongases having substrate specificity tailored to the synthesis of specific downstream products.

1.3.1 Condensing enzymes

The first component of the fatty acid elongase to be genetically identified and characterized in plants was FATTY ACID ELONGATION 1 (FAE1) in a mutant screen for seed VLCFA deficiencies in *Arabidopsis thaliana* (James and Dooner, 1990; Lemieux et al., 1990; Kunst et al., 1992). A single, semi-dominant nuclear mutation in *FAE1* was sufficient to block the elongation of seed 18:1 to 20:1, 20:1 to 22:1, and 18:0 to 20:0 (Kunst et al., 1992). Because three independent screens for mutants defective in VLCFA elongation in seed oils isolated multiple alleles of only *FAE1*, and previous work by Bessoule and coworkers (1989) indicated that elongases consist of multiple protein components, a new model consistent with both biochemical and genetic data designated FAE1 as a single component of a multimeric elongase. In this model, FAE1 would belong to a family of enzymes with distinct substrate specificities and biological roles, while the enzymes that catalyze the three remaining reactions required for elongation would be generalists. Knocking out any generalist component of the elongase would compromise sphingolipid metabolism; therefore, these mutations would be lethal, as suggested by their absence from the mutant screens.

Positional cloning of the *FAE1* gene revealed that it encodes a protein with sequence similarity to polyketide synthases (PKS) such as chalcone synthase and stilbene synthase, and ketoacyl-ACP synthase IIIs (KASIII) (James et al., 1995). These enzymes catalyze the condensation of malonyl-CoA, or malonyl-ACP, with a primer molecule, thereby producing a β–ketoacyl-CoA/ACP product. The homology of FAE1 to these monofunctional condensing enzymes provided strong support for the hypothesis that elongases are multimeric complexes, and that condensing enzymes such as FAE1 provide substrate specificity as they work alongside generalist enzymes of the elongase, β–ketoacyl-CoA reductase (KCR), β–hydroxyacyl-CoA dehydratase (HCD), and enoyl-CoA reductase (ECR) (Figure 1-2).

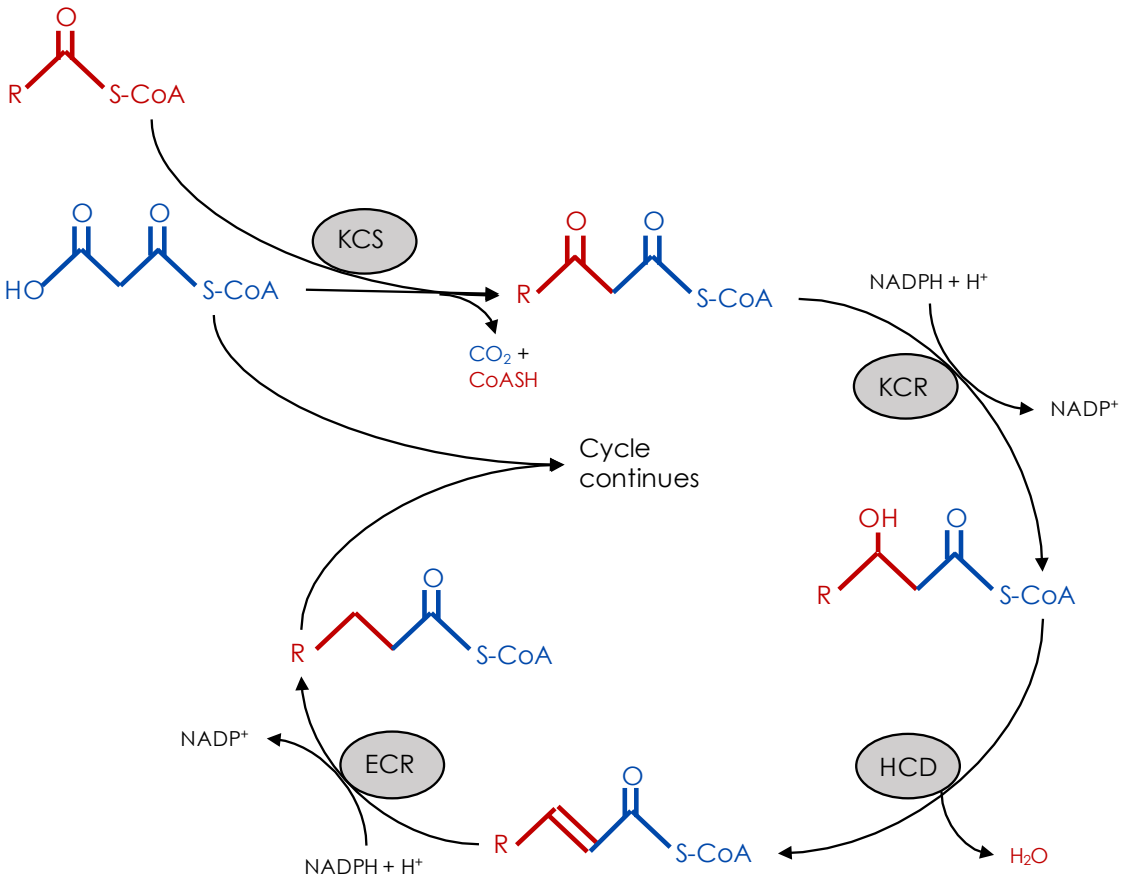

Figure 1-2: Schematic representation of elongation

Malonyl-CoA (**blue**) and an acyl-CoA primer (**red**) are condensed by a ketoacyl-CoA synthase (KCS) to produce a β-ketoacyl-CoA. The β-ketoacyl-CoA is reduced by a β-ketoacyl-CoA reductase (KCR) to yield a β-hydroxyacyl-CoA, which in turn is dehydrated by a β-hydroxyacyl-CoA dehydratase (HCD) to produce an enoyl-CoA. The enoyl-CoA is then reduced by an enoyl-CoA reductase (ECR) to give an acyl-CoA that is two carbons longer than the initial acyl-CoA used as a primer. The acyl-CoA product can then be used as a primer for the same reaction sequence, allowing for repeated elongation of VLCFAs in two carbon units.

Identification of the FAE1 condensing enzyme allowed for further investigation of its activity and specificity in heterologous systems. Millar and Kunst (1997) demonstrated that ectopic expression of FAE1 in both Arabidopsis and tobacco (*N. tabacum*) is sufficient for the synthesis of 20- and 22-carbon VLCFAs. They also found that FAE1 activity could be observed when expressed in yeast; this was an important discovery as it established a simple and fast method to determine KCS specificity. Plant KCSs are able to function alongside generalist components of the native yeast elongase, and take the place of the yeast's native condensing enzymes. It is surprising that plant KCSs function in this system, as yeast ELO condensing enzymes are not homologous to plant FAE1-like KCSs. The first component of the elongase complex that was identified in yeast was *ELONGATION DEFECTIVE 1* (*ELO1*) (Toke and Martin, 1996), which encodes a condensing enzyme responsible for the extension of 14-carbon fatty acids to 16 carbons. Two homologs, *ELO2* (*VBM2/GNS1/FEN1*) and *ELO3* (*SRE1/APA1/VBM1/SUR4*), were subsequently identified, with roles in 16- to 24-carbon and 16- to 26-carbon elongation, respectively (Oh et al., 1997). Yeast Elo proteins are homologous to mammalian ELOVL condensing enzymes. While genes homologous to yeast *ELO*s have been identified in Arabidopsis, their biological functions remain largely unknown.

While ELOs and KCSs are not homologous, the generalist components of the yeast and Arabidopsis elongases are. Elongation of VLCFAs in plants shares many parallels with elongation in yeast, and it is undeniable that yeast research has greatly accelerated our progress in understanding fatty acid elongation in plants. Because of this, and because characterization of yeast elongase enzymes has largely been carried out using biochemical techniques, while molecular genetic approaches have dominated the work done in Arabidopsis, discoveries of both the yeast and Arabidopsis elongase systems will be described here.

1.3.2 β-ketoacyl-CoA reductase

The yeast β-ketoacyl-CoA reductase gene *YBR159* was identified using the reverse genetic approach of searching the yeast genome for oxidoreductases of unknown function predicted to localize to the ER (Beaudoin et al., 2002). Mutants of the candidate oxidoreductases were then screened for their inability to support heterologous activity of *Caenorhabditis elegans* PEA1 (polyunsaturated fatty acid elongating activity 1) and Arabidopsis FAE1 condensing enzymes, which can elongate polyunsaturated fatty acids (PUFAs) and monounsaturated fatty acids (MUFAs), respectively, when expressed in wild-type yeast. Only Ybr159p was identified as essential for elongase activity using this approach, and designation of Ybr159p as a β-ketoacyl-CoA reductase was confirmed by *in vitro* assay (Beaudoin et al.,

2002). Characterization of the *ybr159Δ* mutant revealed that cells have severely impaired growth, but are viable and accumulate residual amounts of VLCFAs (Beaudoin et al., 2002). Ybr159p is localized evenly throughout the endoplasmic reticulum, and co-immunoprecipitates with other components of the elongase, Elo3p and Tsc13p (Han et al., 2002).

Beaudoin et al. (2002) also identified a plant ortholog of *YBR159*, *β-KETOACYL-COA REDUCTASE 1* (*KCR1*) from Arabidopsis. The biochemical function of *KCR1* was confirmed by complementation of *ybr159Δ* mutant yeast. *KCR1* and another putative β-ketoacyl-CoA reductase in Arabidopsis, *KCR2*, have since been further characterized *in planta* (Beaudoin et al., 2009). Despite 45% amino acid identity between KCR1 and KCR2, KCR1 is the only β-ketoacyl-CoA reductase required for VLCFA synthesis in Arabidopsis, as the *kcr1* mutant is lethal, while the *kcr2* mutant has no obvious phenotype. Ectopic expression of *KCR2* cannot complement either the *kcr1* Arabidopsis mutant or the *ybr159Δ* yeast mutant. Intriguingly, both KCR1 and KCR2 contain a putative NADH binding motif and an essential $SX_{16}YX_3K$ catalytic motif, but only KCR1 contains a C-terminal double-lysine endoplasmic reticulum retention motif. The double lysine motif is found in several KCR orthologs from other plant species, and in Ybr159p.

1.3.3 β-hydroxyacyl-CoA dehydratase

The β–hydroxyacyl-CoA dehydratase Phs1p (PTPLA homolog involved in sphingolipid biosynthesis 1 [PTPLA: protein tyrosine phosphatase-like]) was the last component of the elongase to be identified in yeast (Denic and Weissman, 2007). The *phs1Δ* mutation is lethal, indicating that it is an essential component of the yeast elongase with no redundant homologs. Phs1p interacts with other components of the elongase: Elops, Ybr159p, and the enoyl-CoA reductase Tsc13p (described below). Dehydratase activity of Phs1p was demonstrated genetically by analysis of fatty acid elongation intermediates in microsomes derived from wild-type and *PHS1*-downregulated cells. An *in vitro* assay using purified, epitope-tagged Phs1p incubated with β-hydroxyacyl-CoA substrate resulted in the synthesis of the enoyl-CoA product, providing biochemical evidence for Phs1p function (Denic and Weissman, 2007).

The initial characterization of the Arabidopsis hydroxyacyl-CoA dehydratase PAS2 was as a protein-tyrosine phosphatase component of the G2/M cell cycle checkpoint (Bellec et al., 2002; Da Costa et al., 2006). The PAS2 protein bears sequence homology to both the yeast β-hydroxyacyl-CoA dehydratase Phs1p and protein-tyrosine phosphatases, and the *pas2* mutant has phenotypes associated with defects in both VLCFA synthesis and cell cycle control (Bach et

al., 2008; Bellec et al., 2002). Further, PAS2 interacts with both the enoyl-CoA reductase CER10 (Bach et al., 2008) and phosphorylated cyclin-dependent kinases (Da Costa et al., 2006). How these functions are connected remains very poorly understood, however, the separate roles of PAS2 in regulating cell cycle progression and in elongation have been investigated in detail. Similar to *kcr1*, loss-of-transcript alleles of *pas2* are embryo lethal, and knock-down mutants have reduced accumulation of cuticular waxes, seed oil, and sphingolipids (Bach et al., 2008). Ectopic expression of the yeast hydroxyacyl-CoA dehydratase Phs1p in Arabidopsis increased the accumulation of VLCFAs relative to the wild type (Bach et al., 2008). The yeast dehydratase was used in this experiment to avoid any post-translational mechanisms of regulating dehydratase activity in plants. This result indicates that in addition to the demonstrated rate-limiting role of condensing enzymes in elongation (Millar and Kunst, 1997), dehydratase activity can also affect VLCFA yield.

Analogous to *KCR1* and *KCR2*, *PAS2* also has one close homolog, *PTPLA*, which does not have a VLCFA-deficient phenotype, and is unable to complement the *pas2* mutant. However, ectopic *PTPLA* expression in both Arabidopsis and yeast increases VLCFA accumulation, and the *ptpla* mutant accumulates hydroxy-acyl-CoAs (Morineau et al., 2016). Expression profiling of *KCR1*, *KCR2*, *PAS2*, and *PTPLA* in roots revealed that *KCR1* and *PAS2* are highly expressed in the endodermis, which may be anticipated as suberin is synthesized in this tissue. In contrast, *KCR2* and *PTPLA* expression is predominant in the root vasculature. The authors proposed that two fatty elongase complexes might exist in Arabidopsis, with dual functions and expression profiles. This work underscores the fact that there is much that is not yet understood about fatty acid elongation in plants. The current model of a four-enzyme complex is a useful tool, but it is also a simplification of the complexity that exists in nature.

1.3.4 Enoyl-CoA reductase

The first identified generalist component of the yeast elongase was *TEMPERATURE-SENSITIVE csg2Δ 13* (*TSC13* [*csg2Δ*: calcium-sensitive growth 2]), the gene encoding an enoyl-CoA reductase, by means of a forward genetic screen for mutants defective in sphingolipid metabolism (Kohlwein et al., 2001; Dunn et al., 2000). Identity of Tsc13p as the enoyl reductase was supported by four lines of evidence: (1) similar phenotypes of the loss-of-function *tsc13-1* mutant to the *elo2Δ* and *elo3Δ* single mutants, although null *tsc13Δ* mutants were lethal; (2) accumulation of trans-2,3-enoyl-CoA in the *tsc13-1* mutant; (3) homology of Tsc13p with steroid 5-α-reductases, which also reduce double bonds α-β to a carbonyl group; and (4) physical interaction of Tsc13p with Elo2p and Elo3p.

Following the identification and characterization of Tsc13p (Gable et al., 2004) and the identification of its putative Arabidopsis ortholog (Kohlwein et al., 2001), the equivalent enoyl-CoA reductase, ECERIFERUM10 (CER10), was also the first generalist component of the elongase to be characterized in plants (Zheng et al., 2005). Surprisingly, characterization of two mutant alleles, *cer10-1* and *cer10-2*, revealed that the loss of CER10 is not lethal (Zheng et al., 2001) providing a parallel to the non-lethal phenotype of the *ybr159Δ* yeast mutants. In fact, both *cer10* mutants still accumulate low levels of VLCFAs in seed oil, cuticular waxes, and sphingolipids. Thus, the real puzzle brought to light by this study is how VLCFAs are produced in the absence of CER10. As *CER10* has no obvious, closely related homologs in Arabidopsis, Zheng and coworkers (2005) speculated that there could be a functionally equivalent enoyl-CoA reductase existing in plants that has no sequence homology to *CER10* or *TSC13*. They also suggested that alternatively, another reductase with promiscuous activity could act on very-long-chain enoyl-CoAs in the absence of CER10. For example, steroid-5-reductases would be good candidates as they also reduce double bonds α-β to a carbonyl group, and have C-terminal homology with Tsc13p and CER10.

1.4 Plant condensing enzymes

Condensing enzymes are the only core component of the fatty acid elongase that differs markedly between yeast and plants, with yeast using Elops, and plants using FAE1-like KCSs. However, genes with homology to ELOs have also been identified in plant genomes. To date, the function of these genes in flowering plants remains a mystery, however, some *ELO*-like genes have been characterized in bryophytes. Three cDNAs encoding *ELO* homologs have been isolated from the moss *Physcomitrella patens*, and mutant analysis and heterologous expression in yeast have demonstrated that they elongate polyunsaturated VLCFAs (Zank et al., 2002; Eiamsa-ard et al., 2013). These ELO-likes are thought to be necessary for the synthesis of polyunsaturated VLCFAs that are incorporated into diverse membrane lipids in bryophytes.

Four *ELO* homologs have been identified in the Arabidopsis genome. One homolog has been partially characterized (Quist et al., 2009), however, the role of plant ELOs in elongation remains hotly contested. As the role of KCSs in elongation is well established, and it is clear that these condensing enzymes are the major contributors to the elongation of cuticular wax precursors, the remainder of this section will focus on the *FAE1*-like KCS gene family (hereafter referred to as KCSs).

1.4.1 KCS mechanism and catalytic residues

Biochemical characterization of KCSs has been a challenge due to the difficulty inherent in studying membrane-bound proteins. However, homology of KCSs to soluble ketoacyl-ACP synthase IIIs (KASIII) and polyketide synthases (PKS) has been useful in providing a precedent to guide structural and functional studies. KASIIIs, PKSs, and KCSs have been proposed to catalyze similar three-step reaction sequences. First, an acyl group is transferred from acyl-CoA onto a conserved cysteine residue of the condensing enzyme. Next, malonyl-ACP (KASIIIs) or malonyl-CoA (KCSs and PKSs) is decarboxylated, producing an acetyl carbanion intermediate, which remains conjugated to its –CoA or –ACP activating group. The acetyl carbanion then carries out a nucleophilic attack on the carbonyl carbon of the acyl group esterified to cysteine, producing an activated β-keto-acyl (Figure 1-3). It was predicted that Cys223 of FAE1/KCS18 binds the acyl substrate during fatty acid elongation based on the conservation of this residue among condensing enzymes (Lassner et al., 1996). This prediction was later supported by co-crystallization of *E. coli* ketoacyl-ACP synthase III with its acetyl-CoA substrate (Qiu et al., 1999), which demonstrated that the analogous residue in this enzyme forms a thioester bond with acetate. Ghanevati and Jaworski (2001) demonstrated the importance of Cys223 of

FAE1/KCS18 by expressing site-directed mutant isoforms of the gene in yeast, which revealed that the C223A mutation abolishes condensation activity. However, evidence of direct binding of the acyl group to Cys223 of FAE1/KCS18, and on analogous residues of other KCS enzymes, is lacking.

Ghanevati and Jaworski (2002) later developed a soluble *in vitro* assay system for KCSs that allowed them to determine what specific catalytic activities are affected in site-directed mutants. In so doing, they showed that the C223A mutation not only abolishes overall condensation activity of FAE1/KCS18, but that it also inhibits decarboxylation of malonyl-CoA. Decarboxylase activity was also abolished when the assay was conducted with the wild-type enzyme in the absence of acyl-CoA substrate. These observations suggest a "Ping-Pong" mechanism for KCS enzyme activity, wherein decarboxylation of malonyl-ACP/CoA is dependent on transfer of the acyl-CoA substrate to the enzyme. This mechanism is not conserved among all condensing enzymes; *Medicago sativa* chalcone synthase (a PKS) can carry out decarboxylation in the absence of an acyl-CoA substrate and retains some decarboxylase activity even when its catalytic cysteine is mutated, although the reaction becomes much less efficient (Jez et al., 2000).

Witkowski and coworkers (1999) suggested that the "Ping-Pong" dependence of decarboxylation on acyl binding observed in some condensing enzymes enforces a sequence on the reactions required for condensation. There are several bacterial PKSs that lack an active site cysteine, and in its place have a glutamine residue that structurally mimics a bound acyl group; these isoforms very efficiently catalyze malonate decarboxylation in the absence of an acyl-CoA substrate. Similarly, site-directed mutagenesis of otherwise fully functional mammalian fatty acid synthase condensing enzymes has shown that a single amino acid change from cysteine to glutamine is sufficient to induce a change from condensing activity to efficient decarboxylase activity (Witkowski et al., 1999). While this experiment has not been conducted with plant KCSs, the results of Ghanevati and Jaworski (2001) would suggest that a similar regulatory mechanism could exist in this enzyme family. This could serve to prevent the depletion of malonate in the absence of an acyl substrate.

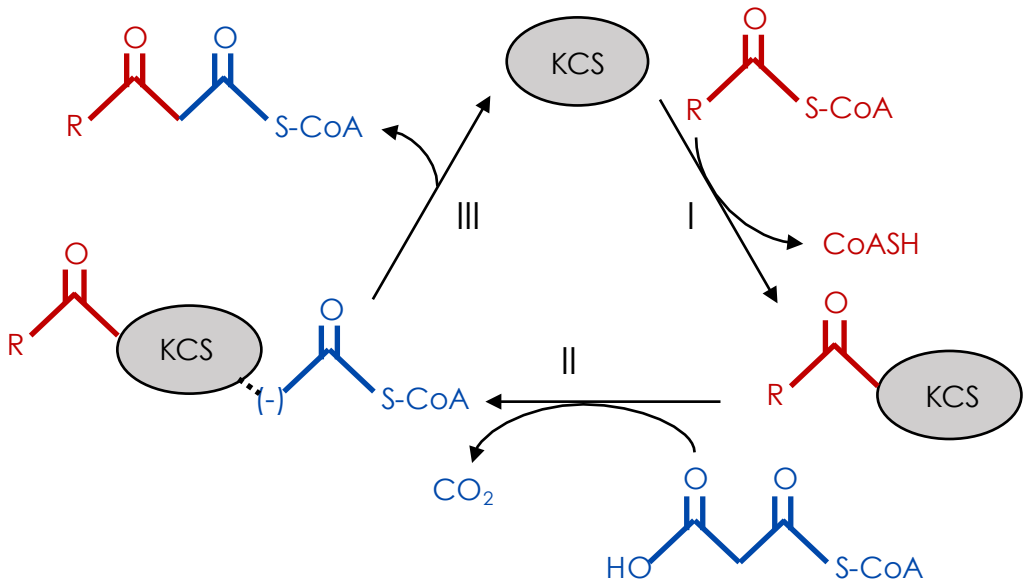

Figure 1-3: Schematic representation of KCS/FAE1-like condensing enzyme catalysis

(I) An acyl group is transferred from acyl-CoA (**red**) on to a cysteine residue of the KCS. (II) Malonyl-CoA (**blue**) is decarboxylated, releasing carbon dioxide, and producing a reactive acetyl-CoA carbanion intermediate (which may be stabilized by histidine and asparagine residues of the KCS enzyme). (III) The nucleophilic carbanion attacks the carbonyl carbon of the acyl group esterified to cysteine, forming a new carbon-carbon bond, releasing the acyl group from the cysteine of KCS, and regenerating the free enzyme.

Comparison of KCSs to KASIIIs and PKSs has also been useful for predicting the mechanism of decarboxylation in KCSs. Two residues, a histidine and an asparagine, are broadly conserved among these condensing enzymes and are thought to facilitate the decarboxylation of the malonyl-ACP/CoA substrate. Ghanevati and Jaworski (2002) used site-directed mutagenesis to probe the function of His391 of FAE1/KCS18, predicted as a catalytic residue based on sequence alignment with KASIIIs and PKSs. Conversion of His391 to several different amino acids abolished both decarboxylation and condensation activities of FAE1. A basic residue in this position has been suggested to function in deprotonating the active-site cysteine to promote the acyl transfer reaction (Abbadi et al., 2000). However, FAE1 His391 substitution with a glutamine residue, which cannot function as a general base, retained significant condensation and decarboxylation activities. A similar outcome was obtained with chalcone synthase (Jez et al., 2000), where glutamine can also substitute for histidine and retain enzyme activity. These results suggest that the conserved histidine is not required for proton abstraction in these enzyme families. Jez and coworkers (2000) suggested, based on the position of the histidine in chalcone synthase known from its crystal structure, it could hydrogen bond with the carbonyl group of malonyl-CoA to stabilize the reactive enol tautomer, and thereby promote decarboxylation of malonyl-CoA to an acetyl anion. Following this reaction, the histidine would also be in a good position to stabilize the acetyl anion product. The analogous histidine residue in plant KCSs may have a similar function.

Work by Jez and coworkers (2000) also provided insight to the function of an asparagine residue conserved among KASIIIs, PKSs, and KCSs; using chalcone synthase they showed that mutation of Asn336 impairs both acyl substrate transfer as well as malonyl-CoA decarboxylation. Ghanevati and Jaworski (2002) demonstrated by site-directed mutagenesis of FAE1/KCS18 that the equivalent residue in this protein, Asn424, is required for both condensation and decarboxylation, but did not test the effect of mutagenizing asparagine on acyl transfer. Based on the position of Asn336, Jez and coworkers (2000) suggested that it could hydrogen bond first with the thioester carbonyl of the acyl-CoA group, priming the transfer of the acyl group from CoA to cysteine. The asparagine could also act similarly to histidine in hydrogen bonding with the carbonyl group of malonyl-CoA to stabilize the enol tautomer and thereby promote decarboxylation, and then stabilize the acetyl anion product.

1.4.2 KCS structure and substrate specificity

While there is no crystal structure for any plant KCS, Joubès and coworkers (2008) used homology modelling to predict and examine the tertiary structure of KCS1. A sequence

homology and threading-based search for structural homologs with known structures revealed *Medicago sativa* chalcone synthase and *E. coli* ketoacyl-ACP synthase III (KASIII/FabH) as good templates for determination of most of the KCS1 structure. Homology modelling was then used to extrapolate the deduced structure of KCS1 to the entire Arabidopsis KCS family. These structure-function comparisons among KCSs demonstrated that all members of the family have a similar structure.

The N-terminus of KCS proteins consists of either one or two alpha helices that for most members of the family are well positioned to serve as a membrane anchor. However, the position of these helices in seven of the 21 KCSs in Arabidopsis is such that the helices are poorly positioned for insertion in a membrane (Joubès et al., 2008). In the absence of a membrane anchor, interactions between protein components of the fatty acid elongase complex may be responsible for the correct localization and orientation of KCS enzymes in the endoplasmic reticulum. This prediction is supported by (1) confirmed endoplasmic reticulum localization of KCSs with membrane anchors predicted to have poor function (Joubès et al., 2008), and (2) demonstration that cleavage of the predicted transmembrane domains from FAE1/KCS18 is insufficient to solubilize the globular portion of the protein, and that salt treatment is necessary to purify FAE1/KCS18 in a soluble cell fraction (Ghanevati and Jaworski, 2002). Domains involved in protein-protein interactions within the fatty acid elongase complex remain unknown.

The remaining, soluble core of the KCS contains all of the catalytic residues (Joubès et al., 2008). By superimposing the catalytic residues involved in both thioester bond formation with the acyl group (cysteine) and decarboxylation of malonyl-CoA (histidine and asparagine), the authors were able to evaluate and compare the sizes and shapes of substrate-binding pockets of different members of the KCS family. Though the metrics of these comparisons were not made explicit in their publication, the authors reported a general correlation between the size of the pocket and the length of the acyl substrate when the latter was known from previous biochemical experiments.

To identify additional features that contribute to the substrate specificity of KCSs, aside from the size of the predicted substrate-binding pocket, Blacklock and Jaworski (2002) carried out domain swaps and site-directed mutagenesis using FAE1/KCS18 from Arabidopsis and its *Brassica napus* homolog (BnFAE1). These proteins have 86% homology, and both elongate 18:1 to 20:1 and 22:1. However, the 22:1/20:1 product ratio varies between 0.12 for FAE1/KCS18 and 0.34 for BnFAE1 when the genes are expressed in yeast. The authors identified a 99-amino acid N-terminal region immediately downstream of the transmembrane

domains of FAE1 as being sufficient to impart either Arabidopsis or *B. napus* FAE1 specificity. On KCS tertiary structure models (Joubès et al., 2008) this region lacks repetitive secondary structure, and its sequence shows high variability within the KCS family compared to the rest of the protein sequence.

Another approach to deciphering structure-function relationships among plant KCSs was explored by Jasinski and coworkers (2012). Natural variation in seed oil accumulation among Arabidopsis ecotypes was used to map quantitative trait loci (QTLs) that strongly impact VLCFA production. A high-VLCFA-producing ecotype, Bay-0, was crossed into a low-VLCFA-producing ecotype, Shahdara, and a single genetic locus responsible for 77% of the observed genetic variation between the two ecotypes was identified. Not surprisingly, their QTL of interest mapped to FAE1/KCS18. This study was not the first of its kind; natural variation in seed oil metabolism among Arabidopsis ecotypes has been surveyed, and the genetic basis for this natural variation has been investigated (O'Neill et al., 2003; Hobbs et al., 2004). However, the work by Jasinski and coworkers is of particular interest because the authors identified and discussed the specific amino acid substitution that strongly impacts VLCFA accumulation in Arabidopsis. The Shahdara ecotype has a polymorphism that converts a well-conserved valine residue near the active site to a leucine. The tertiary structure model (Joubès et al., 2008) predicts that this single amino acid substitution would induce conformational changes resulting in a 25% reduction of the size of the catalytic binding pocket. Heterologous expression of both isoforms in yeast confirmed that the valine to leucine polymorphism in the Shahdara ecotype reduced enzyme activity, as yeast expressing the Bay-0 isoform produced over 8-fold more VLCFAs than yeast expressing the Shahdara isoform. A survey of FAE1/KCS18 in 568 Arabidopsis ecotypes revealed that this valine to leucine substitution is found in 35 ecotypes, and therefore accounts for substantial variation in VLCFA production naturally observed in Arabidopsis.

There is an additional feature common to both KASIIIs and PKSs that is of particular importance for the discussion of KCS structure; both of these enzyme families are known to function as homodimers on the basis of crystal structures (Qiu et al., 1999; Qiu et al., 2001; Jez et al., 2000) as well as biochemical data (Kreuzaler et al., 1979). Considering the void in our understanding of fatty acid elongase complex structure and stoichiometry, confirming whether this is the case with KCSs would be very interesting. A comparison of the crystal structures of free KASIII and ligand-bound KASIII revealed substantial structural changes upon ligand binding, especially at the interface of the two monomers (Qiu et al., 2001). In the case of both KASIIIs and PKSs, there is a single phenylalanine residue from each monomer that protrudes

into the active site of the other, suggesting that dimer formation could play a role in catalysis. The possibility of protein-protein interactions impacting ligand binding is intriguing, and certainly deserves further investigation in the KCS family.

1.4.3 Biological functions of KCSs in Arabidopsis

There are 21 homologous *FAE1*-like *KCS*s in the Arabidopsis genome. The physiological roles of some of these have been determined by mutant analysis, and the substrate specificity has been defined in many using the yeast expression system. Our current knowledge of the Arabidopsis KCS family based on these studies is summarized in Table 1-1.

There is overlap in both the expression patterns (Joubès et al., 2008; Suh et al., 2005) and substrate specificities of many Arabidopsis KCSs (Paul et al., 2006; Tresch et al., 2012; Trenkamp et al., 2004; Blacklock et al., 2006), suggesting that there is functional redundancy within the family. It is particularly striking that the expression of eleven KCSs is up-regulated in the stem epidermis, where cuticular lipids are synthesized (Suh et al., 2005). Large numbers of putative KCS enzymes are also found in barley, rice, maize, and soybean (Tresch et al., 2012). These broad observations suggest that there is an advantage to having multiple specialized, but likely redundant, KCSs in a genome.

There is inconsistency in that so many KCSs are expressed in stem epidermal cells, but very few KCSs produce fatty acids longer than 28 carbons. Aliphatic waxes derived from 30- and 32-carbon fatty acids account for roughly 80% of the total stem wax load in Arabidopsis, and cuticular wax constitutes roughly 50% of the acyl-lipid output of epidermal cells (Suh et al, 2005). Therefore, plants must have a robust mechanism of synthesizing the fatty acid precursors of these waxes, but this is not evident from the analysis of *KCS* genes.

Table 1-1: Summary of KCS genes of *Arabidopsis thaliana*

Gene	Yeast Expression	Biological Function	ER localization confirmed?	Expression patterns	Expression ratio (e)	Expression intensity (e)
At1g01120 (KCS1)	produced 20:0, 20:1, 22:0, 24:0, 26:0 (a); substrate specificity for 16:0, 16:1, 18:0, 20:1; very low activity with 18:1 (b); expressed in *elo2 elo3* yeast, but unable to rescue the mutant phenotype (c); produced 20:0, 20:1, 22:0 (d)	required for cuticular wax accumulation (Todd et al., 1999)	yes (Joubès et al., 2008)	expressed in all tissues, highest in siliques, flowers, stems and cauline leaves (Joubès et al., 2008); high expression in etiolated seedlings (Todd et al., 1999)	4.7	21,884
At1g04220 (KCS2/DAISY)	produced 22:0, 24:0, 26:0 (a); rescued *elo2 elo3*; utilized 16:0, 16:1, 18:0, 18:1, 18:2, 20:0, low activity with 22:0 (c); produced 20:0, 22:0, 24:0 (d)	required for suberin/suberin associated wax biosynthesis in roots, chalaza, and in response to environmental stresses (Franke et al., 2009); has redundant roles in suberin and cuticular wax biosynthesis (Lee et al., 2009)		highest expression in root, silique, and flower (Lee et al., 2009; Franke et al., 2009); enhanced expression in response to osmotic stress (Lee et al., 2009); high expression in stigma, root elongation zone, epidermis, chalaza (Lee et al., 2009); expression detected in all tissues except seedling and rosette leaf, highest in silique (Lee et al., 2009)	8.1	6,599
At1g07720 (KCS3)	expressed in yeast, but no activity detected (b,d)	unknown	yes (Joubès et al., 2008)	expressed in all tissues except root, highest expression in siliques (Joubès et al., 2008)	9.9	2,866
At1g19440 (KCS4)	expressed in yeast, but no activity detected (b,d); expressed in *elo2 elo3* yeast, but unable to rescue the mutant phenotype (c),	unknown		low levels of expression in all tissues, highest in siliques (Joubès et al., 2008)	NA	NA
At1g25450 (KCS5/CER60)	produced 20:1, 26:0, 28:0, 30:0 (a); expressed in *elo2 elo3* yeast, but unable to rescue the mutant phenotype (c); produced 24:0, 26:0, 28:0 (d)	based on phylogeny, heterologous activity in yeast, and expression patterns, thought to be involved in cuticular lipid metabolism, but not confirmed (Fiebig et al., 2000)	yes (Joubès et al., 2008)	expression in all tissues, highest expression in siliques (Joubès et al., 2008)	5.8	1,527
At1g68530 (KCS6/CER6)	produced 24:0, 26:0, 28:0 (d)	required for cuticular wax accumulation throughout Arabidopsis shoots (Millar et al., 1999; Fiebig et al., 2000)	yes (Joubès et al., 2008)	epidermis-specific expression, enhanced by light and osmotic stress (Hooker et al., 2002); expression in all tissues except root, highest expression in siliques (Hooker et al., 2002; Joubès et al., 2008)	3.1	19,397
At1g71160 (KCS7)	expressed in yeast, but no activity detected (b,d)	unknown		only expressed in flowers and siliques (Joubès et al., 2008)	NA	NA
At2g15090 (KCS8)	expressed in yeast, but no activity detected (d)	unknown	yes (Joubès et al., 2008)	highest expression in cauline leaves, some expression in stems, rosette leaves, flowers and siliques (Joubès et al., 2008)	6.6	296

Gene	Yeast Expression	Biological Function	ER localization confirmed?	Expression patterns	Expression ratio (e)	Expression intensity (e)
At2g16280 (KCS9)	rescued *elo2 elo3*; elongated 16-22 substrates, had lower activity for 16:1, 18:1, and 18:2 substrates; mostly produced 24 (c); expressed in yeast, but no activity detected (d)	required for suberin, cuticular wax, sphingolipid, and phospholipid precursor elongation to 24 (Kim et al., 2013)	yes (Kim et al., 2013)	expressed in all tissues tested, highest in stems, cauline leaves, and siliques (Joubès et al., 2008)	3.1	9,337
At2g26250 (KCS10/FDH)	expressed in *elo2 elo3* yeast, but unable to rescue the mutant phenotype (c); expressed in yeast, but no activity detected (d)	required for normal development of the epidermis (Pruitt et al., 2000)	yes (Joubès et al., 2008)	expressed in all tissues except root, highest expression in stems and siliques (Joubès et al., 2008)	4	9,547
At2g26640 (KCS11)	substrate specificity for 16:0, 16:1, 18:0; lower activity level with 18:1, 20:0, 20:1 (b); expressed in *elo2 elo3* yeast, but unable to rescue the mutant phenotype (c); expressed in yeast, but no activity detected (d)	unknown		expressed at a relatively low, consistent levels in all tissues tested (Joubès et al., 2008)	NA	NA
At2g28630 (KCS12)	expressed in yeast, but no activity detected (d)	unknown	yes (Joubès et al., 2008)	expressed in all tissues except root, highest expression in cauline leaves and siliques (Joubès et al., 2008)	5.5	3,857
At2g46720 (KCS13/HIC)		affects guard cell density on leaves; mutants show increased stomatal indices in high [CO2], when wt plants decrease stomatal index in high [CO2] to enhance water use efficiency (Gray et al., 2000)		guard cell-specific expression, low levels of expression except in flowers and siliques (Gray et al., 2000)	NA	NA
At3g10280 (KCS14)		unknown		low levels of expression except in siliques (Joubès et al., 2008)	NA	NA
At3g52160 (KCS15)	expressed in yeast, but no activity detected (d)	unknown		only expressed in flowers (Joubès et al., 2008)	NA	NA
At4g34250 (KCS16)	expressed in yeast, but no activity detected (b)	unknown		low levels of expression except in siliques (Joubès et al., 2008)	NA	NA
At4g34510 (KCS17)	produced 20:0, 20:1, 24:0, 26:0 (a); substrate specificity for 16:0, 18:0, 20:0, 22:0 (b); produced 24:0 (d)	unknown		low levels of expression except in flowers (Joubès et al., 2008)	NA	NA

Gene	Yeast Expression	Biological Function	ER localization confirmed?	Expression patterns	Expression ratio (e)	Expression intensity (e)
At4g34520 (KCS18/FAE1)	produced 20:0, 20:1, 22:0, 22:1, 24:0, 24:1, 26:0 (a); substrate specificity for 16:0, 16:1, 18:0, 18:1; lower activity with 20:0, 20:1 (b); rescued *elo2 elo3*; elongated 16:0, 16:1, 18:0, 18:1, 18:2, lower activity with 20:0 (c); produced 20:0, 20:1, 22:0, 22:1 (d)	required for 20:0, 20:1, and 22:1 VLCFA synthesis for seed storage triacylglycerols (Kunst et al., 1992; James et al., 1995)		only expressed in seeds (James et al., 1995)	NA	NA
At5g04530 (KCS19)	expressed in yeast, but no activity detected (b,d)	unknown		low levels of expression except in siliques (Joubès et al., 2008)	8.7	254
At5g43760 (KCS20)	produced 22:0, 24:0, 26:0 (a); rescued *elo2 elo3*; elongated 16:0, 16:1, 18:0, low activity with 18:1, active with 20 substrate (c); produced 20:0, 22:0, 24:0 (d)	has redundant roles in suberin and cuticular wax biosynthesis (Lee et al., 2009)		expressed at a relatively consistent level in all tissues tested except lower expression in root (Joubès et al., 2008)	4.8	9,032
At5g49070 (KCS21)		unknown		only expressed in flowers (Joubès et al., 2008)	NA	NA

(a) Trenkamp et al. (2004) expressed 17 KCS proteins in yeast; only 6 had activity in this experiment. Differentiation between plant and yeast condensing enzyme products are not clear as this assay was carried out in wild-type yeast. (b) Blacklock et al. (2006) expressed selected His-tagged KCS proteins in yeast, and assayed their activity by feeding the transgenic yeast microsomes labelled malonyl-CoA and assorted acyl-CoAs; 16:0, 16:1, 18:0, 18:1, 20:0, 20:1, 22:0, 22:1. (c) Paul et al. (2006) expressed select KCSs in *elo2 elo3* yeast, determined VLCFA products *in vivo* by GC/MS analysis, then carried out an assay *in vitro* with substrate feeding followed by TLC detection of product. (d) Tresch et al. (2012) expressed 17 KCS proteins in InvSc1, *elo2*, and *elo3* yeast, and compiled and annotated information prior to reporting products of different KCSs. (e) Suh et al. (2005) carried out microarray analysis of gene expression in stem epidermis; the transcript ratio of top stem epidermis/total stem top and the mean signal intensity at the stem top are presented here.

1.5 The *eceriferum2* mutant

In the absence of a condensing enzyme that efficiently elongates fatty acids to the chain lengths required to synthesize cuticular waxes, I hypothesized that there must be other, as yet unknown, genetic components that assist in the elongation of fatty acids beyond 28 carbons. Among the wax-deficient *eceriferum* mutants described by Koornneef et al. (1989), the phenotype of the *cer2* mutant strongly suggests that CER2 may have a role in the final steps of elongation; *cer2* has a dramatic reduction in all stem waxes longer than 28 carbons, and increased accumulation of some wax components 28 carbons and shorter (McNevin et al., 1993). As cuticular waxes derived from fatty acids 30 carbons and longer make up over 80% of the total wax of wild-type Arabidopsis stems, the *cer2* mutant phenotype is obvious; the wax load of *cer2* is approximately one third that of wild type, and *cer2* stems appear glossy and green compared to the glaucous wild type (McNevin et al., 1993).

The *cer2* mutation was mapped to At4g24510 (Negruk et al., 1996; Xia et al., 1996), a gene homologous to plant BAHD acyltransferases. The BAHD acyltransferase family is named for the first four enzymes described in this clade: BEAT, benzylalcohol *O*-acetyltransferase; AHCT, anthocyanin *O*-hydroxycinnamoyltransferase; HCBT, *N*-hydroxycinnamoyl/ benzoyltransferase; and DAT, deacetylvindoline 4-*O*-acetyltransferase. BAHDs are specific to plants and fungi, and have diverse roles in specialized metabolic pathways. BAHDs catalyze the transfer of an acyl group from a CoA-thioester to an alcohol or amine acyl acceptor, generating an ester or amide bond, respectively (Figure 1-4). How an acyl transfer reaction could contribute to the process of fatty acid elongation as we currently understand it is not obvious, much less how an acyl transfer reaction could be required for elongation exclusively at one particular chain length.

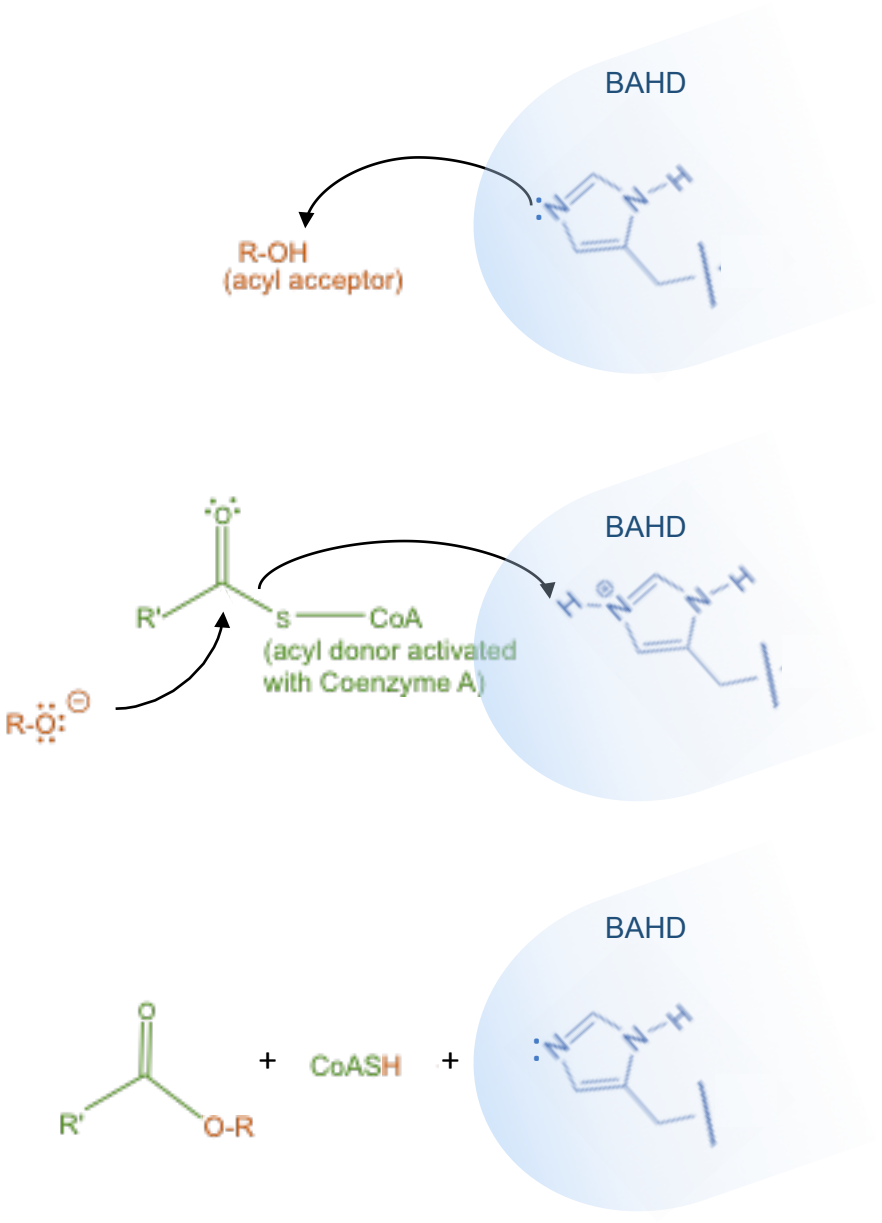

Figure 1-4: Schematic representation of BAHD acyltransferase activity

Acyl transfer proceeds via two steps. First, the acyl acceptor is deprotonated by a catalytic histidine residue on the BAHD. Second, the electronegative acyl acceptor carries our a nucleophilic attack on the carbonyl carbon of the acyl-CoA, the acyl donor. This creates a new ester bond between the acyl donor and acceptor.

1.6 Research questions, objectives, and significance of findings

The canonical mechanism of elongation by FAE complexes is established, and the core machinery has been thoroughly studied. However, characterized components of the FAE complex are insufficient to produce fatty acids longer than 28 carbons, which are required for wax synthesis. The exceptionally long chain length of wax components is one feature of plant cuticles that is reasonably consistent across flowering plant phyla, with most waxes derived from fatty acids 28-34 carbons in length. Other metabolic pathways that incorporate VLCFAs, such as sphingolipid and suberin biosynthesis, use chain lengths shorter than 26 carbons.

The *cer2* mutant is specifically deficient in waxes longer than 28 carbons, but little was known about the *CER2* gene beyond this mutant phenotype. Therefore, my thesis research had three objectives: to characterize *CER2* (Chapter 3), to identify and characterize *CER2* homologs in Arabidopsis (Chapter 4), and to decipher the biochemical activity of the CER2 protein (Chapter 5).

I found that there are five *CER2-LIKE* genes in Arabidopsis, and that these form a unique clade within the BAHD acyltransferase family. CER2-LIKEs are necessary for the elongation of fatty acid precursors of cuticular waxes, and establish the chain-length profiles of waxes on different plant surfaces. CER2-LIKEs pair with specific condensing enzymes to elongate fatty acids longer than 28 carbons. Despite homology to BAHD acyltransferases, CER2-LIKEs do not appear to have acyl transfer function. While the biochemical function of CER2-LIKEs remains a mystery, this work has uncovered an intricacy in the process of elongation that is necessary for the synthesis of cuticular waxes.

Chapter 2: Materials and methods

2.1 Biological material and growth conditions

2.1.1 *Arabidopsis thaliana*

Arabidopsis seed stocks were obtained from the Arabidopsis Biological Resource Center (Alonso et al., 2003; http://www.arabidopsis.org/). Mutants used in this study are summarized in Table 2-1.

Table 2-1: Summary of mutant alleles used in this thesis

ATG	Gene name	Line	Allele	Ecotype	Mutagen
At4g24510	*CER2*	SALK_084443C	*cer2-5*	Col-0	T-DNA
At4g13840	*CER2-LIKE1/CER26*	SALK_087857	*cer2-like1-1*	Col-0	T-DNA
At3g23840	*CER2-LIKE2/CER26-LIKE*	GK-180G04-013602	*cer2-like2-1*	Col-0	T-DNA
At4g29250	*CER2-LIKE3*	SALK_147254C	*cer2-like3-1*	Col-0	T-DNA
At5g02890	*CER2-LIKE4*	N/A	*cer2-like4-1*	Col-0	CRISPR/Cas9
At1g68530	*CER6*	N/A	*ew2*	Col-0	En/Spm transposon

With the exception of Arabidopsis plants grown for the purpose of transformation with *Agrobacterium tumefaciens*, all seeds were germinated on Arabidopsis (*Arabidopsis thaliana*; AT) medium (Somerville and Ogren, 1982) supplemented with 1 % (w/v) agar and, when necessary, with appropriate antibiotics for transgene selection. Seeds were stratified for 2-4 days on AT plates stored in the dark at 4°C, prior to transfer to continuous light (100 $\mu Em^{-2}s^{-1}$ of photosynthetically active radiation) at 20°C. Seven day-old seedlings were transferred to soil (Sunshine Mix 4 or 5, SunGro) supplemented with liquid AT medium under the same light conditions. Pots were covered with cling wrap for 3-4 days after transplanting. Seeds were recovered from mutants with partial male sterility phenotypes by either wrapping young inflorescences in cling wrap for several days or growing plants in a chamber with high relative humidity. Mutant lines were genotyped by PCR as described in Section 2.2.1. Insertion sites of T-DNAs and transposable elements were determined by amplifying the genetic sequence using one insertion-specific and one gene-specific primer. Primers used for this genotyping are specified in Table 2-2. Plants were out-crossed manually to generate double, triple, and quadruple mutants, and homozygous mutants were identified in the F_2 and F_3 generations by PCR-based genotyping.

Arabidopsis seeds grown specifically for transformation with *Agrobacterium tumefaciens* were suspended in a 0.1%(w/v) agarose solution, and distributed on AT-supplemented soil at a

density of 100 seeds/6” pot. Pots were covered with cling wrap for 7-10 days; plants were otherwise grown under the same conditions as described above.

2.1.2 *Nicotiana benthamiana*

Nicotiana benthamiana (tobacco) plants grown for transient expression assays were sown directly on soil (Sunshine Mix 4 or 5, SunGro) supplemented with liquid AT medium. Plants were grown under 16/8 hr day/night cycles, at 100 $\mu Em^{-2}s^{-1}$ of photosynthetically active radiation. Plants were transformed roughly three to four weeks after sowing.

2.1.3 *Saccharomyces cerevisiae*

Saccharomyces cerevisiae strain W3031A (*MATa ade2-1 his3-11,15 leu2-3,112 trp1-1 ura3-1 can1-100*) were used for all yeast expression experiments. Cells were grown on plates of yeast peptone adenine dextrose (YPAD) or synthetic complete (SC) dropout medium solidified with 2% agar (Sherman, 2002). SC medium was prepared lacking nutrients required for selection of prototrophic, transformed cells. Cells were grown at 30°C, and were kept at room temperature for short-term storage.

2.2 Polymerase chain reaction (PCR)

2.2.1 Genotyping

Plant DNA for genotyping was preserved using Whatman FTA cards. Insertional mutants were genotyped using either two gene-specific primers or one gene-specific and one insertion-specific primer, as listed in Table 2-2.

Table 2-2: Primers used for genotyping

Primer Name	Sequence (5'-3')
LBb1-3 (SALK lines)	ATTTTGCCGATTTCGGAAC
LBo8409 (GABI-KAT lines)	ATATTGACCATCATACTCATTGC
En1 RB	GGGTTTTGGCCGACACTCC
CER2 LP	TGGGAAAAACCAAAACAACAC
CER2 RP	ACGTCGAAGAGTTCACAGTGG
CER2-LIKE1 LP	AGGCCCAACCCTAATCCTCC
CER2-LIKE1 RP	TACTCAGCCGAGACAGCACG
CER2-LIKE2 LP	GACTCATCAAGTTCTGCCCTG
CER2-LIKE2 RP	GATCTACTGCCCCAAAACCTC
CER2-LIKE3 LP	AGGGGTTTTCATGAACCCG
CER2-LIKE3 RP	TTCTTTAACCAGTCTCCCGG
CER2-LIKE4 LP	ACATCTGTATTCGCTGTTGGG
CER2-LIKE4 RP1 (for CAPS)	AGGCTCTCCCTAAAGATTCC
CER2-LIKE4 RP2 (for sequencing)	AGAACAATGGAGAGTATTGAGG
CER6 LP	GCCACGCACCATCTACCTCG
CER6 RP	CAACATGGCTCTCTCGTTGCC

2.2.2 RT-PCR & qPCR

RNA was extracted from Arabidopsis tissues by phenol:chloroform:isoamyl alcohol separation and purified by lithium chloride and sodium acetate precipitations (Wilkins and Smart, 1995). Genomic DNA was removed by treatment with DNase I (New England Biolabs) according to the manufacturer's protocol. Single-stranded complementary DNA was synthesized from equal amounts of RNA using Superscript III Reverse Transcriptase (Invitrogen), according to the manufacturer's protocol. *GAPC1* was used as a control for constitutive expression.

cDNA was quantified using iQ SYBR green Supermix (BioRad), according to the manufacturer's protocol, in an MJ Mini Opticon Personal Thermocycler (BioRad). Four technical replicates were prepared for each sample. Expression levels were analyzed using the method described by Pfaffl, 2001. Standard curves were used for each qPCR primer pair, and their efficiencies (*E* values) calculated: *CER2*, 2.45 (122%); *CER2-LIKE1*, 1.83 (91%); *CER2-LIKE2*, 2.01 (101%); *GAPC*, 2.46 (123%). Primers used for RT- and qPCR are listed in Table 2-3.

Table 2-3: Primers used for RT-PCR & qRT-PCR

Primer Name	Sequence (5'-3')
CER2 qPCR F	GTCTACGATCACGTTCTTGGTCCTG
CER2 qPCR R	CCCGATACCAGCTGTCCAAGTG
CER2-LIKE1 RT/q-PCR F	CATCCTATTGGACCGGAATTGACG
CER2-LIKE1 qPCR R	CTTTTCTCCGGTAATGGCCTTAGC
CER2-LIKE1 RT-PCR R	CCGACTCCGGCGACTTCCCC
CER2-LIKE2 RT F	GAGGGAAGCGGTCCTGTTC
CER2-LIKE2 RT R	CTCCTCCACAACCCCCGG
CER2-LIKE2 qPCR F	ACCAGTTGGACCAGATTTGGCA
CER2-LIKE2 qPCR R	CCCACCAGCAAAGGCTTGAGC
GAPC1 RT/q-PCR F	TCAGACTCGAGAAAGCTGCTA
GAPC1 RT/q-PCR R	GATCAAGTCGACCACACGG

2.3 Constructs, transformation, and selection

2.3.1 Stable expression in Arabidopsis

2.3.1.1 *pGWB4-CER2pro::CER2-GFP* and *pGWB6-35Spro::CER2-GFP*

The genomic sequence of *CER2* was amplified beginning from the start codon and extending up until but not including the stop codon for the *pGWB6-35Spro::CER2-GFP* construct, and beginning from the end of the 3' untranslated region of the gene directly upstream of *CER2* and extending up until but not including the stop codon of *CER2* for the *pGWB4-CER2pro::CER2-GFP* construct. Primers used for both constructs are listed in Table 2-4. Both sequences were amplified from Col-0 leaf genomic DNA with Phusion polymerase (NEB), using primers with Gateway attB adaptor sequences. The purified PCR products were transferred into the Donor vector pDONR221 using BP Clonase (Invitrogen), according to the manufacturer's protocol. Positive clones were identified by colony PCR, restriction digestion, and sequencing. The inserts were transferred into pGWB4 and pGWB6 vectors (T. Nakagawa et al., 2007), which have C-terminal GFP tags, using LR Clonase (Invitrogen) according to the manufacturer's protocol. Positive clones were again identified by colony PCR, restriction digestion, and sequencing. Purified constructs were transformed into chemically competent *Agrobacterium tumefaciens* GV3101 cells carrying the pMP90 Ti plasmid, and verified by colony PCR and restriction digestion. Fifty-milliliter cultures of transgenic *A. tumefaciens* in log phase growth were centrifuged, washed, and resuspended in 5% sucrose solution. Four-week-old Col-0 and *cer2-5* plants were sprayed with the *A. tumefaciens* suspensions, and were covered overnight, while the *A. tumefaciens* cells remained infectious. After plant senescence, T1 seeds were collected and screened for hygromycin resistance conferred by the T-DNA, and complementation of the *cer2-5* mutant wax deficiency.

2.3.1.2 *pGWB4-CER2-LIKE1pro::CER2-LIKE1-GFP* and *pGWB4-CER6pro::CER2-LIKE1-GFP*

The *CER2-LIKE1* coding region from the start codon to one codon directly upstream of the stop codon and from 2.6 kb upstream of the *CER2-LIKE1* protein-coding sequence to the codon directly upstream of the *CER2-LIKE1* stop codon were amplified from Col-0 genomic DNA. The *CER6* promoter, consisting of the 1.2-kb fragment upstream of the *CER6* coding sequence, was excised from a *pBI101-CER6pro-GUS* construct (a kind gift from Dr. Patricia Lam, University of British Columbia). The *CER2-LIKE1* genomic sequence with the CER6 promoter and the full-length *CER2-LIKE1* genomic sequence with its native promoter were both cloned by restriction enzyme digestion and ligation into pBluescriptII SK+ (Stratagene).

CER6pro::CER2-LIKE1 and *CER2-LIKE1pro::CER2-LIKE1* were amplified from the Bluescript plasmids using primers with GATEWAY attB adaptor sequences for insertion in pDONR207, and the constructs were confirmed by colony PCR, restriction digests, and sequencing. Primer sequences are listed in Table 2-4. The *CER6pro::CER2-LIKE1* and *CER2-LIKE1pro::CER2-LIKE1* insertions were then transferred to the pGWB4 binary vector using LR Clonase (Invitrogen) with C-terminal GFP tags (T. Nakagawa et al., 2007), for stable expression in Arabidopsis. Purified constructs were transformed into chemically competent *A. tumefaciens* GV3101 cells carrying the pMP90 Ti plasmid, and verified by colony PCR and restriction digestion. Arabidopsis plants were transformed by the floral spray method; the *CER2-LIKE1pro::CER2-LIKE1-GFP* construct was transformed to wild-type Col-0 and *cer2-like1-1* plants, and the *CER6pro::CER2-LIKE1-GFP* construct was transformed to wild-type Col-0 and *cer2-5* plants. Transformed lines were selected by growing the seedlings on hygromycin, and genotypes were confirmed by PCR in lines selected for phenotype analysis.

Table 2-4: Constructs and primers used for stable expression in Arabidopsis

Construct(s)	Primer Name	Sequence (5'-3')
CER2pro::CER2-GFP & 35Spro::CER2-GFP	attB1 - CER2 coding F	GGGGACAAGTTTGTACAAAAAAGCAGGCTTT ATGGAGGGAAGCCCAGTGAC
	attB1 - CER2 promoter F	GGGGACAAGTTTGTACAAAAAAGCAGGCTTT TCAGGACAACTGGCCTAGTG
	attB2 - CER2 coding, no stop R	GGGGACCACTTTGTACAAGAAAGCTGGGTG TATAATCATATTAGTCACCTCCTCC
CER6p::CER2-LIKE1-GFP & CER2-LIKE1p::CER2-LIKE1-GFP	CER6 promoter F	TTAAGTCGACCTTCGATATCGGTTGTTG
	CER6 promoter R	TTAAAAGCTTCGTCGGAGAGTTTTAATG
	CER2-LIKE1 promoter F	AAAATTTTGAATTCACTAGTTTCCGTGTCAAG CCCGATAACTAATCTGGAGG
	CER2-LIKE1 promoter R	AAAATTTTAAGCTTTGGCGCGATCAAACCAA ACTTCTTAAATTCCAATTTTACC
	CER2-LIKE1 coding F	AAAATTTTAAGCTTATGGGTCGATCTCAAGAA CAGGGACAGGGACAGGGTC
	CER2-LIKE1 coding, no stop R	AAAATTTTCTGCAGTGGCGCGATCAAACCAA ACTTCTTAAATTCCAATTTTACC
	attB1 - CER6 promoter F	GGGGACAAGTTTGTACAAAAAAGCAGGCTTT CTTCGATATCGGTTGTTGACG
	attB1 - CER2-LIKE1 promoter F	GGGGACAAGTTTGTACAAAAAAGCAGGCTTT ACTAGTTTCCGTGTCAAGCC
	attB2 - CER2-LIKE1 coding, no stop R	GGGGACCACTTTGTACAAGAAAGCTGGGTG TGGCGCGATCAAACCAAAC

2.3.2 Constitutive and inducible expression in *S. cerevisiae*

cDNA was prepared as described in Section 2.2.2 from Col-0 stem tissue. *CER6* and *CER2* coding DNA sequences were amplified using primers listed in Table 2-5. *CER6* was cloned into the pESC-URA yeast expression vector (Agilent) downstream of the *GAL10* inducible promoter, and *CER2* was cloned into the p423 yeast expression vector with the *HIS3* selection marker, downstream of the strong constitutive *GPD* (glyceraldehyde-3-P-dehydrogenase) promoter (Mumberg et al., 1995). Correct plasmid construction was confirmed by colony PCR, restriction digestion, and sequencing. The yeast strain W3031A was transformed using the protocol described by Gietz and Woods (2002). Transgenic yeast cells were grown on synthetic complete (SC) selection medium (Sherman, 2002) lacking appropriate amino acids. Successful transformation was confirmed by colony PCR. Three to four individual cell lines were selected from each transgenic strain for induction of transgene expression and lipid analysis. Cultures were grown in 5 mL SC medium with 2% glucose overnight, then plated on solid SC medium with 2% galactose and incubated for 2 to 4 d (strains harboring plasmids grew slower than the wild type). A similar method was used for construction and transformation of *CER2-LIKE* expression plasmids. However, when none of the transgenes required galactose to induce expression, the cells were streaked out and grown directly on solid SC medium with 2% glucose and the required amino acids.

To make *CER2* and *CER6* constructs with N-terminal epitope tags, the coding sequences of each gene were amplified with an AvrII restriction site added 3' to the ATG start site. The coding sequence insertions were ligated into p423 (*CER2*) and p426 (*CER6*) vectors. Triple hemagglutinin (HA) and MYC tags were excised from pRS316-HA_3 and pRS316-MYC_3 plasmids using SpeI (a gift from Dr. Frederic Beaudoin, Rothamsted Research, UK). The *p423-AvrII-CER2* and *p426-AvrII-CER6* constructs were cut with AvrII, to allow for the insertion of the SpeI-cut HA and MYC tags. However, a second AvrII site was found in the p423 vector backbone; this site was not present in the p423 sequence downloaded from the ATCC database, but an AvrII site is found in the *HIS3* gene used as a selection marker in the p423 vector. Hence, the AvrII-CER2 cassette was transferred into p426, cut with AvrII, the HA_3 sequence was inserted, and then the HA_3-CER2 sequence was cut and inserted back into p423. Correct plasmid construction was confirmed by colony PCR, restriction digestion, and sequencing.

Over the course of my work with yeast, I found that expression was more consistent and fatty acid profiles were more reproducible when I expressed *CER6* with a constitutive promoter such as *GPD*, instead of the galactose-inducible promoter *GAL10*. Therefore, the p426-AvrII-

CER6 construct (without the MYC_3 tag inserted) was used for all yeast expression experiments described in Chapters 4 and 5. Further, the consistency provided by a Kozak consensus sequence with four adenine bases upstream of the ATG translation start site became clear after some experience with yeast expression. Therefore, the *CER2-LIKE1* and *CER2-LIKE2* yeast expression constructs described in Table 2-7 were used for the yeast expression experiments presented in Chapter 4 of thesis.

Table 2-5: Constructs and primers used for constitutive and inducible expression in yeast

Construct	Primer Name	Sequence (5'-3')
pESC-URA-CER6	CER6-NotI F	AATTGCGGCCGCATGCCTCAGGCACCGATG
	CER6-SpeI R	AATTACTAGTTTAGAGTTTGACAACTTCGGG
p423-CER2	CER2-EcoRI F	AATTGAATTCATGGAGGGAAGCCCAGTGACC
	CER2-SalI R	AATTGTCGACTTATATAATCATATTAGTCACCTCCTC
p424-CER2-LIKE1	CER2-LIKE1-EcoRI F	AATTGAATTCATGGGTCGATCTCAAGAACAGGG
	CER2-LIKE1-SalI R	AATTGTCGACTCATGGCGCGATCAAACC
p425-CER2-LIKE2	CER2-LIKE2-SpeI F	AATTACTAGTATGGGTCTAGTTCAAGAAGAGGG
	CER2-LIKE2-SalI R	AATTGTCGACTTAAACTAACGGCGTGATCAAACC
p423-CER2-LIKE3	CER2-LIKE3-SpeI F	AATTACTAGTAAAAATGTTTGCTAAAGAGAAGAC
	CER2-LIKE3-SalI R	AATTGTCGACTTATAATTGCTTTGTATCTTCC
p425-CER2-LIKE4	CER2-LIKE4-BamHI F	AATTGGATCCAAAAATGGAAACCAAAATCCCTAAGTC
	CER2-LIKE4-SalI R	AATTGTCGACTTACTCTTTTGGCAGTGCAAC
p426-AvrII-CER6	CER6-BamHI F	AATTGGATCCATGCCTAGGCCTCAGGCACCGATGCCAG
	CER6-ClaI R	AATTATCGATTTAGAGTTTGACAACTTCGGGAATAAAG
p423-AvrII-CER2	CER2-EcoRI F	AATTGAATTCATGCCTAGGGAGGGAAGC
	CER2-SalI R	AATTGTCGACTTATATAATCATATTAGTCACCTCCTCC

2.4 Site-directed mutagenesis

Site-directed mutagenesis was carried out by overlap extension mutagenesis as described by Ho et al., 1989.

Different approaches were used for the two site-directed mutagenesis experiments described in Chapter 5. To mutagenize the putative H166 catalytic residue of *CER2* that was annotated based on sequence alignment with BAHD acyltransferases, the genomic CER2 sequence was modified, generating H166A and H166N artificial alleles (Section 5.2.1). The *pGWB4-CER2pro::CER2:GFP* construct was used as a template. 5' and 3' fragments of *CER2* sequence were amplified using the primers specified in Table 2-6, washed on a DNA binding column, and then equal concentrations of each fragment were used for overlap-extension PCR. 5' and 3' end primers were added to the overlap extension PCR reaction, as this was found to increase yield of the final full-length PCR product. The entire, unmodified *CER2* sequence was also amplified from the *pGWB4-CER2pro::CER2-GFP* construct. The constructs were assembled in the pGWB4 gateway vector, introduced into *A. tumefaciens*, and transformed to *cer2-5* mutant Arabidopsis using the method described in Section 2.3.1. The background genotype and the presence of the transgene of all transformed plants selected for analysis were confirmed by PCR amplification. The site-directed mutation of the transgene was sequenced for one representative plant from each transformed line. Complementation of the *cer2-5* phenotype was assessed by the physical appearance of the plant stems, total stem wax load, and stem wax composition (section 2.8.1).

To mutagenize a second putative catalytic site identified based on the structural models of CER2-LIKE proteins (Section 5.2.6), the *CER2* coding sequence was modified, generating an H38A artificial allele. The *p423-CER2* construct was used as a template. To mutagenize *CER2-LIKE4* to mimic *CER2*, the *p425-CER2-LIKE4* construct was used as a template, and the GIFRRTV sequence of CER2-LIKE4 was replaced with LHYV from CER2. Overlap extension mutagenesis was carried out as described above, and detailed in Ho et al., 1989. The modified constructs were transformed to yeast, with wild-type *CER2* and *CER2-LIKE4* cDNA sequences as controls. Function of the mutagenized allele was assessed by FAMEs analysis of the transgenic yeast cell lines (section 2.8.2).

Table 2-6: Constructs and primers used for site-directed mutagenesis

Construct(s)	Primer Name	Sequence (5'-3')
CER2pro::CER2 WT/H166A/H166N SDM	CER2 genomic F	GGGGACAAGTTTGTACAAAAAAGCAGGCTTTTCAGGACAACTGGCCTAGTG
	CER2 genomic R	GGGGACCACTTTGTACAAGAAAGCTGGGTGTTATATAATCATATTAGTCACCTCCTCC
	CER2 H166A mutation, 5' fragment R	CACGTCTCCAAGAATGGCGGCCCAACTCAA
	CER2 H166A mutation, 3' fragment F	TTGAGTTGGGCCGCCATTCTTGGAGACGTG
	CER2 H166N mutation, 5' fragment R	TTGAGTTGGGCCAATATTCTTGGAGACGTG
	CER2 H166N mutation, 3' fragment F	TTGAGTTGGGCCAATATTCTTGGAGACGTG
p423-CER2 H38A SDM	CER2 cDNA F	AATTGAATTCAAAAATGGAGGGAAGCCCAGTGACC
	CER2 cDNA R	AATTGTCGACTTATATAATCATATTAGTCACCTCCTCCTTGAG
	CER2 H38A mutation, 5' fragment R	GCTCGGACGTAGGCGAGCTTCATGG
	CER2 H38A mutation, 3' fragment F	CCATGAAGCTCGCCTACGTCCGAGC
p425-CER2-LIKE4 SDM	CER2-LIKE4 cDNA F	AATTGGATCCAAAAATGGAAACCAAAATCCCTAAGTC
	CER2-LIKE4 cDNA R	AATTGTCGACTTACTCTTTTGGCAGTGCAAC
	CER2-LIKE4 GIFRRTV>LHYV mutation, 5' fragment R	CGTAACTATGTTGACGTAGTGGAGTACTCCGACGGGATCTAC
	CER2-LIKE4 GIFRRTV>LHYV mutation, 3' fragment F	GGAGTACTCCACTACGTCAACATAGTTACGTATTACAAAGAAGC

2.5 Sequence swaps

CER2-LIKE1 and *CER2-LIKE2* coding DNA sequence fragments were amplified from p424/p425 yeast expression plasmids described in section 2.3.2, using primers described in Table 2.7. Regions of homology were selected as swap sites. 5' and 3' fragments amplified in an initial PCR reaction were combined in a second PCR reaction to generate full-length, chimeric products by overlap extension. The chimeras were ligated into the p423 vector, confirmed and co-expressed in yeast with the *CER6* gene as described in section 2.3.2.

Table 2-7: Constructs and primers used for sequence swaps in yeast

Construct (s)	Primer Name	Sequence (5'-3')
p423-CER2-LIKE1	CER2-LIKE1 SpeI F	AATTACTAGTAAAAATGGGTCGATCTCAAG
	CER2-LIKE1 SalI R	AATTGTCGACTCATGGCGCGATCAAAC
p423-CER2-LIKE2	CER2-LIKE2 SpeI F	AATTACTAGTAAAAATGGGTCTAGTTCAAG
	CER2-LIKE2 SalI R	AATTGTCGACTTAAACTAACGGCGTG
p423-chimera A	CER2-LIKE1 SpeI F	AATTACTAGTAAAAATGGGTCGATCTCAAG
	swap 1 R	GCCCATAAGTTGAAG
	swap 1 F	CTTCAACTTATGGGC
	CER2-LIKE2 SalI R	AATTGTCGACTTAAACTAACGGCGTG
p423-chimera B	CER2-LIKE2 SpeI F	AATTACTAGTAAAAATGGGTCTAGTTCAAG
	swap 1 R	GCCCATAAGTTGAAG
	swap 1 F	CTTCAACTTATGGGC
	CER2-LIKE1 SalI R	AATTGTCGACTCATGGCGCGATCAAAC
p423-chimera C	CER2-LIKE1 SpeI F	AATTACTAGTAAAAATGGGTCGATCTCAAG
	swap 2 R	TAAACCGGGTCATCTGAA
	swap 2 F	TTCAGATGACCCGGTTTA
	CER2-LIKE2 SalI R	AATTGTCGACTTAAACTAACGGCGTG
p423-chimera D	CER2-LIKE2 SpeI F	AATTACTAGTAAAAATGGGTCTAGTTCAAG
	swap 2 R	TAAACCGGGTCATCTGAA
	swap 2 F	TTCAGATGACCCGGTTTA
	CER2-LIKE1 SalI R	AATTGTCGACTCATGGCGCGATCAAAC
p423-chimera E	CER2-LIKE1 SpeI F	AATTACTAGTAAAAATGGGTCGATCTCAAG
	swap 3 R	CATTTCCATATGATTCC
	swap 3 F	GGAATCATATGGAAATG
	CER2-LIKE2 SalI R	AATTGTCGACTTAAACTAACGGCGTG

Construct (s)	Primer Name	Sequence (5'-3')
p423-chimera F	CER2-LIKE2 SpeI F	AATTACTAGTAAAAATGGGTCTAGTTCAAG
	swap 3 R	CATTTCCATATGATTCC
	swap 3 F	GGAATCATATGGAAATG
	CER2-LIKE1 SalI R	AATTGTCGACTCATGGCGCGATCAAAC
p423-chimera G	CER2-LIKE1 SpeI F	AATTACTAGTAAAAATGGGTCGATCTCAAG
	swap 4 R	TCCACGAAACGTGTGCC
	swap 4 F	GGCACACGTTTCGTGGA
	CER2-LIKE2 SalI R	AATTGTCGACTTAAACTAACGGCGTG
p423-chimera H	CER2-LIKE2 SpeI F	AATTACTAGTAAAAATGGGTCTAGTTCAAG
	swap 4 R	TCCACGAAACGTGTGCC
	swap 4 F	GGCACACGTTTCGTGGA
	CER2-LIKE1 SalI R	AATTGTCGACTCATGGCGCGATCAAAC
p423-chimera I	CER2-LIKE1 SpeI F	AATTACTAGTAAAAATGGGTCGATCTCAAG
	swap 5 R	GGTAGTGGAGCTTCATGGC
	swap 5 F	GCCATGAAGCTCCACTACC
	CER2-LIKE2 SalI R	AATTGTCGACTTAAACTAACGGCGTG
p423-chimera J	CER2-LIKE2 SpeI F	AATTACTAGTAAAAATGGGTCTAGTTCAAG
	swap 5 R	GGTAGTGGAGCTTCATGGC
	swap 5 F	GCCATGAAGCTCCACTACC
	CER2-LIKE1 SalI R	AATTGTCGACTCATGGCGCGATCAAAC
p423-CER2-LIKE2 truncated	CER2-LIKE2 SpeI F	AATTACTAGTAAAAATGGGTCTAGTTCAAG
	swap 4 R truncation	AATTGTCGACTCACTCCACGAAACGTGTGCC
p423-ASFT	ASFT SpeI F	AATTACTAGTAAAAATGGTTGCTGAGAACAATAAAAAC
	ASFT SalI R	AATTGTCGACTTATATCTGTAAAAACTGTTCTTG
p423-chimera K	CER2-LIKE2 SpeI F	AATTACTAGTAAAAATGGGTCTAGTTCAAG
	swap 4 R	TCCACGAAACGTGTGCC
	swap 4 F ASFT	GGCACACGTTTCGTGGAAGCAGAAGCAAACTG
	ASFT SalI R	AATTGTCGACTTATATCTGTAAAAACTGTTCTTG
p423-CER2-LIKE3	CER2-LIKE3 SpeI F	AATTACTAGTAAAAATGTTTGCTAAAGAGAAGAC
	CER2-LIKE3 SalI R	AATTGTCGACTTATAATTGCTTTGTATCTTCC
p423-chimera L	CER2-LIKE2 SpeI F	AATTACTAGTAAAAATGGGTCTAGTTCAAG
	swap 4 R	TCCACGAAACGTGTGCC
	swap 4 F CER2-LIKE3	GGCACACGTTTCGTGGAGGCCAGAGCAACC
	CER2-LIKE3 SalI R	AATTGTCGACTTATAATTGCTTTGTATCTTCC

2.6 CRISPR/Cas9-mediated mutagenesis

2.6.1 Construct design and assembly

19 and 20 bp target sequences for mutagenesis (protospacers) were selected in the *CER2-LIKE4* gene based on four criteria: (1) they are strictly unique to *CER2-LIKE4*, (2) they have an NGG protospacer adjacent motif (PAM) at the 3' end of the sequence, (3) they are in a position likely to cause a null mutation, and (4) they contain a restriction site within 10 bp of the PAM.

The target selected for mutagenizing the *CER2-LIKE4* gene was TATCCGTCGTAGATCCCGT(CGG) which contains a BstYI digestion site (RGATCY) near the PAM.

Target sites were synthesized as forward and reverse oligonucleotides (Table 2-8) flanked by adaptors to allow for ligation into a BpiI-digested CRISPR array. Complementary oligonucleotides were phosphorylated in the following reaction:

1 µL oligo 1 (100µM)

1 µL oligo 2 (100µM)

1 µL 10X T4 Ligation Buffer (NEB)

6.5 µL ddH2O

0.5 µL T4 Phosphonucleotide Kinase (PNK) (NEB)

The mixture was incubated at 37°C for 30 min, heated to 65°C for 20 min to inactivate the kinase, and then cooled at room temperature to allow the complementary oligonucleotides to form duplexes.

The pGreen-CRISPR vector was digested with BpiI (isoschizomers: BbsI/BpuAI/BstV2I) restriction enzyme (Thermo), and the digested vector was purified on a DNA-binding column, and quantitated on a nanodrop spectrophotometer. Roughly 50 ng of cut vector was used for ligation, with 1 µL of the oligonucleotide duplex diluted 1 in 200:

1 µL (≈50 ng) digested pGreen-CRISPR

1 µL 1:200 dilution phosphorylated primer dimer

2 µL 10X T4 ligase buffer (NEB)

1 µL T4 ligase (NEB)

15 µL distilled H_2O

The ligation was incubated at RT overnight. 5-10 µL of the ligation mixture was transformed to chemically competent DH5α cells. Construct sequences were verified, then transformed to *A. tumefaciens* and into Arabidopsis following the protocol described in section

2.3.1, except that the pGreen-based plasmid used here was co-transformed with the pSoup helper plasmid required for replication of pGreen.

Table 2-8: Constructs and primers used for CRISPR/Cas9 mutagenesis of *CER2-LIKE4*

Construct	Primer Name	Sequence (5'-3')
pGreen-CRISPR-CER2-LIKE4	CRISPR-CER2-LIKE4 F	GATTGTATCCGTCGTAGATCCCGT
	CRISPR-CER2-LIKE4 R	AAACACGGGATCTACGACGGATAC

2.6.2 Identification of CRISPR mutants

T_1, T_2, and T_3 generations were germinated on hygromycin selection medium for the CRISPR/Cas9 T-DNA. The BstYI restriction site within the *CER2-LIKE4* target sequence was used to identify individuals that were mutagenized by the Cas9 nuclease. DNA from all generations was collected on Whatman FTA cards, and a 408 bp sequence surrounding the restriction site was amplified using primers listed in Table 2.2. 1 µL of amplification product from each reaction was digested in a 10 µL reaction volume with BstYI for a minimum of 2 hr. Product that was not cleaved by BstYI was indicative of a putative *cer2-like4* mutant. The *CER2-LIKE4* gene was sequenced from candidate mutants to identify loss-of-function alleles. Additional FTA presses were taken from each putative mutant for a second CAPS and sequencing screen to eliminate obvious chimeras. Homozygous mutations were identified in the T_3 and T_4 generations.

2.7 Microscopy

2.7.1 Confocal Imaging

Subcellular localization of GFP-tagged CER2 and CER2-LIKE1 was carried out on a Perkin-Elmer UltraView VoX Spinning Disk Confocal Microscope, using a 633 glycerol immersion objective. Stem tissue was dyed with hexyl rhodamine B to counterstain the ER. GFP was excited with a 488-nm laser, and hexyl rhodamine B was excited with a 561-nm laser. Cell-specific expression patterns were observed on a Nikon Eclipse 80i Scanning Laser Confocal Microscope using a 203 objective. GFP was excited with a 488-nm laser, and chlorophyll autofluorescence was detected for contrast.

2.7.2 SEM

2.7.2.1 Comparison of *cer2-5* and wild-type stems

Segments from the apical 1 cm of stem were mounted onto SEM stubs, air dried, and sputter coated with gold particles for 10 min at 40 mA in a SEMPrep2 sputter coater (Nanotech). The coated samples were viewed with a Hitachi S4700 field emission SEM using an accelerating voltage of 5 kV and a working distance of 12 mm.

2.7.2.2 Analysis of stems ectopically expressing *CER2-LIKE1*

One centimeter long stem segments approximately 10 cm from the shoot apex were cut, mounted, air dried, and sputter coated with gold particles to a thickness of 10 nm using a Leica EM ACE200 Low Vacuum Coater. Coated samples were viewed with a Hitachi S4700 field emission SEM using an accelerating voltage of 5 kV and a working distance of 12 mm.

2.8 Lipid analyses

2.8.1 GC-FID analysis of wax load and composition

Wax analysis was carried out using the top 10 cm of 3- to 5-week-old primary stems, or 3- to 4-week-old entire rosette leaves. Tissues were photographed to determine sample surface area. Surface area was established by measuring two-dimensional area in Adobe Photoshop, and for stems, by multiplying the flat area by π. Tissues were submerged for 30 s in approximately 8 mL of chloroform containing 10 µg tetracosane as an internal standard. Chloroform was blown off under nitrogen gas, and the waxes silylated by heating in 10 µL pyridine and 10 µL N,O-bis(trimethylsilyl)trifluoroacetamide with 1% trimethylchlorosilane at 80°C for 1 h. Solvent was again blown off under nitrogen gas and the waxes resuspended in 50 µL of chloroform for GC-FID analysis. Waxes were analyzed on an Agilent 7890A gas chromatography system with an HP1 methyl siloxane column, using the method described by Haslam and Kunst, 2013. Leaf wax samples were analyzed using splitless mode, and stem wax samples using a 2.7:1 split. The program ran at 50°C for 2 min, increased temperature by 40°C/min to 200°C and held for 1 min, increased by 3°C/min to 320°C and held for 15 min. The injector was set to 300°C, and the FID was set to 300°C. H_2 was used as a carrier gas with a flow rate of 2 mL/min. Peaks were identified based on comparison of retention times with standards. The analysis was repeated with four biological replicates.

2.8.2 GC-FID analysis of yeast FAMEs

Cells were scraped from plates and resuspended in 2 mL of 1 N methanolic hydrochloric acid and heated at 80°C for 2 hr to transmethylate fatty acids. The fatty acid methyl esters (FAMEs) were then extracted in 2 mL of hexane using 1 mL of 0.9% aqueous sodium chloride to improve phase separation. The hexane phase was dried under a nitrogen stream and resuspended in 50 µL hexane. FAMEs were separated using an Agilent 6890 Plus System with a DB-23 capillary column, using the method described by Kunst et al. (1992). The injection was made with a 10:1 split. The program ran at 180°C for 1 min, increased by 4°C/min to 240°C and held for 7 min. The injector was set to 280°C, and the FID was set to 300°C. H_2 was used as a carrier gas with a flow rate of 0.7 mL/min. Peaks were identified based on comparison of retention times with standards. The analysis was repeated with four biological replicates.

2.8.3 LC/MS analysis of acyl-CoAs

Acyl-CoA extraction roughly followed the protocol described by Larson and Graham (2001). Plant tissue or yeast cell pellets were ground in liquid nitrogen and extraction buffer (1 mL isopropanol / 1 mL 50 mM KH_2PO_4 pH 7.2 /25 µL glacial acetic acid / 40 µL 50 mg/mL BSA). Samples were delipidated by washing three times with saturated petroleum ether, and proteins were salted out by addition of saturated $(NH_4)_2SO_4$. Samples were dried and suspended in 90% H_2O, 10% acetonitrile, 15 mM ammonium hydroxide. Acyl-CoAs were detected and quantitated using electrospray ionization-tandem mass spectrometry (MS/MS) MS/MS + multiple reaction monitoring (MRM) or liquid chromatography (LC)-MS/MS + MRM in positive ion mode. The LC-MS/MS + MRM analysis (using an ABSciex 4000 QTRAP) was performed as described by Haynes et al. (2008) using an Agilent 1200 LC system with a Gemini C18 column (Phenomenex), 2 mm i.d., 150 mm length, 5 mm particle size. For the purpose of identification and calibration, standard acyl-CoA esters with acyl chain lengths from 14 to 20 carbons were purchased from Sigma as free acids or lithium salts.

2.9 Split-luciferase assay for protein-protein interactions

N. benthamiana plants were grown as described in section 2.1.2 and *A. tumefaciens* cultures were prepared and infiltrated as described in section 2.3.3. Genes of interest were fused to firefly luciferase gene fragments in the pCAMBIA-based luciferase vector system developed by Chen et al. (2008). The activity assay followed the floated-leaf luciferase complementation imaging (FLuCI) protocol described by Gehl et al. (2011). *CER2*, *CER6*, *KCR1*, *PAS2*, *CER10*, *3-HYDROXY-3-METHYLGLUTARYL COA REDUCTASE 1* (*HMR1*), and *CALCIUM ATPASE 2* (*ACA2*) coding sequences were amplified from Arabidopsis cDNA prepared as described in section 2.2.2, using primers described in Table 2-9. All genes of interest were inserted in both the pCAMBIA-NLuc vector, with the N-terminal fragment of luciferase tagged to the C-terminus of the gene of interest, and the pCAMBIA-CLuc vector, placing the C-terminal fragment of luciferase at the N-terminus of the gene of interest. The construct that produced the greatest luminescence when co-expressed with a *CER2* construct was interpreted as the best representation of interaction. Interaction with CER6 was only tested with an N-terminal fusion to the C-terminal half of luciferase, as previous work from our lab has shown that N-terminal fusions to condensing enzymes are more stable (Dr. Hugo Zheng and Dr. Ljerka Kunst, unpublished data). Positive clones were identified by colony PCR, restriction digestion, and sequencing.

Constructs prepared for infiltration of tobacco were transformed to electrocompetent *A. tumefaciens* by electroporation. *A. tumefaciens* cells were grown in 5 mL cultures overnight in LB medium with antibiotic selection. Cultures were then diluted 1/20 in an infiltration medium containing 10.5 g/L K_2HPO_4, 4.5 g/L KH_2PO_4, 1.0 g/L $(NH_4)_2SO_4$, 0.5 g/L NaCitrate-H_2O, 0.5% glycerol, 1 mM $MgSO_4$-H_2O, 0.2% glucose, 50 µM acetosyringone, and 10 mM MES, and again grown overnight. Cells were then centrifuged and resuspended in a solution of 4.43 g/L MS, 10 mM MES, and 150 µM acetosyringone to OD_{600} 0.6. Pairs of constructs, either CER2-NLuc or CLuc-CER2, with every other elongase gene fused with the opposite fragment of luciferase, were mixed to make up 2 mL of culture and co-infiltrated to *N. benthamiana* leaves. The contours of the infiltrated tissue were marked with a permanent marker.

After 2-4 days, infiltrated tissues were excised using a paper hole punch. The leaf discs were set, with the abaxial surface facing downwards, on top of 50 µL of the following solution containing the substrate of the firefly luciferase enzyme: 1 mM D-luciferin dissolved in DMSO, 10 mM $MgCl_2$, and 10 mM MES pH 5.6,. Luminescence was detected on a plate reader. Luminescence was captured from each leaf disc for 4 s, every 4 min, for 90 min. The time point with the highest luminescence reading from each disc was used for analysis.

Table 2-9: Constructs and primers for transient expression in tobacco

Construct (s)	Primer Name	Sequence (5'-3')
pCAMBIA-CER2-Nluc	CER2-SacI F	AATTGAGCTCATGGAGGGAAGCCCAGTG
	CER2-SalI R ns	AATTGTCGACTATAATCATATTAGTCACCTCCTCC
pCAMBIA-Cluc-CER2	CER2-KpnI F	AATTGGTACCATGGAGGGAAGCCCAGTG
	CER2-SalI R s	AATTGTCGACTTATATAATCATATTAGTCACCTCCTCC
pCAMBIA-Cluc-CER6	CER6-KpnI F	AATTGGTACCATGCCTCAGGCACCGATG
	CER6-BamHI R s (Cluc-)	AATTGGATCCTTAGAGTTTGACAACTTCGGG
pCAMBIA-KCR1-Nluc/ pCAMBIA-Cluc-KCR1	KCR1-KpnI F	AATTGGTACCATGGAGATCTGCACTTACTTC
	KCR1-SalI R ns (-Nluc)	AATTGTCGACTTCTTTCTTCATGGAGTCTTTTTG
	KCR1-SalI R s (Cluc-)	AATTGTCGACTCATTCTTTCTTCATGGAGTC
pCAMBIA-PAS2-Nluc/ pCAMBIA-Cluc-PAS2	PAS2-KpnI F	AATTGGTACCATGGCGGGCTTTCTCTCCG
	PAS2-SalI R ns (-Nluc)	AATTGTCGACTTCCCTCTTGGATTTGGAGAGAGC
	PAS2-SalI R s (Cluc-)	AATTGTCGACTTATTCCCTCTTGGATTTGGAGAGAGC
pCAMBIA-CER10-Nluc/ pCAMBIA-Cluc-CER10	CER10-KpnI F	AATTGGTACCATGAAGGTCACCGTCGTCTCC
	CER10-SalI R ns (-Nluc)	AATTGTCGACAAGGAATGGAGGAAGTATCACCC
	CER10-SalI R s (Cluc-)	AATTGTCGACCTAAAGGAATGGAGGAAGTATCACCC
pCAMBIA-HMR-Nluc/ pCAMBIA-Cluc-HMR	HMR-KpnI F	AATTGGTACCATGAAGAAAAAGCAAGCTGGTC
	HMR-SalI R ns (-Nluc)	AATTGTCGACTGTTGTTGTTGTTGTCGTTGTC
	HMR-SalI R s (Cluc-)	AATTGTCGACTCATGTTGTTGTTGTTGTCGTTG
pCAMBIA-ACA2-Nluc/ pCAMBIA-Cluc-ACA2	ACA2-KpnI F	AATTGGTACCATGGAGAGTTACCTAAACGAG
	ACA2-SalI R ns (-Nluc)	AATTGTCGACAACGGGAATCGTCTTCAG
	ACA2-SalI R s (Cluc-)	AATTGTCGACTCAAACGGGAATCGTCTTC

2.10 Co-immunoprecipitation

2.10.1 Microsome preparation and solubilization

Yeast cells carrying epitope-tagged CER6 and/or CER2 constructs were grown in 5 mL SD selection medium overnight, which was then used to inoculate 100 mL cultures grown for a further 24 hr to an OD_{600}≈1.0. Cells were centrifuged at 4,500 g at RT for 5 min, washed with water, and centrifuged again. The cell pellets were suspended in 5 mL microsome preparation buffer (below). 0.5 mm glass beads were added to roughly 1 cm below surface of buffer, and vortexed for 1 min, four times. Lysates were transferred to fresh tubes, and the glass beads were washed three times with 5 mL aliquots of buffer, and the lysate/washes for each genotype combined. The lysates were centrifuged at 8,000 g for 10 min at 4°C to remove cell wall debris and nuclei. Supernatants were transferred to polycarbonate tubes and centrifuged at 164,000 g for 1 hr at 4°C to pellet microsomes. Microsomes were resuspended in a mixture of 66% microsome preparation buffer and 33% glycerol, and the volume of each microsome sample

was adjusted to obtain a final protein concentration of 1.1 mg/mL (as determined by a Bradford assay). Microsomes were flash frozen in liquid nitrogen and stored at -80°C.

Microsomes were solubilized by incubating at RT with sucrose monolaurate (SML) at a final concentration of 0.1% (w/v), for 15-30 min. Samples were then centrifuged at 100,000 g for 1 hr at RT to pellet insoluble lipids and proteins. The supernatant from this spin was used for co-immunoprecipitations of the now solubilized, microsomal proteins. The pellet and an aliquot of the supernatant were retained for dot blot or western blot analysis.

2.10.1.1 Microsome preparation buffer

50 mM Tris pH 7.5

1 mM EGTA

1 mM β-mercaptoethanol

1 mM PMSF

1 tablet yeast protease inhibitor cocktail

2.10.2 Co-immunoprecipitation

100 µL of solubilized, microsomal protein was diluted with 900 µL of a 0.1% SML, 50 mM Tris pH 7.5 solution (Tris-SML). 2 µL of antibody against the epitope tag of one of the proteins of interest (here, anti-c-Myc, the tag fused to CER6) was added, and the mixture was incubated at 4°C on a tube rotator for 2-4 hr. 20 µL of protein A/G-agarose beads (Santa Cruz) (4 µL beads suspended in 16 µL buffer) were added to each immunoprecipitation, and incubated overnight on the tube rotator at 4°C. The following day, beads were centrifuged, and the supernatant kept for western blot analysis – this was labelled as the free/unbound fraction. The beads were washed 4x with Tris-SML, and retained as the bound fraction for western blot analysis.

2.10.3 Western blotting

10-20 µL of each protein fraction was loaded in 10% acrylamide gels with 1% SDS. Proteins were separated at a constant voltage of 200 V for 60 min, and transferred to nitrocellulose membrane in semi-dry blotting apparatus in Bjerrum Schafer-Nielsen buffer (recipe below), at a constant voltage of 15 V for 50 min. The membranes were blocked with 5% skim milk powder in Tris buffer saline with 0.1% tween (TBST) for either 30 min at RT, or at 4°C overnight.

Membranes were blotted with primary antibodies for 1 hr at RT. Both anti-c-Myc (mouse) and anti-HA (rat) antibodies were diluted 1:10,000 in TBST with 5% milk. The membranes were washed 3x with TBST, then incubated with secondary antibodies diluted 1:50,000 in TBST with 5% milk for 1hr at RT. The blots were finally washed 3x with TBST, and horseradish peroxidase activity was detected with the GE Healthcare ECL Prime western blotting detection kit.

2.10.3.1 Tris buffer saline

50 mM Tris
150 mM NaCl
pH 7.6

2.10.3.2 Bjerrum Schafer-Nielsen buffer

48 mM Tris
39 mM glycine
20% methanol
pH 9.2

2.11 Homology-based tertiary structure modelling of CER2-LIKEs

Deduced amino acid sequences for the five CER2-LIKE proteins were input into the Phyre2 server. Multiple structural homologs were found for all of the CER2-LIKEs, however, the hydroxycinnamoyltransferase from *Sorghum bicolor* (SbHCT) was the best candidate for all CER2-LIKEs as it had the highest sequence homology of all proteins with experimentally determined structures. Therefore, models of CER2-LIKEs generated using SbHCT were used for analysis. Graphics were generated, annotated, and analyzed with UCFS Chimera. Chimera was developed by the Resource for Biocomputing, Visualization, and Information at the University of California, San Francisco, supported by NIGMS P41-GM103311; Pettersen et al., 2004.

Chapter 3: ECERIFERUM2 is a component of the fatty acid elongation machinery required for extension to exceptional lengths

3.1 Introduction

Eceriferum2 was among the most severe wax-deficient mutants identified in a visual screen for glossy stem wax phenotypes in ethylmethane sulfonate (EMS)-induced and irradiated mutant populations of Arabidopsis (Koornneef et al., 1989). Several *cer2* mutants have been isolated in subsequent screens for wax deficiency; these are summarized in Table 3-1. Characterization of the *cer2-4* allele by McNevin et al. (1993) revealed that the *cer2* mutant specifically lacks stem cuticular waxes longer than 28 carbons, and accumulates more 26- and 28-carbon waxes than wild type. The authors suggested that the *CER2* gene could regulate the activity of the elongase complex, but as the *cer2* mutation was mapped to a gene with homology to BAHD acyltransferases (Xia et al., 1996), a mechanism by which this could occur was not obvious. Basic characterization of the CER2 protein was necessary to make predictions about its activity.

Given that the four characterized enzymes of the FAE complex are localized to the ER (Zheng et al., 2005; Bach et al., 2008; Joubès et al., 2008; Beaudoin et al., 2009), I predicted that the *CER2* gene product would localize to the ER as well. However, all characterized BAHDs are soluble, cytosolic proteins (D'Auria, 2006; Panikashvili et al., 2009; Rautengarten et al., 2012), with the exception of one of three splice variants of At1g65450, which contains a nuclear localization signal and is localized to the nucleus (Leshem et al., 2012). Localization and topology prediction algorithms reveal that CER2 has no transmembrane domains and no transit peptide (Aramemnon; Schwacke et al., 2003). In light of this information, one might anticipate that CER2 could localize to the cytosol. Inconsistent with both of these predictions, the CER2 protein was previously reported to localize to the nucleus, based on cell fractionation and immunoblotting experiments (Xia et al., 1997). Velasco et al. (2002) used the same technique to localize the CER2 homolog of *Zea mays*, GLOSSY2, but found the protein enriched in a cellular fraction containing ER and mitochondria, as well as in a soluble, cytosolic fraction. Hence, there was an obvious need to determine the true localization of CER2 *in planta*.

Previous work has established that FAE complexes carry out VLCFA elongation for wax biosynthesis. Mutant analysis in Arabidopsis has demonstrated that the condensing enzyme CER6 is required to elongate VLCFA precursors of cuticular waxes greater than 24 carbons in length (Millar et al., 1999). When expressed in yeast, CER6 elongates VLCFAs up to 28

carbons. However, waxes derived from 30- and 32-carbon VLCFAs are by far the most abundant constituents of Arabidopsis stem and leaf wax. No other known condensing enzymes from Arabidopsis efficiently elongate VLCFAs in yeast beyond 28 carbons. The capacity of yeast cells to support the production of VLCFAs longer than 28 carbons is not in question, as the production of 30-carbon VLCFAs in yeast by engineered yeast Elops was previously reported (Denic and Weissman, 2007).

To confirm previous work on the *cer2* mutant phenotype, a new T-DNA allele, *cer2-5*, was obtained. *CER2* expression patterns were examined using qPCR, and a *CER2-GFP* fusion driven by the native *CER2* promoter. CER2-GFP localization was determined using a similar construct driven by the *35S* promoter. Finally, because yeast has proven to be a powerful system for characterizing components of the plant fatty acid elongation machinery, CER2 was expressed in yeast cells to study its function.

Table 3-1: Summary of characterized *cer2* alleles of Arabidopsis

Line	Allele	Ecotype	Mutagen	Source
CS32	*cer2-1*	?	EMS	Maarten Koornneef (Koornneef *et al.*, 1989)
CS2014	*cer2-1*	WS-1 / Ler	EMS	Pablo Scolnik
CS2077	*cer2-1*	WS-1 / Ler	EMS	Pablo Scolnik
CS2122	*cer2-1*	WS-1 / Ler	EMS	Pablo Scolnik
CS2124	*cer2-1*	WS-1 / Ler	EMS	Pablo Scolnik
CS2207	*cer2-1*	WS-1 / Ler	EMS	Pablo Scolnik
CS8	*cer2-2*	Ler	EMS	Maarten Koornneef; further characterized in Xia *et al.,* 1996 and Xia *et al.,* 1997.
BRL5	*cer2-3*	WS	T-DNA	Bertrand Lemieux (McNevin *et al.*, 1993)
BRL9	*cer2-4*	WS	T-DNA	Bertrand Lemieux (McNevin *et al.*, 1993); further characterized by Negruk *et al.*, 1996, and Jenks *et al.*, 1995.
SALK_084443C	*cer2-5*	Col	T-DNA	Joseph Ecker. Characterized in the present work.

3.2 Results

3.2.1 The *cer2* mutant is deficient in waxes longer than 28 carbons

To further investigate *CER2* function, a T-DNA insertional mutant in Col-0 ecotype was obtained from the Arabidopsis Biological Resource Center (ABRC), SALK_084443 (Alonso et al., 2003), hereafter referred to as *cer2-5*. Homozygous mutants were identified by PCR-based genotyping, and direct sequencing of genomic DNA located a T-DNA insertion in the second exon of the *CER2* gene (Figure 3-1A). Stems of *cer2-5* individuals had a glossy appearance characteristic of *eceriferum* mutants with decreased wax load (Figure 3-1B). This phenotype was further examined using SEM; stems of wild-type Col-0 plants were densely coated with rod-shaped, tubular, and platelet-shaped wax crystals, whereas *cer2-5* stems appeared completely devoid of such structures (Figure 3-1C). Stem waxes were analyzed by GC-FID to determine how wax load and composition of the *cer2-5* mutant compare with that of the wild type and other previously described *cer2* alleles. The total stem wax load of *cer2-5* was approximately 30% that of wild type (Figure 3-1D). All wax components longer than 28 carbons were reduced to trace amounts in the mutant, and relative increases were observed for several wax components shorter than 28 carbons (Figure 3-1E). These results suggest a block in acyl chain elongation past 28 carbons in *cer2-5*. The load and composition of *cer2-5* mutant rosette leaf wax was also examined; no change compared with the wild type was detected (data not shown). These results agree with the published data for other *cer2* alleles.

Male sterility dependent on environmental humidity is a phenotype associated with pollen coat deficiencies, and has been observed in several Arabidopsis mutants with deficiencies in cuticular wax metabolism (Koornneef et al., 1989; Preuss et al., 1993) including one *cer2* allele (Preuss et al., 1993; Eisner et al., 1998). The most abundant acyl lipids in pollen coat are 29-carbon alkane and ketone, and 31-carbon alkene (Jessen et al., 2011), and so it is not surprising that the biosynthesis of cuticular waxes and pollen coat could require the same or similar enzymes. No reduction in the seed set of the *cer2-5* mutant was observed. This discrepancy may be due to subtle differences in growth conditions, or the different alleles selected for study. The subject of VLCFA elongation and pollen coat function is discussed further in Chapter 4.

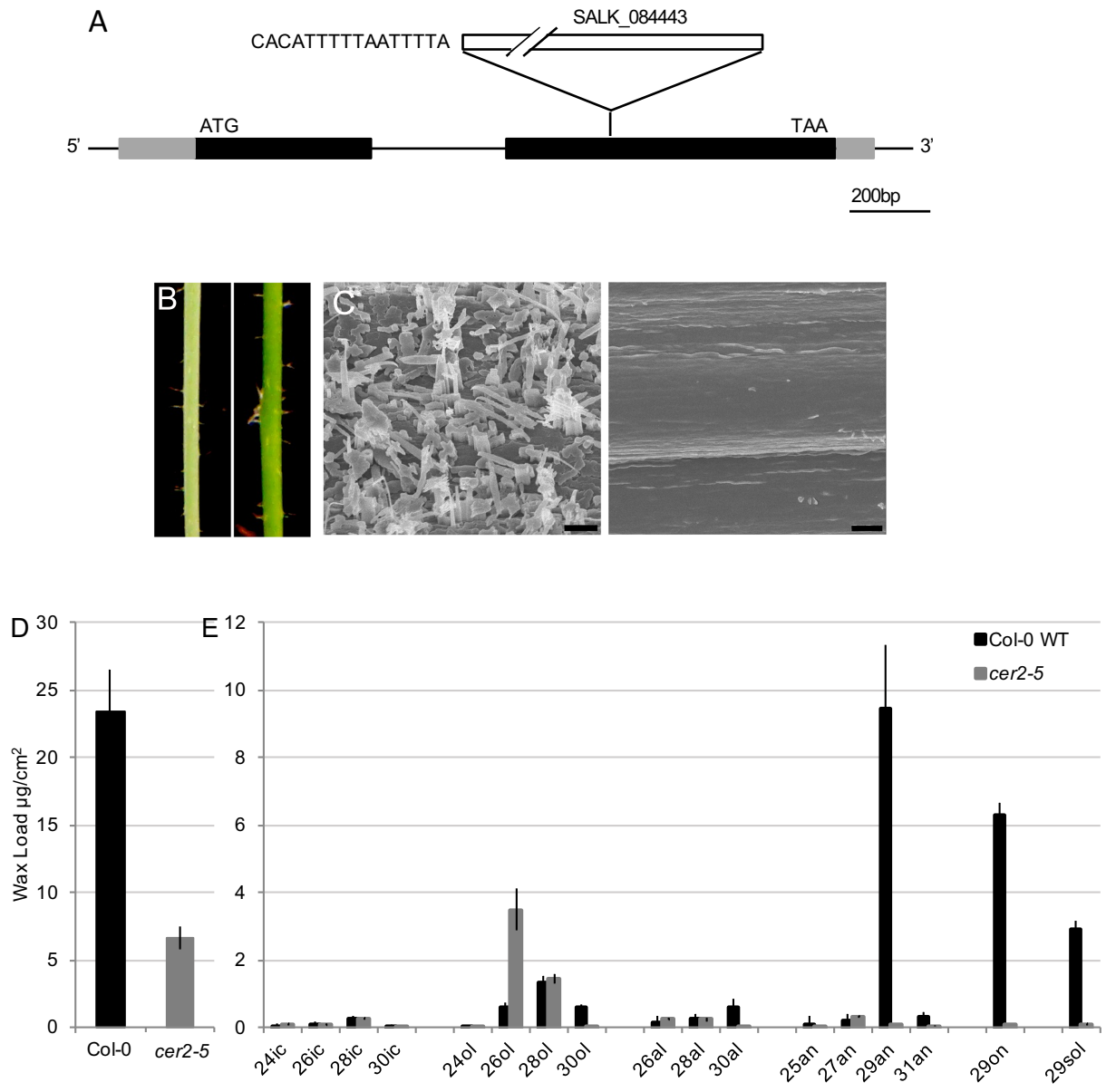

Figure 3-1: Characterization of the *cer2-5* mutant phenotype

A, T-DNA insertion site in the second exon of *CER2*. B, stems of wild-type Col-0 (left) and *cer2-5* (right) plants. C, SEM of wild-type Col-0 (left) and *cer2-5* (right) inflorescence stems. Scale bars = 20 µm. Wild-type Col-0 and *cer2-5* total stem wax loads are shown in D, and wax compositions in E. Both are measured as the average of four biological replicates, with error bars representing SD. Ic, free fatty acid; ol, primary alcohol; al, aldehyde; an, alkane; on, ketone; sol, secondary alcohol. Reproduced with permission from Haslam et al., 2012; Copyright American Society of Plant Biologists © 2012 (www.plantphysiology.org)

3.2.2 The *CER2* gene is expressed in epidermal cells of aerial organs

Organ-specific expression patterns of *CER2* were investigated by qPCR. *CER2* transcript was detected in all tissues except roots (Figure 3-2A), suggesting that CER2 may contribute to wax biosynthesis in organs other than stem. To determine tissue- and cell type-specific expression patterns of *CER2*, GFP fluorescence was examined in wild-type and *cer2-5* plants transformed with a *CER2-GFP* transgene driven by the native *CER2* promoter. This construct complemented the *cer2-5* wax-deficient phenotype (data not shown).

In stems, siliques, rosette leaves, and cauline leaves, GFP fluorescence was unique to epidermal cells (Figure 3-2B,D,E,F). This result supports the notion that CER2 function is specific to cuticular lipid synthesis, which occurs exclusively in the epidermis, and is similar to previous *CER2* expression patterns reported by Xia et al. (1996, 1997). GFP fluorescence was very strong in epidermal cells near the stem apex (Figure 3-2B) and there was a stark reduction in fluorescence at a distance of only 3 cm from the apex (Figure 3-2C). This observation corroborates previous findings that wax biosynthesis occurs predominantly at the shoot tip (Suh et al., 2005).

3.2.3 The CER2 protein is localized to the ER membrane

To determine the localization of the CER2 protein, the genomic *CER2* sequence was fused to GFP and expressed downstream of the *35S* promoter in *cer2-5* and wild-type plants. Multiple *cer2-5* transgenic individuals were recovered that displayed complementation of the *cer2-5* wax-deficient phenotype (i.e. they had glaucous stems, and restored wax load and composition as determined by GC-FID analysis). In both genetic backgrounds, GFP fluorescence strongly labelled a reticulate structure in young, wax-producing stem epidermal cells (Figure 3-3A). When plant stems were stained with the ER dye hexyl rhodamine B (Boevink et al., 1996), the stain and GFP fluorescence showed clear co-localization (Figure 3-3B,C). The GFP signal was also observed in the nuclei of some cells, in addition to the strong and consistent signal from the ER. ER localization of CER2 supports a role for CER2 in wax biosynthesis.

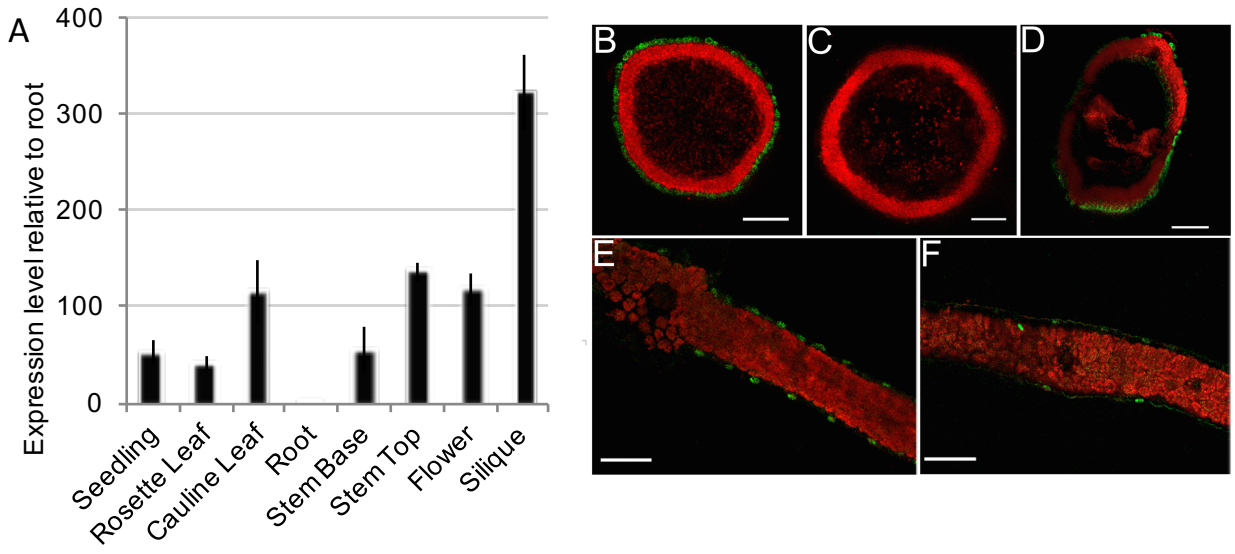

Figure 3-2: *CER2* expression determined by qPCR and CER2pro::CER2-GFP fluorescence

A, qPCR analysis of *CER2* expression patterns in the wild type normalized to *GAPC1*, shown as the average of four technical replicates; error bars represent SD. *CER2pro::CER2-GFP* expression in stem sections 1 cm from the apex (B), stem sections 3 cm from the apex (C), developing siliques (D), young rosette leaf (E), and young cauline leaf (F). Scale bars = 50 μm. Reproduced with permission from Haslam et al., 2012; Copyright American Society of Plant Biologists © 2012 (www.plantphysiology.org)

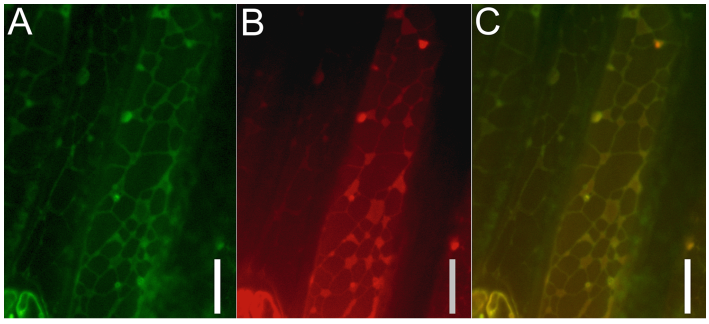

Figure 3-3: CER2 localization to the ER

A, GFP fluorescence in the stem epidermis of Col-0 transformed with *35S::CER2-GFP*. B, Hexyl rhodamine B staining. C, Merge of images A and B, showing co-localization of CER2-GFP and hexyl rhodamine B. Scale bars = 10 μm. Reproduced with permission from Haslam et al., 2012; Copyright American Society of Plant Biologists © 2012 (www.plantphysiology.org)

3.2.4 CER2 modifies the output of elongation when co-expressed with CER6

The wax phenotype of the *cer2-5* mutant demonstrates a role for CER2 in a specific step of VLCFA elongation required for wax synthesis. However, the biochemical function of CER2 is unknown. CER2 could serve as a condensing enzyme in the elongation of VLCFAs longer than 28 carbons, or facilitate acyl chain extension past 28 carbons catalyzed by a condensing enzyme such as CER6. To establish whether CER2 is sufficient for elongation to 30 carbons, CER2 was expressed alone in yeast, but these cells showed no substantial change in fatty acid profile relative to the wild type (Figure 3-4). Changes in the yield of 26-carbon FAME were observed in some experimental replicates. However, subtle, quantitative changes in the fatty acid profile were difficult to interpret given that the VLCFA composition of wild-type yeast cells can vary markedly with growth phase, conditions, and growth medium.

The phenotype of the *cer2-5* mutant suggests that CER2 might require 28-carbon fatty acid as a substrate for elongation, and so CER2 was expressed in yeast cells in combination with LfKCS45, a condensing enzyme from the crucifer *Lesquerella fendleri* (Moon et al., 2004). LfKCS45 efficiently elongates 26-carbon fatty acid to 28 carbons, the proposed substrate for CER2, and also produces a small amount of 30-carbon fatty acid. 28-carbon FAME and trace amounts of 30-carbon FAME were detected in yeast cells co-transformed with CER2 and LfKCS45, equivalent to what was produced when LfKCS45 was expressed alone. These results indicate that CER2 is not sufficient for 28-carbon VLCFA elongation.

The dominant role of the CER6 condensing enzyme in cuticular wax elongation suggested that concerted activity of CER2 and CER6 might be required for the production of 30-carbon VLCFAs. Therefore, CER2 and CER6 were co-expressed in yeast. As previously reported, cells expressing CER6 alone accumulated a much greater amount of 28-carbon FAME relative to wild type, but no 30-carbon FAME. Remarkably, in yeast cells expressing both CER6 and CER2, an additional peak was detected, which was identified as 30-carbon FAME. Therefore, the combined activity of CER6 and CER2 is necessary and sufficient for acyl chain elongation to 30 carbons.

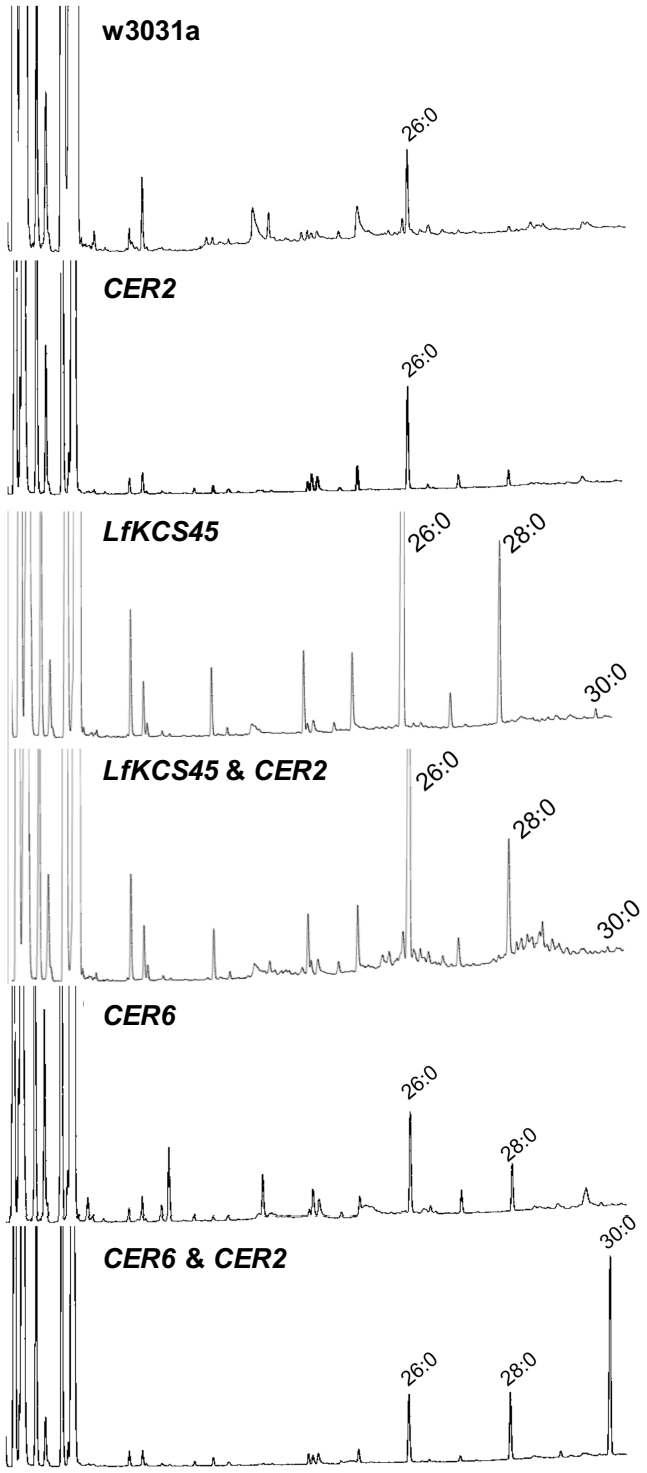

Figure 3-4: Co-expression of *CER2* with plant condensing enzymes in *S. cerevisiae*

Yeast total lipid profiles measured as FAMEs extracted from W3031A, W3031A transformed with *CER2*, *LfKCS45*, *LfKCS45*+*CER2*, *CER6*, and *CER6*+*CER2*. Modified from Haslam et al., 2012, and reproduced with permission; Copyright American Society of Plant Biologists © 2012 (www.plantphysiology.org).

3.3 Discussion

3.3.1 CER2 localizes to the ER in young epidermal cells that are active in cuticular wax biosynthesis

My characterization of the *cer2-5* mutant was consistent with previous reports from McNevin et al. (1993) and Jenks et al. (1995), and suggests a function for CER2 in the elongation of cuticular wax precursors from 28- to 30-carbons in stems. In addition to the stem wax deficiency of *cer2* that was examined by GC-FID, the glossy phenotype of *cer2* was also obvious on siliques. I analyzed leaf wax of *cer2-5* by GC-FID because wax deficiency on leaves cannot be detected by eye, but there was no difference in composition relative to wild type, as reported by Jenks et al. (1995). qPCR analysis of CER2 expression revealed CER2 transcript in all organs except root, and *CER2-GFP* expression was observed in epidermal cells of stems, leaves, and siliques. While the phenotype of *cer2* was only obvious on stems and siliques, *CER2* could also contribute to wax precursor elongation in leaves and in floral organs, but its function may be masked by genetic redundancy.

The enzymes of the FAE complex that generate VLCFA wax precursors, as well as all of the characterized wax biosynthetic enzymes, reside on ER membranes (Samuels et al., 2008). I anticipated that likewise, if CER2 were involved in fatty acid elongation, it would localize to the ER. Confocal microscopy performed on transgenic lines expressing CER2-GFP driven by the *35S* promoter confirmed CER2 localization to the ER in epidermal cells of the inflorescence stem, which actively synthesize cuticular lipids. In these cells, strong CER2-GFP fluorescence was clear throughout the ER: the reticulate cortical ER, trans-vacuolar strands, and the nuclear envelope. Such localization is consistent with a metabolic function for CER2 in VLCFA biosynthesis.

Whereas ER localization of CER2 is compatible with a biochemical function in wax synthesis, it presents yet another peculiarity of CER2 in the context of homology to BAHD acyltransferases, as all BAHDs localized to date are soluble, cytosolic enzymes (D'Auria, 2006; Panikashvili et al., 2009; Rautengarten et al., 2012). Furthermore, localization of maize *GL2* to both the ER and the cytoplasm suggests that CER2 may reside in both compartments and be both soluble and membrane bound. At present, it is not clear how CER2 associates with the ER. Further work is needed to determine if ER localization of CER2 requires interaction with proteins in the FAE complex such as CER6, or other wax biosynthetic enzymes.

3.3.2 CER2 and CER6 are necessary and sufficient for 30-carbon VLCFA synthesis

Plant KCS enzymes expressed in yeast can work with other components of the native yeast FAE complex to synthesize their specific products (Millar and Kunst, 1997). Therefore, yeast has been an invaluable system for the functional characterization of KCS enzymes from Arabidopsis. This approach has revealed an inconsistency in that CER6, the key KCS enzyme associated with VLCFA elongation for cuticular wax synthesis, is unable to elongate VLCFAs longer than 28 carbons. Arabidopsis CER60 (Trenkamp et al., 2004) and *L. fendleri* LfKCS45 (Moon et al., 2004) are the only plant KCSs with demonstrated 28- to 30-carbon elongation activity, and both produce very small amounts of 30-carbon fatty acid when expressed in yeast.

When I expressed LfKCS45 alone in yeast cells, 28- and a small amount of 30-carbon fatty acid were produced, as previously reported by Moon et al. (2004). When CER2 alone was introduced to yeast cells, no effect on the fatty acid profile was obvious from the GC traces. However, analysis of the FAMEs composition did reveal a decrease in 26-carbon FAME in *CER2*-expressing cells compared to the wild type, in some experimental replicates. The reason for this is unclear, and is particularly difficult to interpret given that the amount of 26-carbon fatty acid accumulating in wild-type yeast cells varies substantially between assays. The fatty acid profile of cells expressing CER2 alongside LfKCS45 was no different from that of cells expressing only LfKCS45, demonstrating that CER2 is insufficient for VLCFA elongation past 28 carbons. Expression of CER6 alone in yeast resulted in 28-carbon FAME accumulation, as expected. In contrast, co-expression of CER2 and CER6 in yeast cells resulted in a remarkably high yield of 30-carbon FAME. These findings demonstrate that CER2 and CER6 are necessary and sufficient for 30-carbon VLCFA synthesis. My results also indicate that the CER6 condensing enzyme has a property absent from LfKCS45 that is necessary for CER2-associated elongation. What this property is and how unique it is to CER6 remains unknown. It also remains to be determined whether CER2 has a distinct activity that contributes to VLCFA elongation, if it plays a structural or stabilizing role necessary for the elongation of VLCFAs by CER6, or has a role in allosteric regulation of condensing enzymes.

VLCFAs longer than 28 carbons are not common in nature, and I am not aware of any reports of KCSs that can produce more than trace amounts of 30-carbon fatty acids or longer. It would seem that the canonical FAE complex-catalyzed mechanism of elongation holds exceptions after 28-carbon fatty acid synthesis. Previous phylogenetic analyses have revealed that CER2-type proteins are pervasive among flowering plants (Yu et al., 2009; Tuominen et al., 2011). This suggests that the CER2 family has a necessary, conserved role in VLCFA elongation, and that CER2 activity is important for cuticular wax biosynthesis in flowering plants.

Chapter 4: ECERIFERUM2-LIKE proteins have unique biochemical and physiological functions in very-long-chain fatty acid elongation

4.1 Introduction

In the previous chapter, the central role of *CER2* in the elongation of fatty acids to 30 carbons was demonstrated, and the importance of these VLCFAs for the synthesis of stem cuticular wax was described. However, cuticular waxes derived from fatty acids 30 carbons and longer coat all of the primary aerial surfaces of Arabidopsis. Similar lipids are also found in the pollen coat, where they are required for pollen hydration and germination on dry stigma (Elleman et al., 1992; Preuss et al., 1993). Accordingly, public microarray data (Winter et al., 2007), qPCR data, and CER2-GFP expression patterns all indicate that the *CER2* gene is expressed in the epidermis throughout the shoot. Yet, characterization of the *cer2-4* mutant by Jenks et al. (1995) showed that leaf waxes of *cer2-4* do not differ significantly from the wild type, and the *cer2* allele I studied was fertile. This information suggests that other Arabidopsis genes might contribute to the synthesis of VLCFA precursors of leaf cuticular wax and pollen coat.

CER2 orthologs are found in diverse flowering plant lineages, and many species have multiple *CER2* paralogs (Yu et al., 2009; Tuominen et al., 2011). Previous analyses of the BAHD acyltransferase family of Arabidopsis have identified several genes with high sequence identity to CER2. Tuominen and coworkers (2011) reported that there are two CER2 homologs in Arabidopsis, At3g23840 and At4g29250. Yu and coworkers (2009) also reported the existence of two CER2 homologs in Arabidopsis, but identified At3g23840 and At4g13840. The inconsistency between these publications was not immediately obvious to me, and I began characterizing the "CER2-LIKE" family of Arabidopsis using the gene identities specified by Yu et al. (2009). After noticing the discrepancy between these publications, I compared CER2 homologs that I could find through NCBI and the BAHDs in the Yu et al. (2009) and Tuominen et al. (2011) phylogenies, and found that there are in total five CER2-LIKE genes in Arabidopsis. The genes and their assigned names are specified in Table 4-1. A phylogeny for the Arabidopsis BAHD acyltransferase family that includes all of these proteins was published as supplementary material by Molina et al., 2009, and is reproduced in Figure 4-1.

Table 4-1: Identities of CER2 homologs from Arabidopsis

		Identified by		
Gene locus	**Name**	**Yu et al.**	**Tuominen et al.**	**HXXXD***
At4g24510	*CER2*	Y	Y	HILDG
At4g13840	*CER2-LIKE1*	Y	N	NIIDG
At3g23840	*CER2-LIKE2*	Y	Y	HIMGD
At4g29250	*CER2-LIKE3*	N	Y	HLLAD
At5g02890	*CER2-LIKE4*	N	N	ILIAD

*HXXXD is the conserved acyltransferase catalytic motif. H = histidine, D = aspartic acid, X = any amino acid.

It is not clear why CER2-LIKE3 and CER2-LIKE4 were omitted from the phylogeny published by Yu et al. (2009). CER2-LIKE1 and CER2-LIKE4 were excluded from the phylogeny published by Tuominen et al. (2011) because both of these proteins lack an HXXXD motif characteristic of BAHD acyltransferases. The authors reasoned that this divergent feature indicates that CER2-LIKE1 and CER2-LIKE4 cannot be true BAHDs. My work has since shown that the CER2-LIKEs have biochemical function distinct from other characterized BAHDs (Chapter 5). In light of this, the absence of the HXXXD motif in two CER2-LIKEs reflects novelty in the CER2-LIKE clade, and does not preclude CER2-LIKE1 and CER2-LIKE4 from having common function with CER2, CER2-LIKE2, and CER2-LIKE3.

It is necessary to characterize the metabolic and physiological functions of CER2-LIKE proteins. Beyond the value of knowing the specific roles of each homolog, such an investigation has the potential to elucidate the biochemical nature of CER2-LIKE activity. The present chapter will address the following questions: (1) Can CER2-LIKE proteins function with condensing enzymes other than CER6, and if so, is the effect of the CER2-LIKE constant? (2) Do different CER2-LIKE proteins have different effects on the substrate specificity of the same condensing enzyme? (3) What is the physiological relevance of the subtle changes in acyl lipid chain length that CER2-LIKE proteins induce?

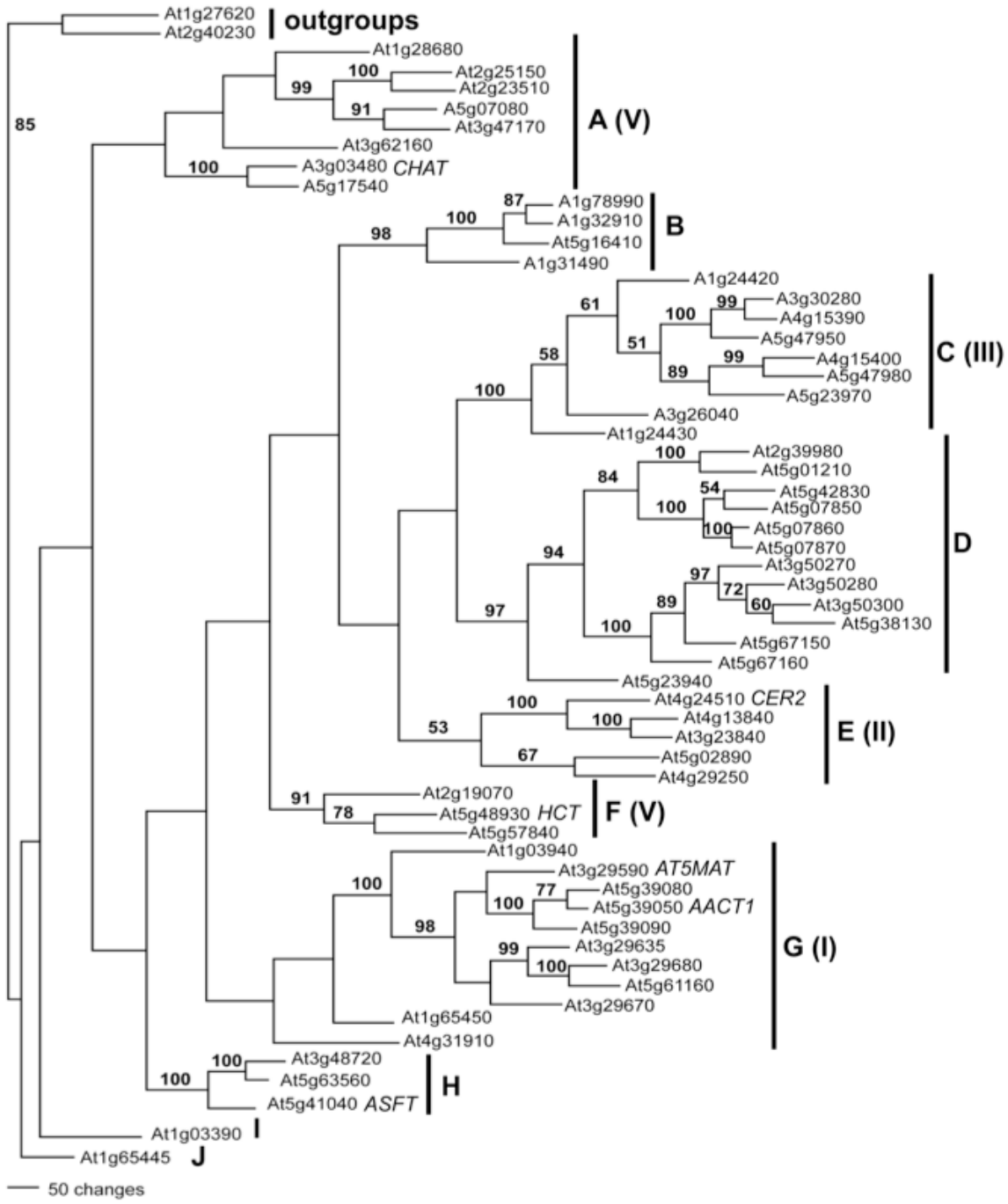

Figure 4-1: Phylogeny of the Arabidopsis BAHD acyltransferase family

Numbers on branches represent bootstrap values as percentages. Roman numerals correspond to BAHD clades designated by D'Auria, 2006. Several BAHDs are labelled: AACT1: Anthocyanin 5-aromatic acyltransferase1; AT5MAT: O-malonyltransferase; CHAT: acetyl-CoA:(Z)-3-hexen-1-ol acetyltransferase; HCT: hydroxycinnamoyl-CoA:shikimate/quinate hydroxycinnamoyltransferase. Reproduced with permission from Molina et al., 2009; Copyright American Society of Plant Biologists © 2009 (www.plantphysiology.org)

4.2 Results

4.2.1 CER2-LIKEs have different expression patterns

Based on the phylogeny of Yu et al. (2009), my work initially focused on only three of the five *CER2-LIKEs*: *CER2*, *CER2-LIKE1*, and *CER2-LIKE2*. Characterization of *CER2* was presented in the previous chapter. To guide phenotypic analyses of *cer2-like1* and *cer2-like2* mutants, gene expression patterns were examined. Organ-specific expression patterns of both genes were investigated by qPCR, as described in Section 2.2.2. *CER2-LIKE1* transcript was detected in seedlings, rosette and cauline leaves, and siliques (Figure 4-2A). *CER2-LIKE2* transcript was detected in seedlings, rosette and cauline leaves, and flowers (Figure 4-3A). Expression of both genes in leaves is consistent with the notion that they may contribute to cuticular wax biosynthesis. High expression levels of *CER2-LIKE2* in flowers suggest that it could be required for the production of the unique cuticular lipids on floral organs, the synthesis of lipidic components of the pollen coat, or sporopollenin.

A *CER2-LIKE1-GFP* fusion driven by the native *CER2-LIKE1* promoter was constructed to examine cell-type specific expression patterns. This construct complemented the *cer2-like1* leaf wax phenotype (complementation not shown). Unfortunately, GFP fluorescence was too weak to discern cell-type specific fluorescence patterns in hand-sectioned material. However, this construct was useful as localization of *CER2-LIKE1-GFP* to the ER in intact rosette leaf pavement cells was easily observed (Figure 4-2B).

Characterization of *CER2-LIKE1* and *CER2-LIKE2* was carried out in collaboration with Dr. Jérôme Joubès' lab at the University of Bordeaux, France. Dr. Joubès' lab used qPCR to examine *CER2-LIKE2* expression throughout floral development following the staging described by Smyth et al. (1990). Temporal patterns of *CER2-LIKE2* expression were compared to those of *FATTY ACYL REDUCTASE2* (*FAR2*), *CER1*, and *CER2* (Figure 4-3B). *FAR2* contributes to the synthesis of fatty alcohols in sporopollenin (Aarts et al., 1997). *CER1* encodes an alkane-forming enzyme required for cuticular wax biosynthesis (Bernard et al., 2012). *CER2* and *CER1* are both expressed in different floral organs throughout development and contribute to cuticle formation (Bourdenx et al., 2011; Pascal et al., 2013). Further, specific mutant alleles of both of these *CER* genes cause conditional male sterility at low humidity (Koornneef et al., 1989; Preuss et al., 1993), suggesting that they contribute to the synthesis of pollen coat lipids. *FAR2* transcript could be detected only until stage eight, which fits with a role for *FAR2* in sporopollenin synthesis. *CER1* and *CER2* were expressed throughout all of the developmental stages profiled, consistent with functions of both genes in both floral cuticular wax and pollen

coat lipid biosynthesis. *CER2-LIKE2* expression was highest in flower buds collected at stage eight or younger, decreased to approximately 25% of that level at stage nine, and was not detected later in development.

Dr. Joubès' lab further examined patterns of *CER2-LIKE2* expression using a *CER2-LIKE2pro::GUS* construct stably expressed in wild-type Col-0 plants (Figure 4-3C). When whole inflorescences were stained, GUS activity could be detected only in young anthers (Figure 4-3C[a]). Flowers were fixed, embedded, and cut in semi-thin sections at developmental stages eight, nine, and eleven to observe cell type-specific expression patterns (Figure 4-3C, [b–d]). In stage eight flowers, GUS activity was present in the tapetum and on microspores within the locule. I was skeptical of microspore staining, as several promoters that drive gene expression uniquely in the tapetum have resulted in blue microspores when fused to GUS (Yokoi et al., 1997; Kapoor et al., 2002; Choi et al., 2014). It is possible that secretion of either the GUS protein or its ClBr-indigo product, or the release of either upon degeneration of tapetal cells, may have caused the observed staining of microspores. In stage nine flowers, GUS staining was exclusive to tapetal cells, and no staining was observed in stage eleven flowers. Together, the spatial and temporal expression patterns of *CER2-LIKE2* suggest that its gene product is required for pollen coat or sporopollenin biosynthesis.

While *CER2-LIKE3* and *CER2-LIKE4* were not extensively characterized in the present work, their expression profiles can be generally described based on microarray data publicly available in the Arabidopsis eFP browser (Winter et al., 2007). *CER2-LIKE3* expression is only detected in young flower buds, between developmental stages 9-11. *CER2-LIKE4* expression is broader, with transcript detected in leaves, stems, floral organs, roots, and siliques. Notably, expression is up-regulated in young stem epidermal cells, in the developing seed coat, and in the L1 layer of the shoot meristem.

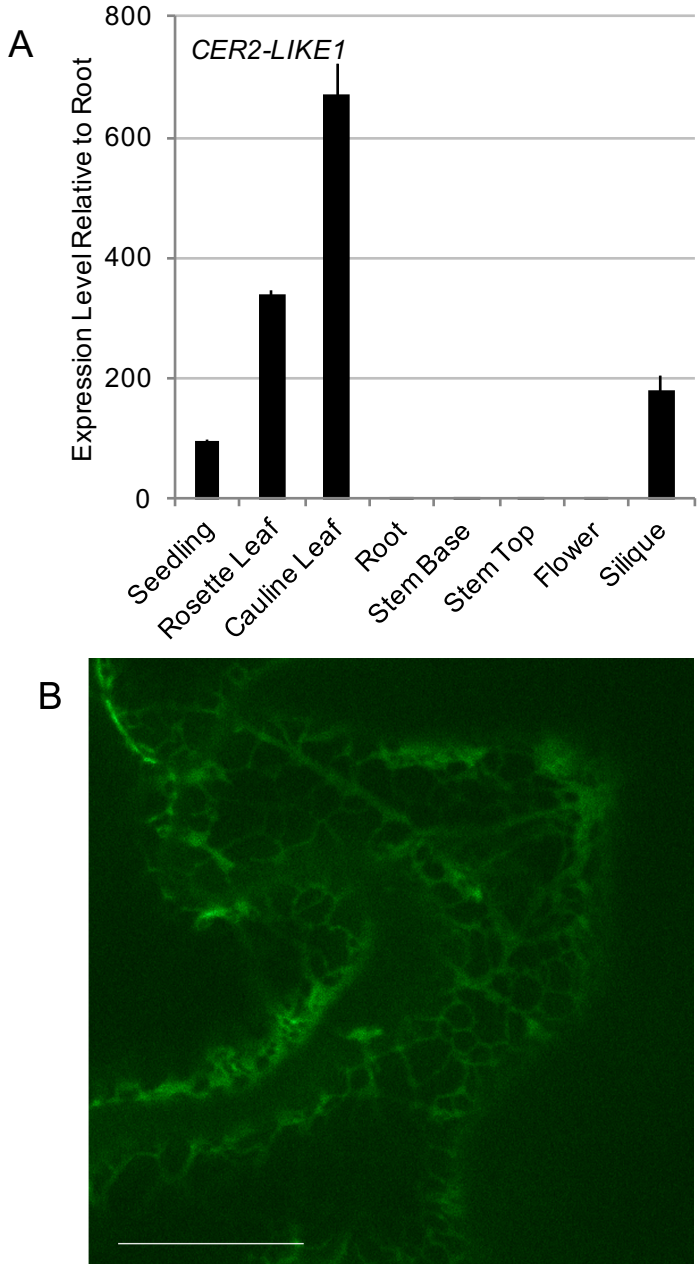

Figure 4-2: Expression pattern and localization of *CER2-LIKE1*

(A) qPCR analysis of *CER2-LIKE1* expression patterns in the wild type normalized to *GAPC1*, shown as the average of four technical replicates; error bars represent SD. Reproduced with permission from Haslam et al., 2012; Copyright American Society of Plant Biologists © 2012 (www.plantphysiology.org) (B) Sub-cellular localization of CER2-LIKE1 in rosette leaf pavement cells of the *cer2-like1* mutant, complemented with *CER2-LIKE1pro::CER2-LIKE1-GFP*. Scale bar = 18 μm.

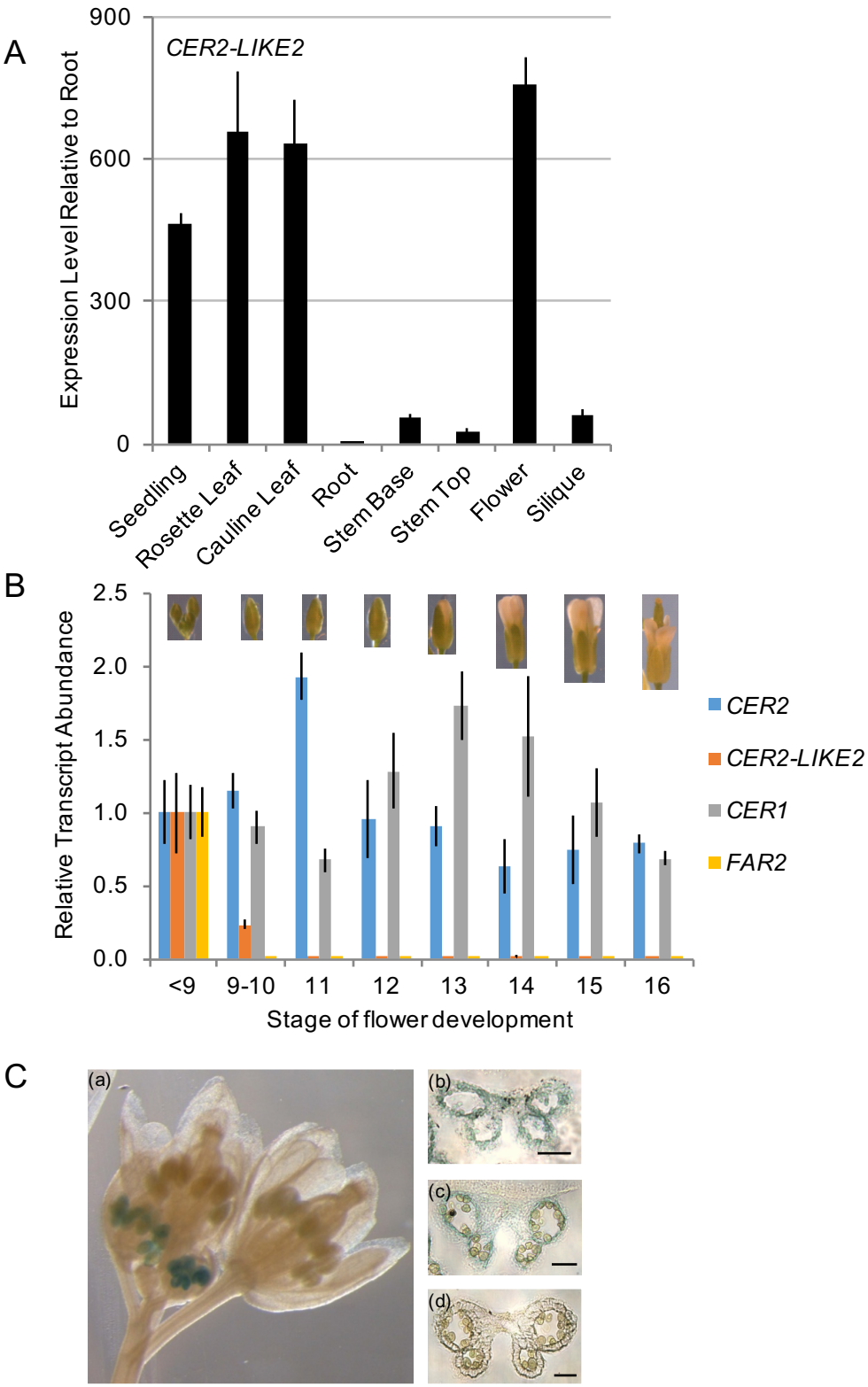

Figure 4-3: Expression profiling of *CER2-LIKE2*

(cont'd on following page)

(A) qPCR analysis of *CER2-LIKE2* expression patterns in the wild type normalized to *GAPC1*, shown as the average of four technical replicates; error bars represent SD. Reproduced with permission from Haslam et al., 2012; Copyright American Society of Plant Biologists © 2012 (www.plantphysiology.org) (B) Differential expression analysis of *CER2, CER2-LIKE2, CER1 and FAR2* genes in Arabidopsis flowers. Gene expression level was determined by real-time PCR analysis. The relative transcript abundance of *ACT2* and *eIF-4A-1* in each sample was determined and used to normalize for differences of total RNA amount. Results are presented as transcript abundance for each gene compared to expression levels at stage <9. The data represent the means ±SD of three replicates. (C) Anther-specific staining of GUS in flowers in transgenic Arabidopsis plants harbouring the *CER2-LIKE2* promoter fused to the *GUS* reporter gene. Promoter activity was visualized through histochemical GUS staining of a flower bud (a) and on semi-thin sections of anthers at stage 8 (a), 9 (b) and 11 (c) of flower development. Scale bar = 0.5 mm. B and C reproduced with permission from Haslam et al., 2015; Copyright American Society of Plant Biologists © 2015 (www.plantphysiology.org)

4.2.2 Isolation of *cer2-like* mutants

T-DNA mutant alleles of *CER2-LIKE1*, *CER2-LIKE2*, and *CER2-LIKE3* were obtained to investigate the biological functions of *CER2-LIKE* genes in Arabidopsis. The *cer2-like1* mutant was ordered directly from ABRC, and the *cer2-like2* and *cer2-like3* mutants were kind gifts from Dr. Carl Douglas and Lexcy Li. Individual plants were genotyped to identify homozygous mutants, and the precise sites of T-DNA insertions were determined by PCR and sequencing, as described in Section 2.2 (Figure 4-4). *cer2 cer2-like1*, *cer2 cer2-like2*, and *cer2-like1 cer2-like2* double mutants and a *cer2 cer2-like1 cer2-like2* triple mutant were generated to investigate some of the possible overlapping biological roles within this gene family.

Because the T-DNA insertion in the *cer2-like1* mutant is situated in an intron, and the T-DNA insertion in *cer2-like2* is situated near the 3' end of the gene, RT-PCR was used to determine whether full-length transcript was produced in either mutant. No full-length transcript was detected in either line (Figure 4-5).

No T-DNA lines were available with insertions in the coding sequence of *CER2-LIKE4*, so the CRISPR/Cas9 system was used to generate loss-of-function mutants. A 19 bp sequence located 100 bp from the start of the coding region was selected as a target. Two alleles were chosen for analysis, which were named *cer2-like4-1* and *cer2-like4-2*. Both had small deletions that caused frame-shift mutations. The mutations in these genes are shown in Figure 4-6.

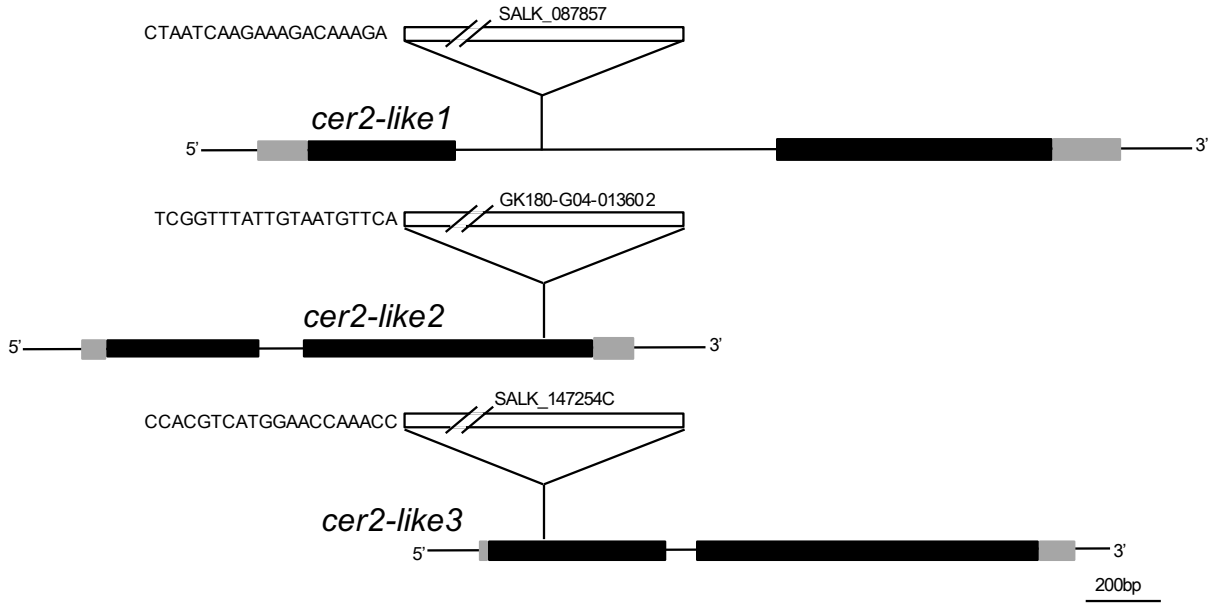

Figure 4-4: Schematic representation of T-DNA insertions in *cer2-like1*, *cer2-like2*, and *cer2-like3*

Coding sequences are represented as black boxes, UTRs as grey boxes, and introns and un-transcribed flanking genomic DNA as a straight black line. The T-DNA insertion sites were determined by PCR and sequencing. Modified and reproduced with permission from Haslam et al., 2012; Copyright American Society of Plant Biologists © 2012 (www.plantphysiology.org)

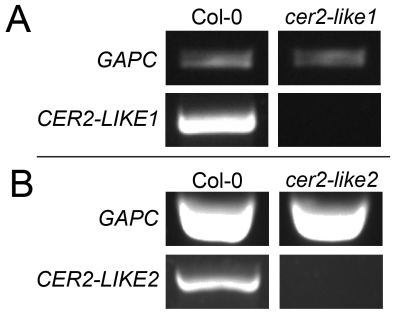

Figure 4-5: RT-PCR of *cer2-like1* and *cer2-like2* mutants

(A) RT-PCR of *CER2-LIKE1* expression in rosette leaves of the wild type and in the *cer2-like1* mutant. *CER2-LIKE1*-specific primers annealed to the first and second exons, flanking the intron that contains the T-DNA. 30 amplification cycles were used for *GAPC*, 32 for *CER2-LIKE1*. Reproduced with permission from Haslam et al., 2012; Copyright American Society of Plant Biologists © 2012 (www.plantphysiology.org) (B) RT-PCR of *CER2-LIKE2* expression in cauline leaves of the wild type and in the *cer2-like2* mutant. *CER2-LIKE2*-specific primers annealed near the start and stop of the open reading frame. 28 amplification cycles were used for GAPC, and 30 for *CER2-LIKE2.* All primers are specified in Table 2-3. Reproduced with permission from Haslam et al., 2015; Copyright American Society of Plant Biologists © 2015 (www.plantphysiology.org)

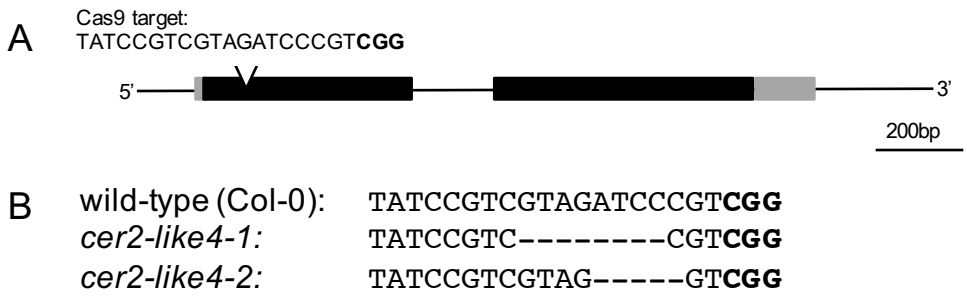

Figure 4-6:CRISPR/Cas9 target site and mutants generated in *CER2-LIKE4*

(A) Schematic representation of *CER2-LIKE4* and the target sequence selected for CRISPR/Cas9-mediated mutagenesis. The protospacer adjacent motif (PAM) is in bold type. (B) Mutations in *cer2-like4-1* and *cer2-like4-2*. Eight base pairs are deleted in *cer2-like4-1*, and five are deleted in *cer2-like4-2*, both causing frame shift mutations.

4.2.3 CER2-LIKE1 has an analogous role to CER2 in the elongation of leaf wax precursors

Because *CER2* is expressed in leaves, but *cer2* has no leaf wax phenotype, possible roles of *CER2-LIKEs* in rosette leaf cuticular wax metabolism were examined. Wax composition of *cer2-like1* rosette leaves was analyzed first. Strikingly, *cer2-like1* leaves accumulated approximately 60% less 31-carbon alkane and four times more 29-carbon alkane than the wild type (Figure 4-7A). Increased accumulation of 30-carbon primary alcohol and aldehyde was also observed. The shift in wax component chain length distribution suggests a function for CER2-LIKE1 in the elongation of fatty acids from 30 to 32 carbons in leaf, parallel to the role of CER2 in the elongation of fatty acids from 28 to 30 carbons in stems.

To explore the possibility of functional redundancy between *CER2* and *CER2-LIKE1*, rosette leaf wax composition of a *cer2 cer2-like1* double mutant was examined. *cer2 cer2-like1* rosette leaf wax accumulated roughly triple the wild-type load of 28-carbon primary alcohol and VLCFA, and roughly 85% less 31-carbon alkane. Unlike the *cer2-like1* single mutant, the double mutant did not accumulate excess 29-carbon alkane (Figure 4-7A). Overall, this result was interpreted as an accumulation of leaf cuticular waxes 28-carbons and shorter, and a reduction in waxes longer than 28 carbons in *cer2 cer2-like1*. That the block in leaf wax elongation occurred at 28 carbons in the double mutant suggests that *CER2-LIKE1*, like *CER2*, contributes to the elongation of 28-carbon fatty acids to 30.

The fact that the *cer2-like1* mutant does accumulate some 31 and 33 carbon alkane implies that there are more genes that contribute to the elongation of VLCFAs from 30 to 34 carbons. Because *CER2-LIKE2* is also expressed in rosette leaves (Figure 4-3A, Section 4.2.1), *CER2-LIKE2* or one of the many condensing enzymes expressed in leaves could contribute to the elongation of these VLCFAs. Analysis of the rosette leaf cuticular wax of a *cer2 cer2-like1 cer2-like2* triple mutant revealed that while the triple accumulated slightly less 30 to 34 carbon waxes than the *cer2 cer2-like1* double mutant, these waxes could still be detected (data not shown). This might be in part due to presence of truncated, but functional, CER2-LIKE2 protein, as the T-DNA insertion site in the GK180-G04 allele was located near the 3' end of the gene. Alternatively, other condensing enzymes or CER2-LIKEs could contribute to elongation in leaf epidermal cells.

Surprisingly, the total leaf wax load of the *cer2-like1* single mutant was nearly 50% greater than that of the wild type. Although there is considerable variability in total wax load measurements between individual plants, this difference was statistically significant (Figure 4-7A). The reason for increased wax load in the mutant is unclear. Perhaps it reflects a

compensatory effort by the plant to build an effective cuticular barrier by producing more wax when the cuticle structure is compromised by altered composition. Alternatively, the alkane synthetic pathway that produces most of the rosette leaf wax of Arabidopsis may have preference for the 30-carbon acyl-CoA substrate that might accumulate when CER2, but not CER2-LIKE1, is present.

4.2.4 The acyl-CoA pools of *cer2-like* mutants are unusual

The cuticular wax phenotypes of *cer2-like* mutants and the activity of CER2 in yeast suggest that CER2-LIKE proteins modify the substrate specificity of fatty acid elongation. Therefore, characterization of *cer2-like* mutants based on their wax composition, though convenient, is indirect. Subsequent modification of VLC-acyl-CoAs to different wax components, and secretion of the waxes to the cuticle might obscure the precise effect of *cer2-like* mutations on elongation. Hence, the phenotypes of *cer2*, *cer2-like1*, and *cer2 cer2-like1* mutants were further investigated by profiling the acyl-CoA pools of rosette leaves by LC-MS (Figure 4-7B).

The leaf acyl-CoA profile of *cer2* was no different from the wild type. The *cer2-like1* mutant had a 3-fold increase in 30-carbon acyl-CoA, a 50% reduction in the amount of 32-carbon acyl-CoA, and only trace amounts of 34-carbon acyl-CoA. *cer2 cer2-like1* had a 2-fold increase in the amount of 28-carbon acyl-CoA, no difference compared to wild type in the amount of 30-carbon acyl-CoA, and the same reduction in 32- and 34-carbon acyl-CoAs as observed in the *cer2-like1* single mutant. These results are consistent with conclusions drawn based on cuticular wax phenotypes: *CER2* and *CER2-LIKE1* both contribute to the elongation of acyl-CoAs from 28 to 30 carbons in leaf, and *CER2-LIKE1* is involved in elongation up to 34 carbons. Accumulation of 28-carbon acyl-CoAs is much more dramatic than the cuticular wax phenotype for the double mutant.

4.2.5 CER2 and CER2-LIKE2 contribute to male fertility

The *cer2 cer2-like2* double mutant and the *cer2 cer2-like1 cer2-like2* triple mutant had stunted siliques, which were largely devoid of viable seeds at maturity (Figure 4-8A). This phenotype was rescued by growing the mutants in high humidity, suggesting that they may be male sterile due to a pollen coat defect. To investigate this possibility, reciprocal crosses were made between the triple mutant line and the wild type. Normal seed set and siliques were produced when wild-type pollen was applied to triple mutant pistils (Figure 4-8B), but few or no seeds could be recovered with the reciprocal cross (Figure 4-8C). These results indicate that *CER2* and *CER2-LIKE2* have redundant functions required for male fertility.

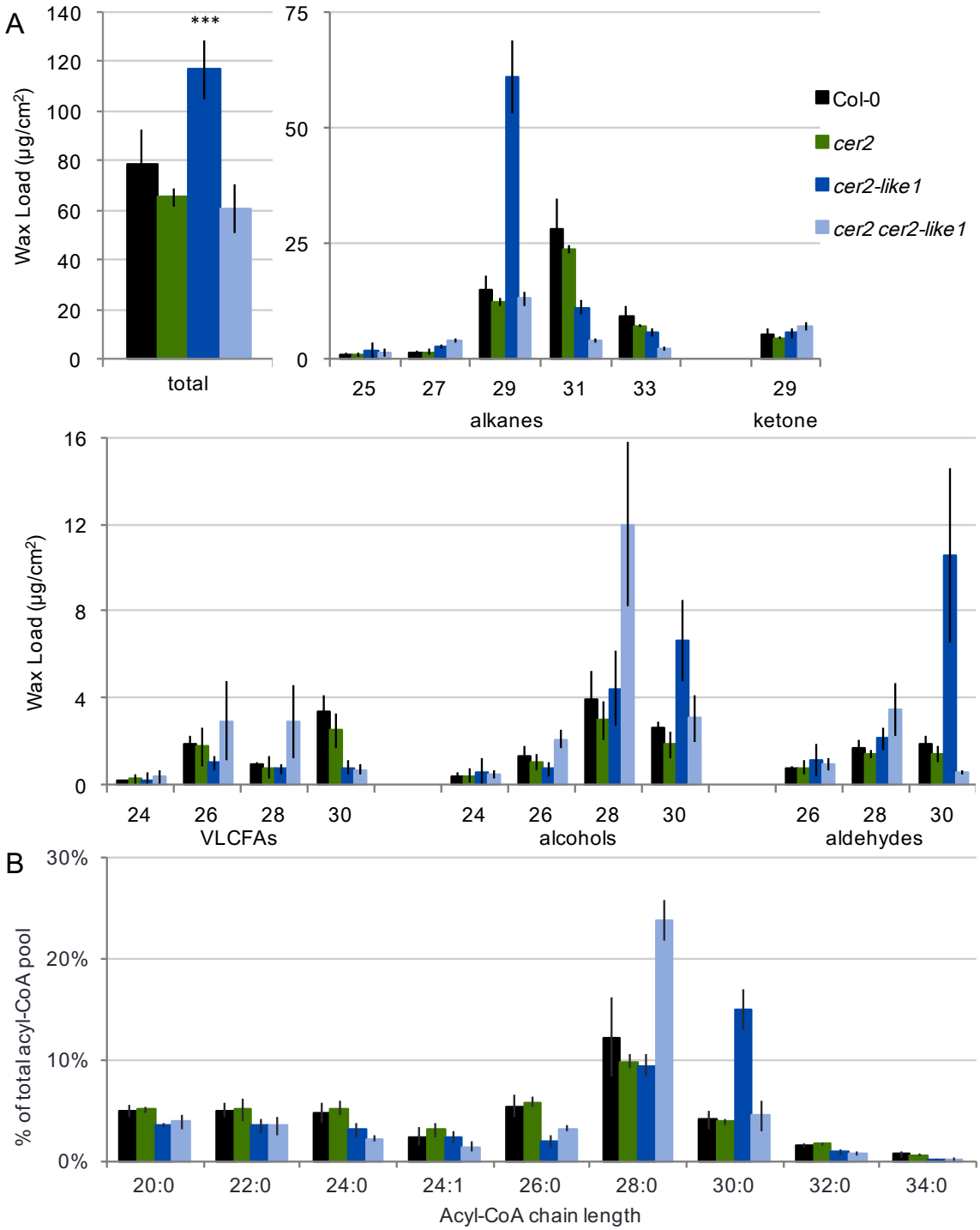

Figure 4-7: Rosette leaf wax and acyl CoAs of the *cer2*, *cer2-like1*, and *cer2 cer2-like1* mutants

(A) Load and composition determined by GC-FID. Values are averages of at least four biological replicates, error bars are SD. Asterisk denotes significant difference between *cer2-like1* and wild type determined by a Student's T-test, ***p<0.001. (B) Acyl-CoA profiles determined by LC-MS. Values are averages of at least four biological replicates, error bars are SD. Reproduced with permission from Haslam et al., 2015; Copyright American Society of Plant Biologists © 2015 (www.plantphysiology.org)

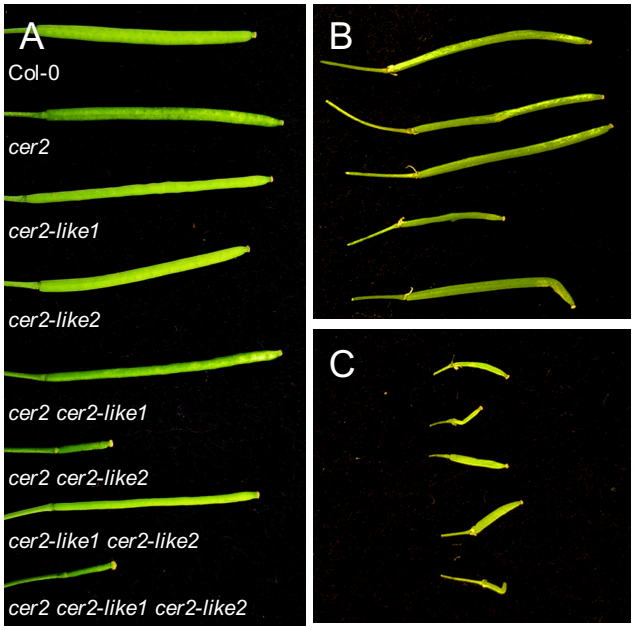

Figure 4-8: Male sterility phenotypes of select *cer2-like* mutants

(A) Mature siliques of single, double, and triple mutants. Siliques of *cer2-5 cer2-like2-1* and *cer2-5 cer2-like1-1 cer2-like2-1* are stunted and contain few or no seeds at maturity. (B) Siliques of *cer2-5 cer2-like1-1 cer2-like2-1* triple mutant manually pollinated with wild-type pollen. (C) Siliques of wild-type plants manually pollinated with *cer2-5 cer2-like1-1 cer2-like2-1* triple mutant pollen. Reproduced with permission from Haslam et al., 2015; Copyright American Society of Plant Biologists © 2015 (www.plantphysiology.org)

4.2.6 Substitution of *CER2-LIKE*s is sufficient to modify the plant cuticle structure

The phenotypes of the *cer2-like* mutants do not reveal whether the activities of CER2-LIKE proteins are competitive, nor whether they can substitute for the functions of one another *in planta*. To address these unknowns, a *CER2-LIKE1-GFP* transgene was ectopically expressed in the stem epidermis of wild type and *cer2-5* mutants, using the promoter of the condensing enzyme gene *CER6* (Hooker et al., 2002). GC-FID analysis of stem wax revealed that there was no significant difference in the total wax load when *CER2-LIKE1* was expressed in wild-type plants (Figure 4-9A). *CER2-LIKE1* expression in the *cer2-5* mutant background recovered more than one-half the wild-type wax load (Figure 4-9B). The wax chain length profiles of the transgenics indicate that CER2-LIKE activity is sufficient to modify the specificity of elongation *in planta*; when *CER2-LIKE1* was expressed in both wild-type and *cer2-5* backgrounds, the ratio of 31:29-carbon wax components was greater than 1, whereas it was 0.03 in Col-0 wild type. The increased accumulation of 31- and 33-carbon waxes at the expense of 29-carbon waxes in wild-type background suggests that the activities of CER2 and CER2-LIKE1 are competitive.

Plants carrying the *CER2-LIKE1-GFP* transgene in either wild-type or *cer2-5* background appeared glossy, despite the fact that they had completely or partially recovered stem wax loads, respectively. A similar observation has been made when *cer2-like1* was complemented with a *35Spro::CER2-LIKE1* construct (Pascal et al., 2013). Examination of the progeny of three independent transgenic lines in each background by scanning electron microscopy (SEM) revealed that their stems had reduced wax crystal density relative to wild type. Crystals that did form on the stems of transgenic plants consisted of irregularly shaped, thin flakes (Fig. 4-9C).

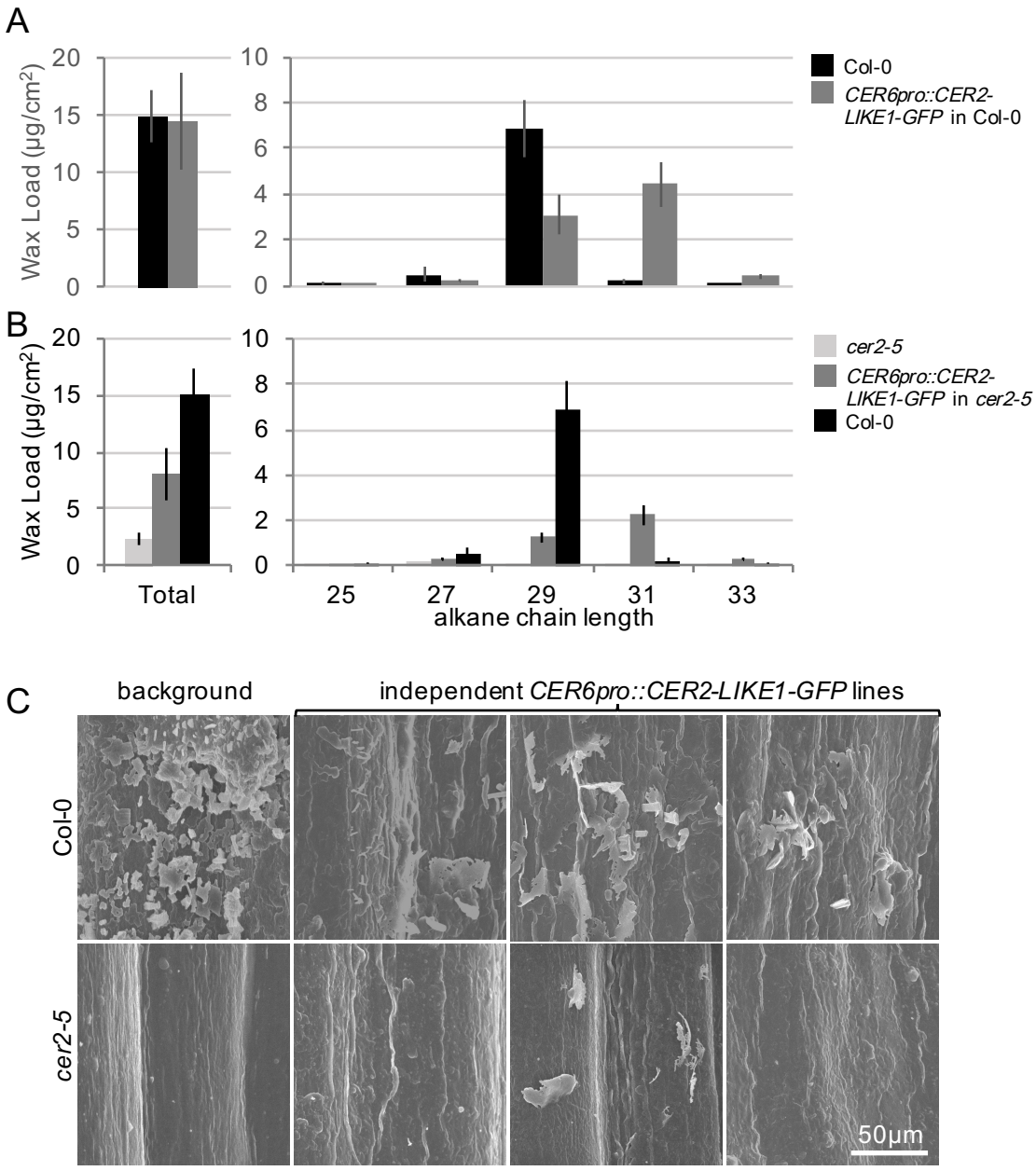

Figure 4-9: Ectopic expression of *CER2-LIKE1* in stem epidermis

(A) Expression of *CER2-LIKE1* in wild-type stem. (B) Expression of *CER2-LIKE1* in *cer2-5* stem. Total wax load includes all aliphatic wax components, and the alkane composition shows the chain length profile. Values represent averages of 3 (A) and 4 (B) independent T_1 lines. Error bars represent standard deviation. (C) SEM images of stems from transgenics in wild-type (top) and *cer2-5* (bottom) background. Each image was taken of a different T_1 line. Modified and reproduced with permission from Haslam et al., 2015; Copyright American Society of Plant Biologists © 2015 (www.plantphysiology.org)

4.2.7 CER2-LIKEs impart different substrate specificities to the same condensing enzyme

The *cer2-like* phenotypes indicate that different CER2-LIKEs have distinct roles in VLCFA elongation. These differences could be due to either (1) each CER2-LIKE protein functioning with a different condensing enzyme, or (2) CER2-LIKEs imparting their own unique substrate specificities to the same condensing enzyme. To differentiate between these two possibilities, each of the five Arabidopsis *CER2-LIKE*s was co-expressed with *CER6* in yeast, and yeast FAMEs were analyzed by GC-FID. As reported, *CER2* and *CER6* co-expression produced 30-carbon fatty acid (Figure 4-10A). Yeast cells co-expressing *CER2-LIKE1* with *CER6* accumulated 30-, 32-, and 34-carbon fatty acids. The specificity of *CER2-LIKE1* observed here is in agreement with the fact that the *cer2-like1* mutant rosette leaf wax has reduced amounts of 31-, 32-, and 33-carbon waxes, which are abundant in wild-type leaf cuticular wax. Yeast cells co-expressing *CER6* and *CER2-LIKE2* synthesized 30-, and traces of 32-carbon fatty acids. *CER6* with *CER2-LIKE3* had a similar FAMEs profile to *CER6* with *CER2*, producing 30-carbon fatty acids. Finally, *CER2-LIKE4* was unique among the homologs in that it did not extend the substrate specificity of *CER6*, and only reduced the accumulation of 26-carbon FAMEs detected when *CER6* was expressed alone. CER2, CER2-LIKE1, CER2-LIKE2, and CER2-LIKE3 have a similar negative effect on the accumulation of 26-carbon fatty acid when co-expressed with CER6, however, this may simply be due to 26-carbon fatty acid being used as substrate for elongation to longer chain lengths. Why less 26-carbon VLCFA accumulates when CER2-LIKE4 is co-expressed with CER6 is less clear. Curiously, co-expression of each of the CER2-LIKEs except CER2-LIKE4 with CER6 reduced the accumulation of 28-carbon fatty acid in comparison to CER6 alone.

Together, these results demonstrate that *CER2-LIKE* proteins have unique substrate specificities in the presence of the same condensing enzyme. Co-expression of *CER2*, *CER2-LIKE1*, and *CER6* produced VLCFA profiles similar to *CER2-LIKE1* and *CER6* (Figure 4-10B), indicating that there is no synergistic effect of having multiple CER2-LIKE proteins.

CER2 can alter chain length specificity of the elongation complex when it is co-expressed with CER6, but not when it is co-expressed with the LfKCS45 condensing enzyme from the crucifer *L. fendleri* (Chapter 3). This implies that a particular feature of CER6 is required for CER2 activity, but how unique this feature is to CER6 is unknown. To determine if other KCS enzymes can pair with CER2-LIKEs to produce VLCFAs 30 carbons and longer, another suite of yeast expression experiments was devised. This work was done in

collaboration with Dr. Jérôme Joubès at the University of Bordeaux. Dr. Joubès' lab co-expressed *CER2, CER2-LIKE1*, and *CER2-LIKE2* with the following condensing enzyme genes from Arabidopsis: *ECERIFERUM60* (*CER60/KCS5*; Fiebig et al., 2000), *FIDDLEHEAD* (*KCS10*; Pruitt et al., 2000), *KCS1* (Todd et al., 1999), *KCS9* (Lü et al., 2012), and *KCS20* (Lee et al., 2009). These condensing enzymes were selected because their null mutants have cuticle defects, they belong to different subclasses of the FAE1-like KCS family (Joubès et al., 2008), and because they have demonstrated activity in yeast (Tresch et al., 2012). CER2-LIKE activity was not tested with ELO-LIKE proteins. All three CER2-LIKEs tested had an effect on the specificity of CER60, which is 88 % identical to CER6, and had the same substrate specificity as CER6 in this assay. The effects of CER2-LIKEs on CER60 were identical to their effects on CER6. None of the other KCSs tested had different activity when paired with CER2-LIKEs (data not shown; Haslam et al., 2015).

4.2.8 CER2-LIKE4 has a negative effect on CER6 + CER2 activity in yeast

The effect of CER2-LIKE4 on CER6 activity in yeast was unique in that *CER2-LIKE4* expression reduced the accumulation of 26-carbon fatty acids, but was not correlated with increased accumulation of any longer fatty acids. It is unknown whether and how CER2-LIKE4 might contribute to wax metabolism. The Arabidopsis eFP browser (Winter et al., 2007) indicates that *CER2-LIKE4* is expressed in both stem and leaf epidermal cells. As only *CER2* among the remaining *CER2-LIKEs* is expressed in stem, *CER6*, *CER2*, and *CER2-LIKE4* were co-expressed in yeast to mimic the Arabidopsis stem epidermal elongase (Figure 4-10C). Accumulation of 26-carbon fatty acid was not substantially different in cells expressing *CER6* and *CER2* compared to cells expressing *CER6*, *CER2*, and *CER2-LIKE4*. However, *CER2-LIKE4* did have a negative effect on elongation in that 50% less 30-carbon fatty acid accumulated in *CER6*, *CER2*, and *CER2-LIKE4*-expressing cells than in yeast cells expressing only *CER6* and *CER2*. Accumulation of 28-carbon fatty acid was maintained at similar levels as in cells transformed with either *CER6* or *CER6* and *CER2-LIKE4.*

4.2.9 The *cer2-like4* mutant does not have a cuticular wax phenotype

To investigate the *in planta* function of CER2-LIKE4, *cer2-like4* mutants were generated using the CRISPR/Cas9 system. Preliminary analyses of two *cer2-like4* mutant alleles did not reveal any obvious phenotype. The stems of the mutants appeared glaucous, and analysis by GC/FID did not uncover any significant changes in the total wax load or chain length distribution of wax components (Figure 4-11).

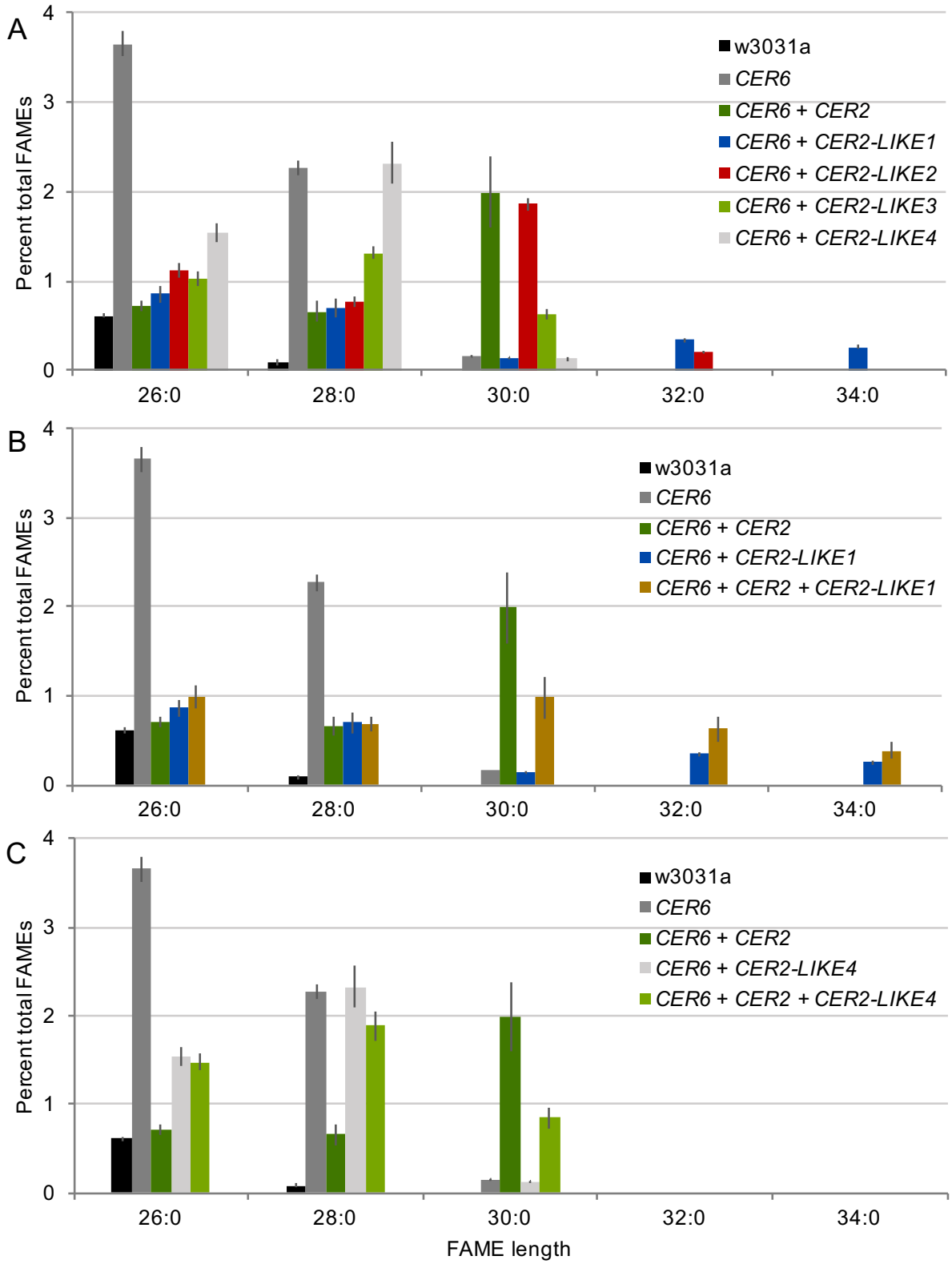

Figure 4-10: FAMEs profiles of yeast cells expressing CER6 and CER2-LIKE proteins

Values represent averages of four biological replicates; error bars represent standard deviation.

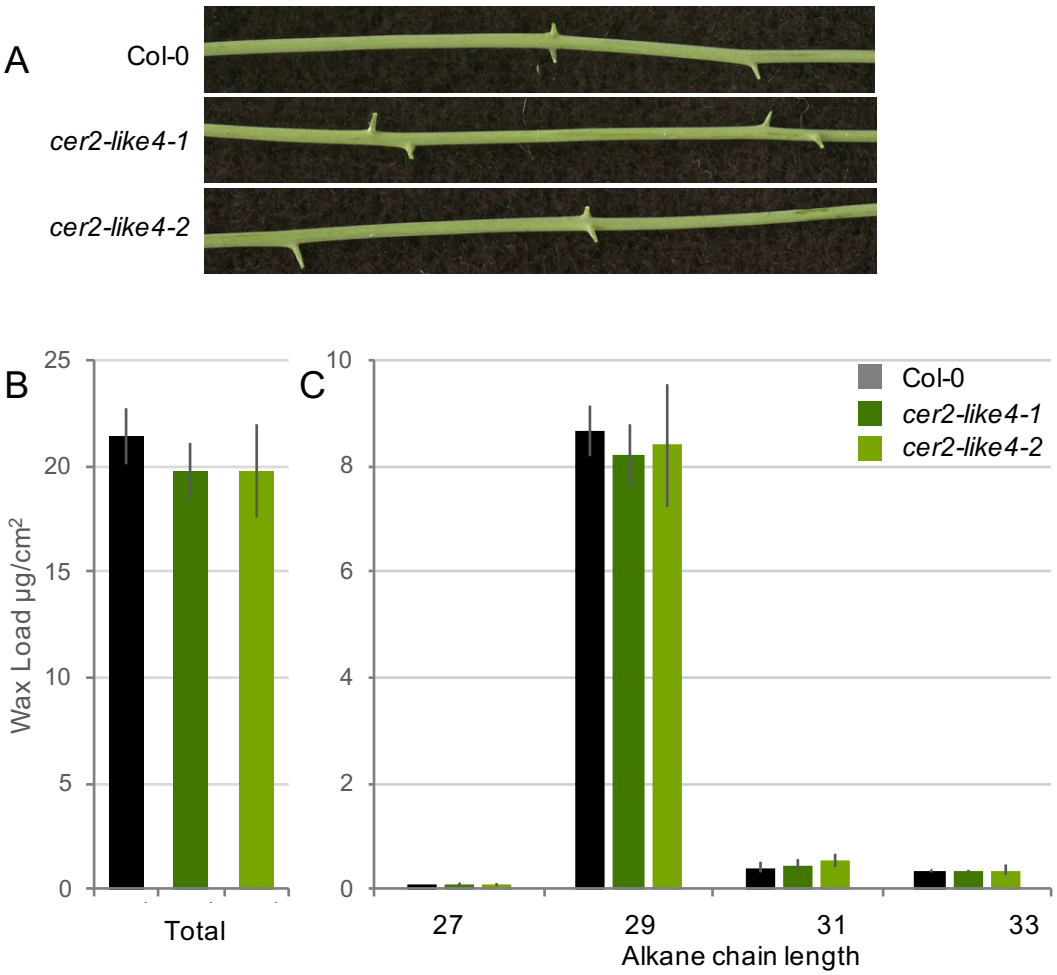

Figure 4-11: Phenotypes of *cer2-like4* mutants

(A) Stems of wild-type and *cer2-like4* mutant plants. (B) Total load and (C) alkane composition of stem cuticular wax for wild type and *cer2-like4* mutants. Values are averages of at least four biological replicates; error bars represent standard deviation.

4.3 Discussion

4.3.1 CER2-LIKEs impart unique substrate specificities to fatty acid elongation

Cuticular wax and acyl-CoA profiles of *cer2*, *cer2-like1*, and *cer2 cer2-like1* mutants demonstrate that CER2 and CER2-LIKE1 contribute to the elongation of fatty acids to different chain lengths. Building off the conclusions of Chapter 3, this observation suggests two hypotheses: (1) different CER2-LIKE proteins could associate with and thereby alter the specificity of different condensing enzymes; and/or (2) different CER2-LIKE proteins could have unique effects on the specificity of the same condensing enzyme. These possibilities are not mutually exclusive, but at least one of them must be true to account for the different phenotypes observed.

Co-expression of each of the *CER2-LIKE* genes with *CER6* in yeast demonstrated that all of the CER2-LIKEs have unique product specificity. CER2-LIKE1 and CER2-LIKE2 amino acid sequences are 66% identical, and are the most similar among the CER2-LIKE proteins. As such, I was surprised to find that CER2-LIKE1 uniquely supports elongation up to 34 carbons, while CER2-LIKE2 is similar to CER2 and CER2-LIKE3 in primarily contributing to the accumulation of 30-carbon fatty acids. This observation will be valuable in designing experiments to dissect the basis of substrate specificity of CER2-LIKE proteins.

When CER6, CER2, and CER2-LIKE1 are co-expressed, the yeast FAMEs profile is similar to that of only CER2-LIKE1 and CER6 together in that fatty acids up to 34 carbons in length are produced. CER6 + CER2 + CER2-LIKE1 cells accumulate less 30-carbon fatty acid than only CER6 + CER2, but substantially more than CER6 + CER2-LIKE1. This result suggests that there could be competition among CER2-LIKEs for activity alongside the core elongation machinery. This idea is further supported by the dramatic accumulation of 30 carbon acyl-CoAs and 29-carbon waxes in the *cer2-like1* single mutant, which greatly exceeds the loss of 32-carbon acyl-CoAs and 31-carbon waxes observed in this mutant.

When CER2, CER2-LIKE1, and CER2-LIKE2 were co-expressed with several condensing enzymes from Arabidopsis known to contribute to the synthesis of cuticular lipid precursors, they only had activity with CER6 and CER60/KCS5. The specificity of CER2-LIKEs was not changed by the identity of the condensing enzyme. That the CER2-LIKEs functioned with CER6 and CER60 was not surprising, as the amino acid sequences of these two condensing enzymes are 88.6% identical and they belong to the same clade within the FAE1-like KCS family (Joubès et al., 2008). I conclude that CER2-LIKE proteins are active only when they are co-expressed with an appropriate condensing enzyme partner. Although the identical

effects of CER2-LIKEs on CER6 and CER60 suggest that the specificity of CER2-LIKEs does not vary with different condensing enzymes, it remains a possibility that CER2-LIKE activity may be different with other condensing enzymes that were not investigated here. Without knowing what specific property of CER6 and CER60 enables them to pair with CER2-LIKEs, it is difficult to make logical predictions and design experiments to further explore this question.

4.3.2 Modification of KCS specificity by CER2-LIKEs has physiological importance

To better understand the physiological importance of CER2-LIKEs, the impact of a modified acyl-chain length profile on the downstream synthesis of cuticular waxes and on the assembly of a cuticular barrier was investigated. The strong, epidermis-specific *CER6* promoter was used to drive expression of a *CER2-LIKE1-GFP* transgene in stems of both wild-type and *cer2* plants. This resulted in a substantial increase in 31- and 33-carbon waxes, and a decrease in 29-carbon waxes in the transgenic plants compared to both genetic backgrounds. The *CER2-LIKE1-GFP* construct was able to partially complement the total wax load deficiency of the *cer2-5* mutant, demonstrating that CER2-LIKE proteins can substitute for one another's function *in vivo*. The total wax load of the transgenics in the wild-type background did not differ substantially from the non-transformed controls. This was somewhat counterintuitive, as the stems of the transgenics of both genetic backgrounds were glossy, suggesting a wax load deficiency. As the changes in relative amounts of different types of acyl lipids (e.g. ketones, alkanes, secondary alcohols, etc.) were minor compared to the relative changes in amounts of acyl chain lengths, this result suggests that wax component chain length affects the formation of wax crystals. This is in agreement with the fact that Arabidopsis leaf cuticular waxes, which are predominantly composed of 31-carbon alkanes, do not appear white or waxy, while stem cuticular wax that is largely composed of 29-carbon alkanes, secondary alcohols, and ketones, imparts a glaucous appearance to the stem. Hence, the effects of CER2-LIKE proteins on the final steps of VLCFA elongation affect the assembly and physical properties of the cuticle.

Male sterility dependent on low environmental humidity is a phenotype associated with pollen coat deficiencies, and has been observed in several Arabidopsis wax-deficient mutants (Koornneef et al., 1989; Preuss et al., 1993) including one *cer2* allele (Preuss et al., 1993; Eisner et al., 1998). The most abundant acyl lipids in the pollen coat are 29-carbon alkane, 29-carbon ketone, and 31-carbon alkene (Jessen et al., 2011), so it is not surprising that the biosynthesis of cuticular waxes and pollen coat could require the same or related gene products. I did not detect any reduction in seed set in the single *cer2-5* mutant relative to the wild type. This discrepancy with previous work could be due to subtle differences in growth

conditions, or the different alleles selected for study. However, I did observe that inactivation of both *CER2* and *CER2-LIKE2* caused male sterility in low-humidity environments. This suggests that the chain length of acyl-lipid pollen coat components is relevant to function, or that the chain length of VLCFAs is important for their conversion to alkanes and other aliphatics found in the pollen coat. The precise role of VLC-acyl lipids in the pollen coat remains unknown. It has been suggested that they could be required to create physical contact between the pollen grain and stigmatic papillae to enable the diffusion of signalling molecules, that they could provide a matrix that could stabilize other pollen coat components, or that VLC-acyl lipids could themselves function as signalling molecules (Preuss et al., 1993). Regardless of which of these functions VLC-acyl lipids fulfill in the pollen coat, my data show that CER2-LIKEs are required for fertilization.

4.3.3 The function of CER2-LIKE4 remains unknown

The role of CER2-LIKE4 in VLCFA metabolism remains unknown. Co-expression of *CER6* with *CER2-LIKE4* in yeast resulted in reduced 26-carbon fatty acid accumulation, and co-expression of *CER6*, *CER2*, and *CER2-LIKE4* resulted in lower accumulation of 30-carbon fatty acid. This suggests that *CER2-LIKE4* could function as a negative regulator of wax biosynthesis by restricting the production of VLCFA precursors of cuticular wax. However, as previously discussed, quantitative changes in fatty acid production in the heterologous yeast system are difficult to interpret, and are arguably meaningless in the absence of a *cer2-like4* mutant phenotype.

Unfortunately, no change in stem cuticular wax load and composition was detected in *cer2-like4* mutant plants. It remains a possibility that CER2-LIKE4 could affect wax biosynthesis under stress conditions, or that CER2-LIKE4 could contribute to or regulate VLCFA flux into other lipid biosynthetic pathways. Cursory evaluation of *CER2-LIKE4* expression patterns reported on the Arabidopsis eFP browser (Winter et al., 2007) reveals that its expression is up-regulated in the L1 layer of the shoot apical meristem. In these rapidly dividing, polarized epithelial cells, I expect that both wax and sphingolipid biosynthesis are highly active. Recent work has demonstrated that hydroxylated 24- and 26-acyl chains incorporated in ceramides are required to support polarized secretion in young root epithelial cells (Wattelet-Boyer et al., 2016). I anticipate that similar sphingolipids could be required in the L1 of the shoot apical meristem to support polar secretion of cuticular lipids and cell wall carbohydrates. Because ceramides incorporate shorter VLCFAs than are used for wax metabolism, one hypothesis for the function of CER2-LIKE4 is that it could serve as a ‘brake’ that limits substrate channelling

into wax biosynthesis by reducing the production of VLCFAs 26 carbons and longer. This would ensure that sufficient VLCFAs are available for ceramide synthesis, and would be particularly important when wax metabolism is up-regulated under stress conditions. Therefore, it will be important to examine the *cer2-like4* wax and sphingolipid phenotypes of plants subjected to conditions known to up-regulate wax production, including drought, cold, and high light intensity.

An alternative hypothesis is that CER2-LIKE4 could support the production of 28-carbon fatty acids. This is suggested by the fact that yeast cells expressing CER6, CER2, and CER2-LIKE4 accumulated more 28-carbon FAME than cells co-expressing CER6 and CER2. 28-carbon acyl-CoAs are preferentially used by the fatty acyl reductase, CER4/FAR3, which generates cuticular fatty alcohols. While this hypothesis is not supported by wax analysis of *cer2-like4* mutants, it is possible that a reduction in primary alcohol load might be observed when the *cer2-like4* mutation is introduced to a genotype and cell type that accumulates more of these particular waxes, such as stems of the *cer2* single mutant. Analysis of the *cer2-like4* phenotype in stems and leaves of *cer2 cer2-like1 cer2-like2* mutants is currently underway.

4.3.4 Summary of implications for models of CER2-LIKE metabolic function

While the focus of this chapter has been a descriptive characterization of the breadth of biological functions of CER2-LIKEs, I can also make inferences from these results that pertain to the biochemical, mechanistic contribution of these proteins to elongation. CER2-LIKEs contribute to the chain-length specificity of elongation, and functionally partner only with specific condensing enzymes. Further, the functions of CER2-LIKEs are unique and competitive, with individual proteins having the capacity to positively or negatively affect elongation. These conclusions will be incorporated in models of activity of CER2-LIKEs developed at the end of Chapter 5.

Chapter 5: Biochemical characterization of ECERIFERUM2

5.1 Introduction

Based on sequence homology, CER2 was annotated as a BAHD acyltransferase. BAHDs transfer an acyl group from a CoA-thioester to either an alcohol or amine acyl acceptor, generating an ester or amide bond, respectively (Figure 1-4). BAHD acyltransferases are plant- and fungi-specific enzymes that use diverse substrates in a wide variety of specialized metabolic pathways, are soluble, monomeric, and are localized to the cytosol. Their catalytic mechanism has been characterized extensively using protein modelling and site-directed mutagenesis (reviewed in D'Auria, 2006). While CER2 is homologous to this family of enzymes, and was, in fact, one of the first members of the family to be identified, CER2 differs markedly from other characterized BAHDs in two respects.

First, CER2 with C-terminally fused green fluorescent protein (GFP) localizes predominantly to the ER (Section 3.2.3). This makes biological sense in that the ER is the site of VLCFA elongation. However, it is unusual for a BAHD acyltransferase, particularly since CER2 does not have any predicted transmembrane domains or an ER targeting signal (Aramemnon; Schwacke et al., 2003). Therefore, either post-translational modifications of the CER2 protein or interactions between CER2 and ER membrane-localized proteins may be involved in CER2 localization. It is tempting to speculate that CER2 interaction with other protein components of the fatty acid elongase complex may account for CER2 association with the ER.

Second, two conserved motifs have been described for BAHDs: carboxy-terminal DFGWG, which is predicted to have a function in retaining structural stability of the enzyme but is not present in all BAHDs, and HXXXD, which catalyzes the acyl transfer reaction (D'Auria, 2006). All of the CER2-LIKEs that I identified lack the putatively stabilizing DFGWG motif. However, this may not be surprising given that BAHDs are soluble enzymes (D'Auria, 2006; Panikashvili et al., 2009; Rautengarten et al., 2012), while CER2 and CER2-LIKE1 localize to the ER membrane. Perhaps the DFGWG motif is not required when these proteins are in association with the ER.

Site-directed mutagenesis experiments on anthocyanin malonyltransferase of *Salvia splendens* (Suzuki et al., 2003), vinorine synthase of *Rauvolfia serpentina* (Bayer et al., 2004), hydroxycinnamoyltransferases of *Coffea canefora* (Lallemande et al., 2012), and *Sorghum bicolor* (Walker et al., 2013) have demonstrated that the histidine residue within the HXXXD motif is essential for enzyme activity. The histidine residue is thought to be responsible for deprotonating the alcohol or amine acyl acceptor, creating a nucleophile that attacks the carbonyl carbon of the acyl-CoA, and resulting in the release of CoASH and formation of a new ester or amide bond (Figure 1-4). The importance of the conserved histidine residue is supported by the crystal structures of vinorine synthase from *Rauvolfia* and anthocyanin malonyltransferase from *Chrysanthemum*, in which the histidine residue is ideally positioned at the junction of the acyl donor and acyl acceptors within the active site (Ma et al, 2005; Unno et al, 2007).

Both *CER2-LIKE1* and *CER2-LIKE4* lack a histidine in their predicted HXXXD motifs (Figure 5-1). Genetic analysis of a null *cer2-like1* mutant (Chapter 4) revealed that despite this abnormality, CER2-LIKE1 has an analogous role to CER2 in VLCFA elongation. This, and the absence of an obvious purpose of an acyl transfer reaction in the elongation of VLCFAs to specific chain lengths, led me to question whether CER2-LIKEs have acyl transfer activity.

Beyond the transferase domain and its catalytic motif, there are no recognizable features in CER2-LIKE proteins that suggest a biochemical function. I took several approaches to search for clues as to how CER2 might participate in elongation. First, I used site-directed mutagenesis to determine whether CER2 requires its HXXXD motif for function. I characterized interactions between CER2 and components of the core elongase complex using the split-luciferase system, and used co-immunoprecipitation to confirm CER2-CER6 interaction. I also tested whether interaction with CER6 was required for CER2 targeting to the ER by comparing the localization of CER2-GFP in *cer2* and *cer2 cer6* genetic backgrounds. I generated sequence chimeras of CER2-LIKE1 and CER2-LIKE2, the two CER2-LIKEs with the greatest sequence identity in Arabidopsis, to investigate what features determine their distinct substrate-specificities. Finally, I used homology-based tertiary structure models to compare CER2-LIKE structures to each other, and to BAHDs with confirmed acyl transfer function.

Figure 5-1: Amino acid alignment of CER2-LIKE BAHD acyltransferases from Arabidopsis

The HXXXD motif of CER2 is marked with a black box. The predicted catalytic histidine residues of all five homologs are shaded red. The sequence swap sites discussed in Section 5.2.3 are marked S#. The histidine residues discussed in Section 5.2.4 are highlighted in blue.

5.2 Results

5.2.1 CER2-LIKEs do not require a conserved acyltransferase motif for function

Site-directed mutagenesis was used to modify the putatively catalytic histidine 166 of CER2 to determine if it is required for CER2 function. Histidine was replaced with alanine (H166A), to knock out any catalytic activity at this site, and asparagine (H166N), to mimic CER2-LIKE1. Constructs with these mutant alleles, as well as a wild-type control (H166H), were transformed into *cer2* mutant plants. In each case, insertion of the transgene and the mutant background were confirmed by PCR-based genotyping, and Sanger sequencing of the transgene verified the mutations. Plants were visually examined for glossiness/glaucousness, and wax load and composition were measured by GC-FID. Both mutant alleles fully complemented the background mutant phenotype, indicating that CER2 does not have the described catalytic mechanism of characterized members of the BAHD acyltransferase family (Figure 5-2).

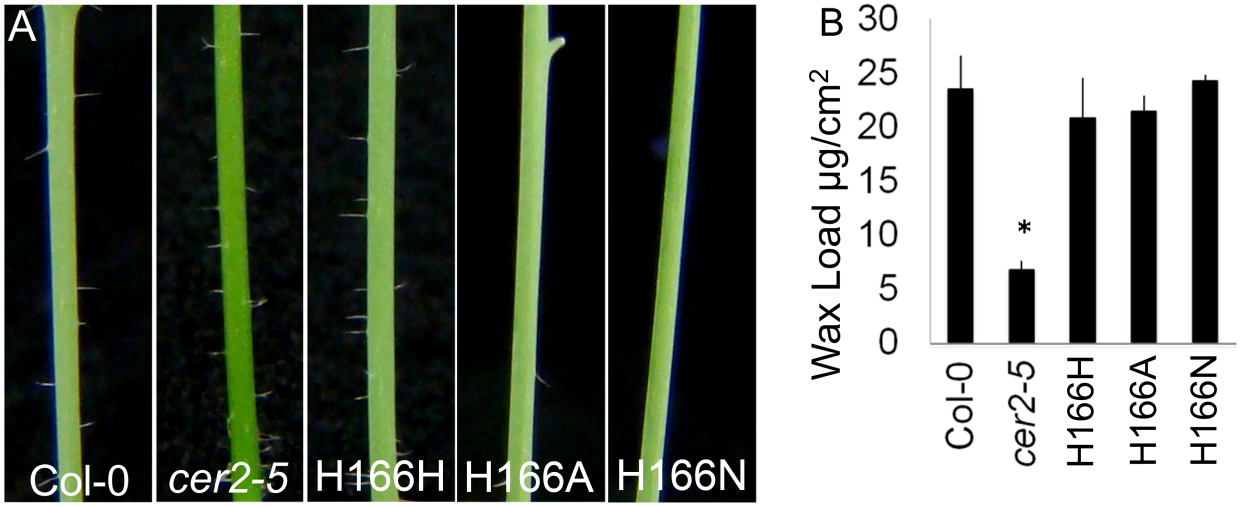

Figure 5-2: Phenotypes of the *cer2-5* mutant transformed with H166-modified *CER2* sequences

(A) Inflorescence stems of (left to right) Col-0 wild type, *cer2-5*, *cer2-5* complemented with wild-type, H166A, and H166N CER2 sequences. (B) Total wax load of inflorescence stems from the same genotypes. Values are the average of four biological replicates. Error bars represent SD. The asterisk denotes significant difference between the total wax loads as determined by a Student's T-test ($p<0.05$). Reproduced with permission from Haslam et al., 2012; Copyright American Society of Plant Biologists © 2012 (www.plantphysiology.org).

5.2.2 CER2 and CER6 physically interact

5.2.2.1 Split-luciferase

Interactions between CER2 and the core elongase complex were investigated using the split-luciferase system in *Nicotiana benthamiana* (tobacco) leaf. All of the elongase components were cloned to produce either N- or C-terminal fusions to either the C-terminal or N-terminal half of the firefly luciferase enzyme, respectively, and co-expressed with CER2 fused with the opposite luciferase half. Luminescence is produced when the two co-expressed fusion proteins interact or come in such close physical proximity as to allow the luciferase enzyme halves to reconstitute the entire, light-producing enzyme.

Luminescent signal was anticipated even when observing negative controls, as all of the proteins were over-expressed, and localize to the ER. Another complication of working in tobacco leaf is that the capacity for infiltration, and competency for transformation, varies greatly among plants, and between different stages of leaf development. Hence, each technical replicate for each putative interaction pair was normalized against a negative control interaction pair infiltrated symmetrically to the same tobacco leaf. Hydroxymethylglutaryl-CoA reductase (HMG1) was used as a negative control as it is not expected to interact with CER2, but is similar to elongase enzymes in that it is an ER-localized transmembrane protein (Leivar et al., 2005). Protein pairs that truly interact were expected to produce more luminescence than their coupled negative control pair. The validity of the HMG1 + CER2 negative control was confirmed using a second negative control, ACA2, to ensure that both HMG1 and ACA2 produce equal luminescence levels when co-expressed with CER2. *ACA2* is *CALCIUM ATPASE2,* a calcium transporter localized to the ER (Hong et al., 1999). A sample, hypothetical experiment is presented in Figure 5-3 to illustrate how data was collected.

Sources of error that produce falsely negative results, such as protein degradation, mis-folding, or mis-targeting were anticipated, but these were expected to vary among different proteins, and different protein fusions. Therefore, while there are two construct pairs possible for each interaction tested (e.g. CLuc-CER2 + CER6-NLuc vs. CER2-NLuc + CLuc-CER6), whichever pair produced the greatest luminescence was considered to be the most accurate, and is presented in Figure 5-4. Interaction was detected between CER2 and all components of the core elongase complex (Figure 5-4). CER2 interactions with CER6, PAS2, and CER10 were all 7- to 9-fold greater than the negative control, and CER2-KCR1 interaction was nearly 5-fold greater than the negative control. CER2 co-expressed with itself, in the opposite luciferase fusion, also interacted, producing roughly 7-fold more luminescence than the negative control.

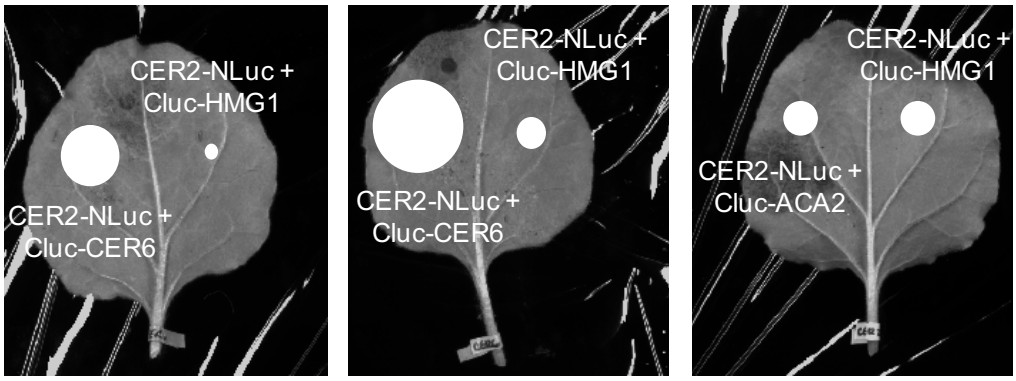

Figure 5-3: Schematic representation of the split luciferase assay

Each technical replicate was normalized using the CER2-HMG1 interaction pair infiltrated symmetrically to the same *N. benthamiana* leaf. While luminescence of the CER2-CER6 pairs is different between the two technical "replicates" shown here at the left and centre, the ratio between light emitted by the test and control pairs is the same. On the right, the second negative control used, ACA2, produces the same luminescence paired with CER2 as does HMG1.

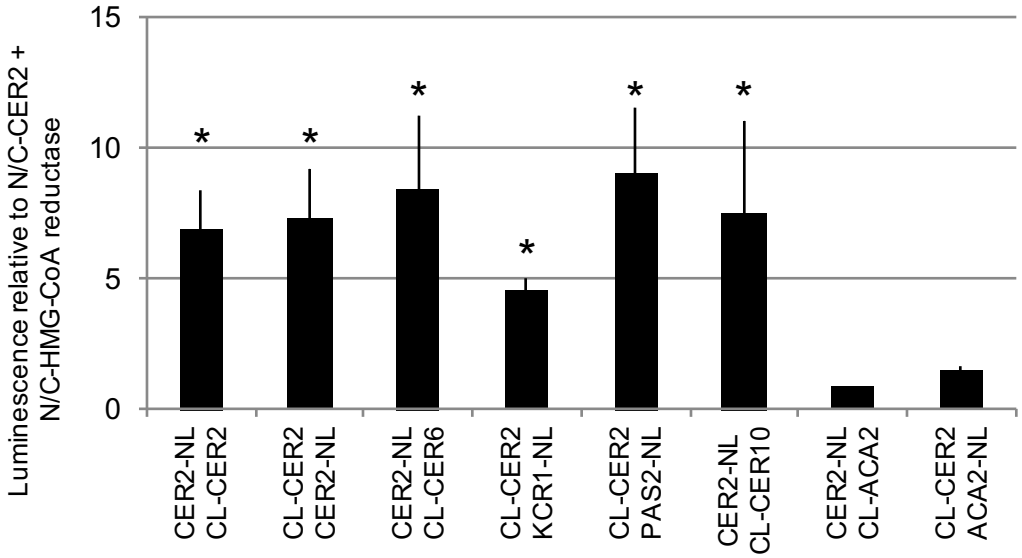

Figure 5-4: Split luciferase assay of CER2 paired with core components of the fatty acid elongase

NL= N-terminal fragment of luciferase, CL= C-terminal fragment of luciferase. All proteins were fused to both N- and C-terminal fragments of luciferase; the pair that showed the greatest luminescence is presented. ACA2 = calcium ATPase, an ER-localized protein used as a negative control. Bars are mean +/- SD, n=3, asterisks denote significance in a Student's T-test compared to corresponding assay with CER2 paired with ACA2, $p<0.05$.

5.2.2.2 Co-Immunoprecipitation

To confirm that CER2 and CER6 physically interact, I attempted to co-immunoprecipitate the two proteins from solubilized microsomes of yeast cells co-expressing epitope-tagged CER2 and CER6. A triple hemagglutinin tag was fused to the N-terminus of CER2, and a triple c-MYC tag was fused to the N-terminus of CER6. Both were constitutively expressed in yeast cells using the GPD promoter. Microsomes were prepared and solubilized from cells co-transformed with HA_3-CER2 and MYC_3-CER6 constructs.

Solubilization of the microsomes was inconsistent. Frequently, more protein was detected in the insoluble fraction compared to the soluble fraction used for the immunoprecipitation, and the efficiency of CER2 and CER6 solubilization did not always match. Therefore, the efficiency of each solubilization was checked by dot blot before proceeding with immunoprecipitation and western blot.

anti-c-MYC antibody coupled with protein-A/G beads were used to immunoprecipitate MYC_3-CER6. MYC_3-CER6 was not consistently pulled down; some MYC_3-CER6 could almost always be detected in the free, unbound fraction. However, when MYC_3-CER6 was immunoprecipitated, so was HA_3-CER2 (Figure 5-5). This result confirms that CER2 and CER6 interact. Further, given that HA_3-CER2 and MYC_3-CER6 were heterologously expressed and isolated from yeast cells, co-immunoprecipitation of CER2 indicates that the two proteins interact directly.

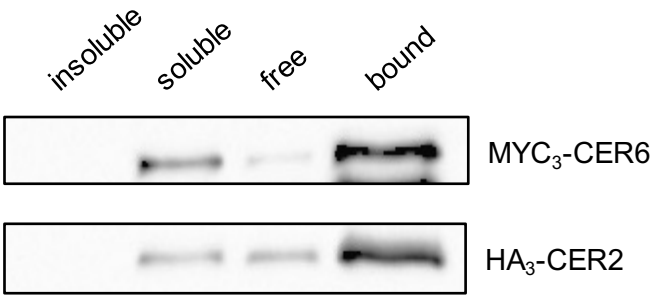

Figure 5-5: Co-Immunoprecipitation of HA_3-CER2 with MYC_3-CER6

Insoluble, soluble, free and bound fractions of yeast microsomes separated by SDS-PAGE and probed with either anti-MYC (top) or anti-HA (bottom). The soluble fraction was the input for co-immunoprecipitation. The band visible below CER6 in the bound product lane is the heavy chain of the immunoglobulin used for the immunoprecipitation.

5.2.2.3 CER6 is required for correct localization of CER2

Localization of CER2 to the ER membrane is curious in that CER2 does not have an ER-targeting signal, nor any transmembrane domains. Additionally, other members of the BAHD acytransferase family have all been found to be soluble, cytosolic proteins. I suggested in Chapter 3 that CER2 interactions with CER6 might be required for correct CER2 localization to the ER. To test this hypothesis, localization of the CER2-GFP protein (construct described in section 2.3.1, initial experiment in section 3.2.2) was examined in a null *cer6* mutant background, *ew2*. The *ew2* mutant was a gift from Dr. Ellen Wisman; the mutant was generated in a screen for phenylpropanoid-deficient mutants using the *En-1* transposable element as a mutagen (Wisman et al., 1998). In *ew2*, the transposable element is located 782 bp from the start codon of *CER6* (Figure 5-6A), and no full-length *CER6* transcript is produced (Figure 5-6B). The *En-1* transposable element is mobile in Arabidopsis, but no reverting or chimeric progeny were observed. Analysis of the stem cuticular wax of *ew2* revealed a 97% reduction in the stem cuticular wax load (Figure 5-6C).

The *ew2* mutant was crossed with *cer2* mutants carrying the *35Spro::CER2-GFP* construct. F_2 progeny carrying the transgene were selected by sowing seeds on hygromycin, and genotypes of the *ew2* and *cer2-5* mutants were determined by PCR-based genotyping. Three double mutant lines derived from independent *35Spro::CER2-GFP* transgenic plants were selected for analysis, as well as three *cer2-5* single mutants (also independent lines carrying the *35Spro::CER2-GFP* transgene) for comparison.

As described in section 3.2.3, GFP fluorescence in the *cer2-5* single mutant was consistently observed in a fine, bright, reticulate pattern. In the *cer2-5 ew2* double mutant background, GFP fluorescence was diffuse, taking shape in the contours of organelles. This pattern of fluorescence matched that of free, cytosolic GFP. This result indicates that CER6 is needed for localization of CER2 to the ER.

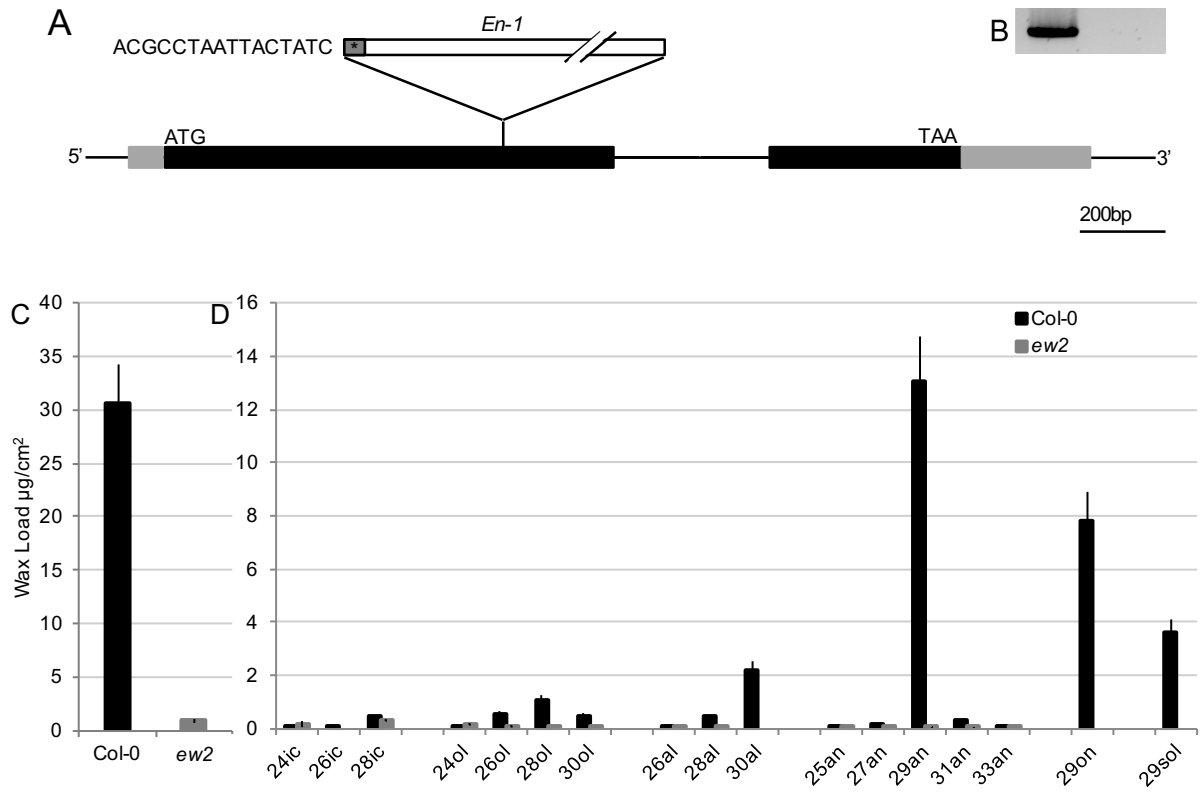

Figure 5-6: Characterization of the *ew2* mutant allele of *CER6*

A, *En-1* insertion site in the first exon of *CER6*. The *En-1* transposable element is represented with an open white box. The dark grey box marked with an asterix adjacent to *En-1* represents additional, chimeric sequence that was found inserted between *En-1* and the *CER6* gene. A part of this fragment is identical to non-coding sequence downstream of the gene At1g68490, and a second part is identical to non-coding sequence downstream of At1g68875. Coding sequence of *CER6* is marked with a solid black box, and the untranslated regions (UTRs) are marked in pale grey boxes. Introns and un-transcribed flanking genomic DNA is presented as a straight black line. B, RT-PCR of full-length *CER6* transcript in wild-type Col-0 (left) and *ew2* (right). No full-length transcript was detected in the *ew2* mutant. C, Wild-type and *ew2* total stem wax loads and, D, stem wax compositions. Load and composition are both measured as the average of at least four biological replicates, with error bars representing SD.

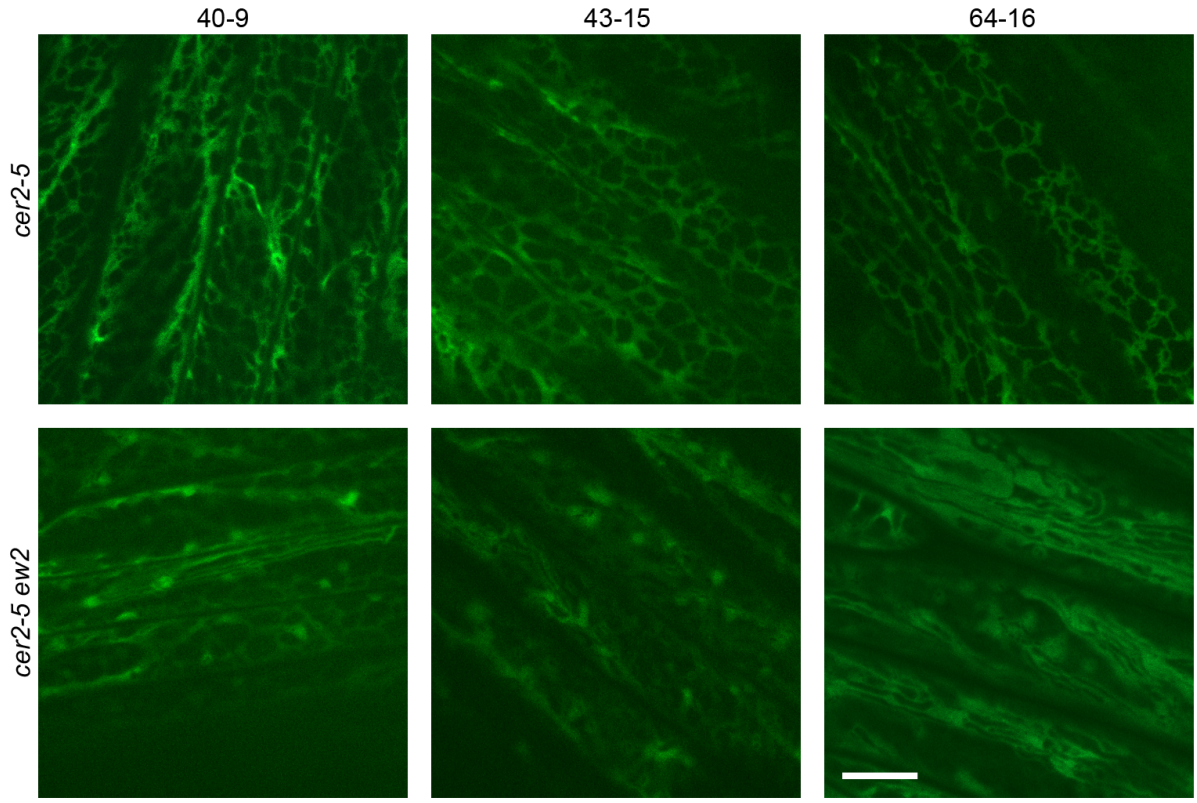

Figure 5-7: Localization of CER2-GFP in *cer2-5* and *cer2-5 ew2* mutant backgrounds

cer2-5 and *cer2-5 ew2* individuals derived from the same lines carrying the *CER2-GFP* transgene. Images were taken 10 cm from the stem apex, where fine, reticulate ER can be easily and consistently observed. Scale bar = 10 μm.

5.2.3 CER2-LIKE substrate specificity is determined by an N-terminal sequence

Conserved domains and motifs often help predict protein function. The only domain annotated for the CER2-LIKE proteins is a transferase; this designation is questionable in light of the fact that the HXXXD catalytic motif of this domain is not required for CER2-LIKE function. To break down the amino acid sequences of CER2-LIKEs into functional units, sequence swaps were carried out between *CER2-LIKE1* and *CER2-LIKE2* coding sequences. The chimeric genes were then expressed in a yeast elongation assay to determine what sequences affect CER6/CER2-LIKE product specificity.

CER2-LIKE1 and CER2-LIKE2 were selected for this experiment because they have the greatest sequence identity among the CER2-LIKE proteins of Arabidopsis (Table 5-1) but they have distinct substrate specificities. Percent identity was determined with Clustal 2.1.

Table 5-1: Percent identity matrix of CER2-LIKE proteins from Arabidopsis

	CER2	CER2-LIKE1	CER2-LIKE2	CER2-LIKE3	CER2-LIKE4
CER2	100.00	36.23	37.37	21.90	19.82
CER2-LIKE1	36.23	100.00	65.55	21.46	21.43
CER2-LIKE2	37.37	65.55	100.00	22.36	20.61
CER2-LIKE3	21.90	21.46	22.36	100.00	25.57
CER2-LIKE4	19.82	21.43	20.61	25.57	100.00

Primers used for domain swaps are listed in Table 2-7. All CER2-LIKE chimera and control constructs were cloned in the p423 vector with histidine selection, using the same restriction sites and with identical AAAA Kozak consensus sequences inserted upstream of the ATG start codon (S. Nakagawa et al., 2007). All of the chimeras generated for this experiment are illustrated in Figure 5-8, and the swap sites are marked in the sequence alignment presented at the beginning of this chapter (Figure 5-1). The swap sites were selected in regions of identical sequence for CER2-LIKE1 and CER2-LIKE2, so that chimeras could be generated by overlap extension PCR. All chimeras were co-expressed with the CER6 condensing enzyme. Unmodified CER2-LIKE1 and CER2-LIKE2 constructs were used as controls.

The first pair of chimeras, A and B, have sequence swap sites just downstream of the predicted HXXXD motif. Chimera A has the N-terminus of CER2-LIKE1 and the C-terminus of CER2-LIKE2; Chimera B has the N-terminus of CER2-LIKE2, and the C

terminus of CER2-LIKE1. Chimera A had no activity; the yeast cells co-expressing CER6 and chimera A had the same FAMEs profile as cells transformed with only CER6. Chimera B had the same substrate specificity as CER2-LIKE2, producing 30-carbon VLCFA, and a lesser amount of 32-carbon VLCFA (Figure 5-9). The position of the sequence swap site might have produced an unstable chimera A, so a second set of chimeras was created, chimeras C/D/E/F, with the swap site moved both up- and down-stream of the swap site selected for chimeras A and B.

Chimeras C and D have a swap site positioned one third of the coding sequence downstream from the ATG, and chimeras E and F have a swap site positioned two thirds of the coding sequence downstream from the ATG. C and E have the N-terminus of CER2-LIKE1 and the C-terminus of CER2-LIKE2. Both had activity similar to CER2-LIKE1 when co-expressed with CER6 in yeast; that is, they produced small amounts of both 32- and 34-carbon VLCFAs. D and F, on the other hand, have the N-terminus of CER2-LIKE2 and the C-terminus of CER2-LIKE1, and both had similar activity to CER2-LIKE2. The major product of elongation with these chimeras was 30-carbon fatty acid, with some 32-carbon fatty acid accumulating as well (Figure 5-9). These results indicate that product specificity is determined by the N-terminal third of the CER2-LIKE1 and CER2-LIKE2 protein sequences.

Another set of chimeras was generated to narrow down the N-terminal sequence required for product specificity. Chimeras G and H have a swap site positioned roughly 100 amino acids from the start codon. Chimera G has the 100 N-terminal amino acids from CER2-LIKE1, and displayed activity similar to CER2-LIKE1. Chimera H, which has the opposite composition, had activity similar to CER2-LIKE2 (Figure 5-9). The last set of chimeras, I and J, finally broke this trend, as neither had activity that could be described as similar to either CER2-LIKE1 or CER2-LIKE2. Chimera I, which has only the N-terminal 50 amino acids of CER2-LIKE1 and the remaining sequence from CER2-LIKE2, was similar to CER2-LIKE2 in that its major product was 30-carbon VLCFA with a lesser amount of 32-carbon VLCFA. However, the yield of both of these products with chimera I was roughly 50% that of CER2-LIKE2. Chimera J, which has the N-terminal 50 amino acids from CER2-LIKE2 and the remaining sequence from CER2-LIKE1, produced 30-carbon VLCFA and a large amount of 32-carbon VLCFA, which is not a major product for any of the wild-type Arabidopsis CER2-LIKE proteins (Figure 5-9). These results indicate that N-terminal 100 amino acid fragments of CER2-LIKE1 and CER2-LIKE2 are necessary to confer product specificity, and that further divisions within these proteins disrupt specificity.

5.2.4 The N-terminal sequence is not sufficient for CER2-LIKE activity

The 100 N-terminal amino acids of CER2-LIKE1 and CER2-LIKE2 are necessary to confer their product specificity when paired with the CER6 condensing enzyme. However, whether this sequence is sufficient for CER2-LIKE activity is unclear. To test this, the CER2-LIKE2 protein was truncated after only the first 100 amino acids, and co-expressed with CER6 in yeast. Not surprisingly, the truncated CER2-LIKE2 was not functional (Figure 5-9).

Cleaving the C-terminal fragment from CER2-LIKE2, which accounts for more than 75% of the protein, is a very drastic modification. The tertiary structure of the N-terminus, and by extension any putative function of the N-terminus, could easily be compromised by this truncation. Therefore, the N-terminal fragment of CER2-LIKE2 was tagged onto CER2-LIKE3 and aliphatic suberin feruloyl-transferase (ASFT) proteins with their N-terminal fragments removed. This was done in an attempt to provide the N-terminal peptide fragment of CER2-LIKE2 some structural support. CER2-LIKE3 and ASFT were selected as they have high and low levels of sequence identity with CER2-LIKE2, respectively. Unmodified ASFT and CER2-LIKE3 were also co-expressed with CER6 as controls in the elongation assay. At the time that this experiment was designed, it was not known that CER2-LIKE3 is a CER2-LIKE. It was only clear that the gene encoding CER2-LIKE3, At4g29250, was homologous to BAHDs, was not characterized, and had relatively high sequence identity to CER2-LIKE2. Because the phylogenetic tree used as reference (Yu et al., 2009) did not cluster At4g29250 with the other CER2-LIKEs, it was not expected to have similar activity.

The entire ASFT protein did not function with CER6, and neither did chimera K, which has the N-terminal sequence of CER2-LIKE2 tagged to the C-terminus of ASFT. Unmodified At4g29250 elongated VLCFAs to 30-carbons. This experiment serendipitously revealed that there was something important missing from the phylogeny I used as reference. Chimera L, which has the N-terminus of CER2-LIKE2 tagged on to the C-terminus of At4g29250, was non-functional (Figure 5-9). This demonstrates that the role of the 100 N-terminal amino acids in product specificity is a character unique to the CER2-LIKE1 - CER2-LIKE2 pair.

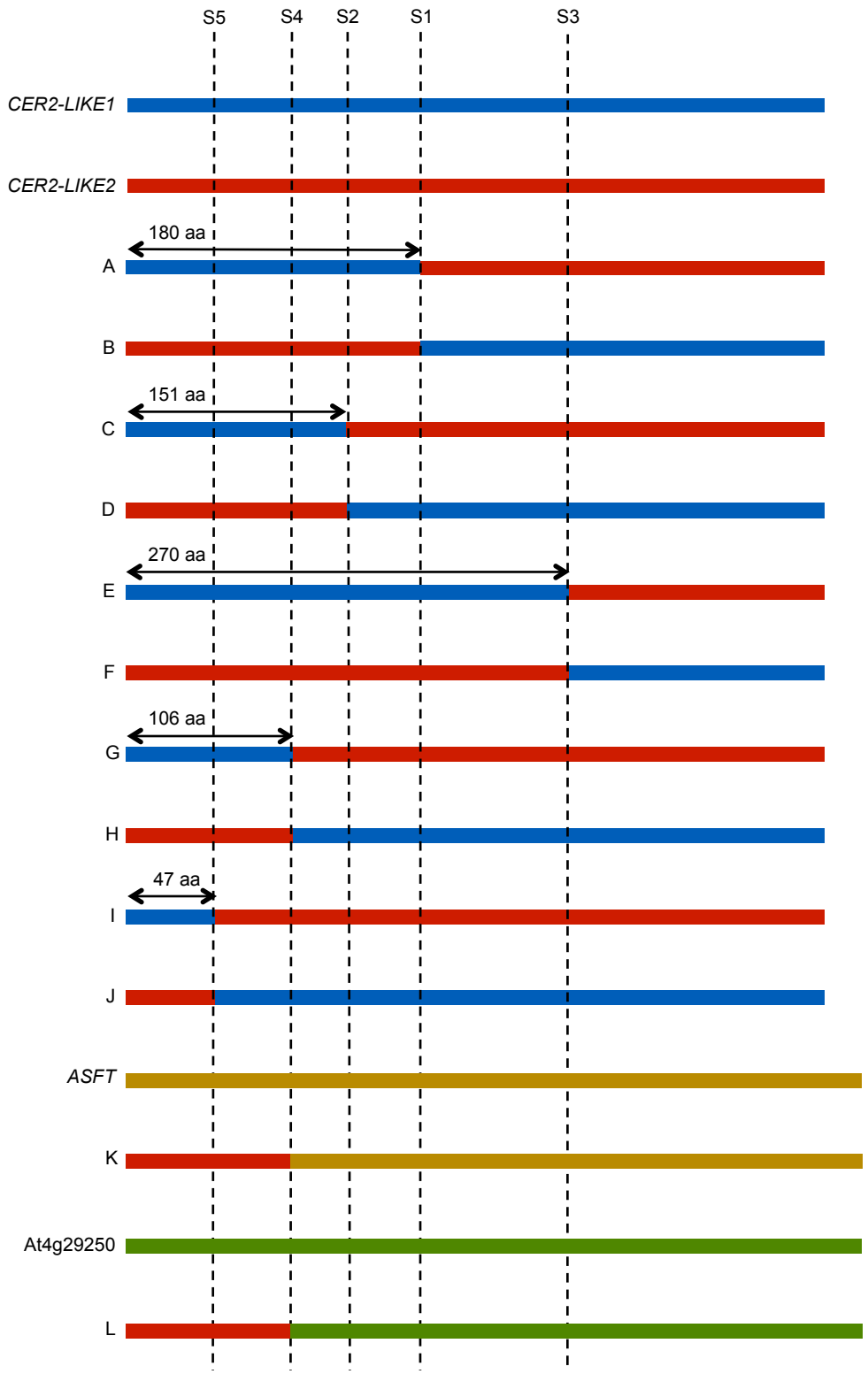

Figure 5-8: CER2-LIKE1 and CER2-LIKE2 chimeras used for yeast elongation assay with CER6

Chimeras were generated by overlap extension PCR. CER2-LIKE1 sequence is represented in blue, CER2-LIKE2 sequence in red, ASFT in gold, and CER2-LIKE3 in green.

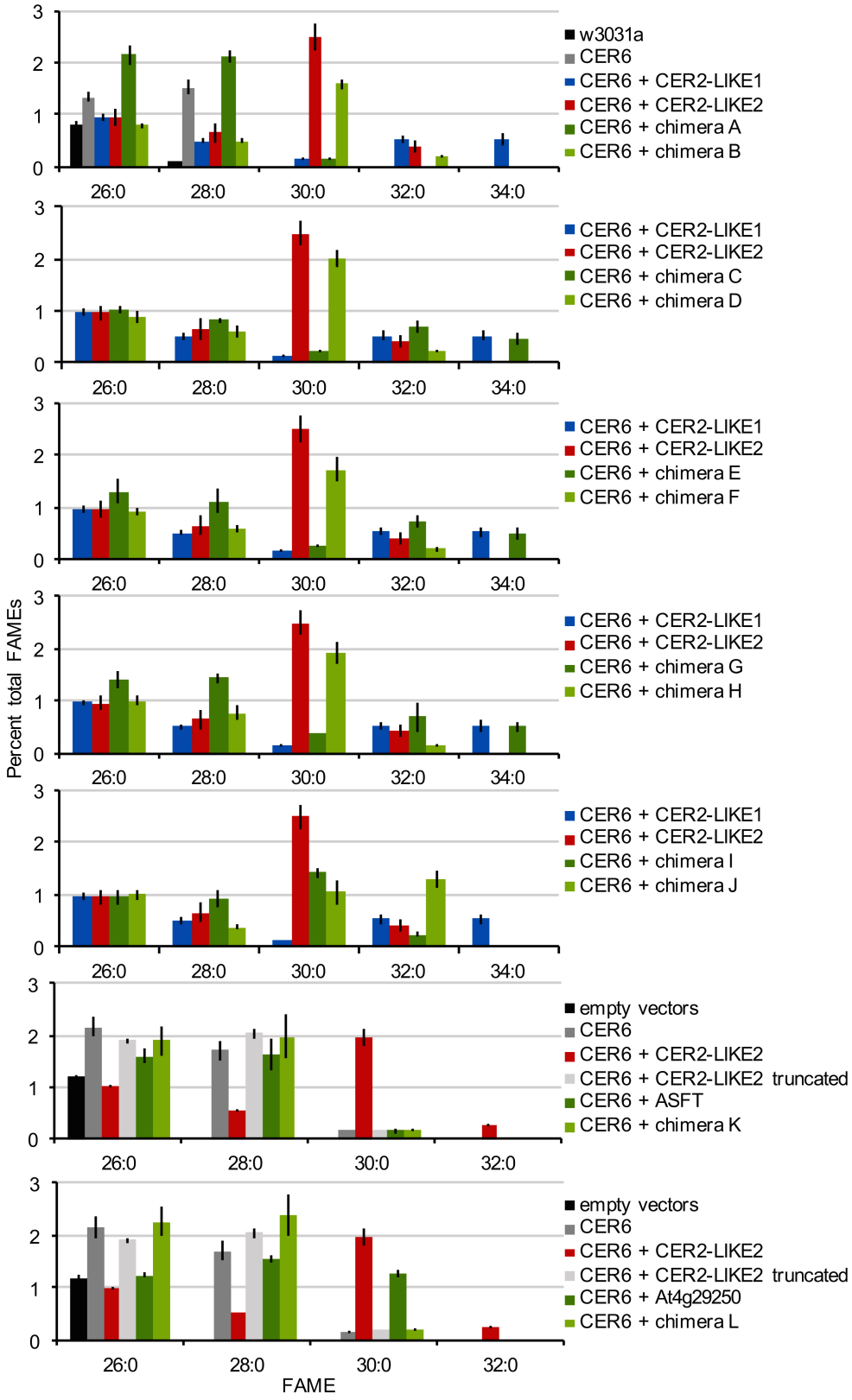

Figure 5-9: Elongation assay of chimeric CER2-LIKE proteins with CER6 in *S. cerevisiae*

Values are averages of at least four biological replicates, and error bars represent standard deviation.

5.2.5 Insight from CER2-LIKE structural models

Crystal structures have been solved for several plant BAHD acyltransferases; vinorine synthase from *Rauvolfia* (Ma et al., 2005), anthocyanin malonyltransferase from *Chrysanthemum* (Unno et al., 2007), hydroxycinnamoyl transferases from *Sorghum bicolor* (Walker et al., 2013) and *Coffea canefora* (Lallemand et al., 2012), and a promiscuous malonyltransferase from tobacco (Manjasetty et al., 2012) (Protein Databank). There are also crystal structures available for several unrelated acyltransferases that have similar catalytic functions to BAHDs. While there are no structures available for CER2-LIKEs, homology modelling based on known BAHD structures has the potential to reveal similarities and differences both among CER2-LIKEs and between CER2-LIKEs and BAHDs that might cast light on CER2-LIKE metabolic function.

Phyre2 (protein homology/analogy recognition engine) was used to model all five CER2-LIKEs from Arabidopsis (Kelley and Sternberg, 2009). Phyre2 compares a query sequence with sequences of proteins with known crystal structures. A protein that will serve as the best structural template for the query is selected based on sequence homology, secondary structure homology, and the presence of insertions and deletions. An alignment between the template and the query is then used to generate a tertiary structure prediction for the query. Phyre2 identified hydroxycinnamoyl-CoA shikimate hydroxycinnamoyl transferase from *Sorghum bicolor* (SbHCT) as the best structural template for CER2, and generated a model for CER2 based on SbHCT that covers 96% of the CER2 sequence (Figure 5-10).

The position of the N-terminal sequence that affects substrate specificity (Section 5.2.3) was examined on the CER2 model. Largely, this peptide sequence was positioned on the surface of the protein, removed from a channel running through its core. That a surface feature of CER2 could determine its product specificity supports the notion that the activity of CER2 could be mediated by physical interaction with other proteins, namely the CER6 condensing enzyme.

Structural models for all of the remaining CER2-LIKE proteins were also generated based on SbHCT (Figures 5-11, 5-12, 5-13, 5-14). With the exception of CER2-LIKE4, all of the CER2-LIKE models had comparable shapes, with channels that passed through the core of each protein. The N-terminal portions of the peptides were largely positioned on the surface of each protein.

A channel running through the core the protein was evident in CER2 model. Interestingly, the predicted catalytic histidine of the HXXXD motif (H166) was positioned with its imidazole side chain pointing inwards near the center of the channel, similar to true BAHD

acyltransferases. Examination of other residues lining the channel revealed the presence of another histidine, H38, positioned in very close proximity and with similar orientation to H166, despite being distant from the catalytic motif in the amino acid sequence. Notably, H38 lies within the N-terminal sequence that affects product specificity.

It is clear from the CER2-LIKE sequence alignment (Figure 5-1) that CER2-LIKE1, CER2-LIKE2, and CER2-LIKE3 all have N-terminal histidine residues that align with H38 of CER2; the only CER2-LIKE that lacks this N-terminal histidine residue is CER2-LIKE4. Importantly, the positions of the N-terminal histidines in each CER2-LIKE structural model were also consistently in close proximity to the HXXXD histidine (Figures 5-10, 5-11, 5-12, 5-13, 5-14). It seems possible that these N-terminal histidines could take the role ascribed to HXXXD histidine residues based on sequence homology, and act as base catalysts for an acyl transfer reaction. This would explain why the HXXXD histidine is absent from some CER2-LIKEs (CER2-LIKE1) and is simply not required for function in others (CER2). However, it remains completely obscure how an acyl transfer could be useful in the process of elongation, should CER2-LIKEs have such activity. To determine if this second-site N-terminal histidine is required for CER2 function in VLCFA elongation, and by extension, whether CER2-LIKEs are likely to contribute to elongation via acyl transfer function, site-directed mutagenesis on H38 of CER2 was performed (Section 5.2.6).

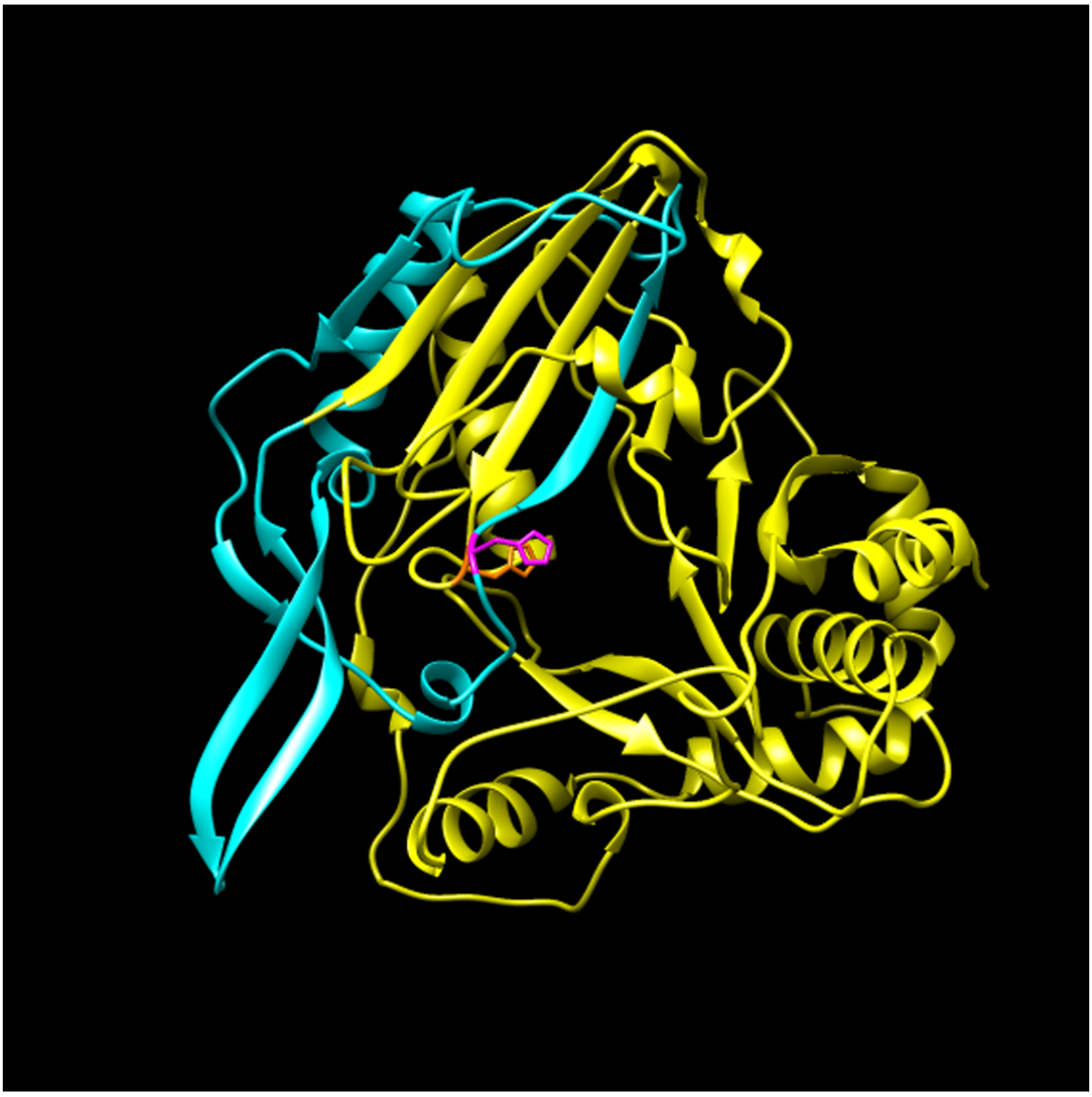

Figure 5-10: Homology-based model of CER2 tertiary structure

The N-terminal 100 amino acids are colored blue, the histidine of the predicted HXXXD catalytic motif (H166) is colored orange, and a second, N-terminal histidine residue (H38) is colored magenta. Side chains of both labelled histidines point in towards a predicted channel.

Figure 5-11: Homology-based model of CER2-LIKE1 tertiary structure

The N-terminal 100 amino acids are colored blue, the asparagine which substitutes for histidine in the predicted HXXXD catalytic motif is colored orange, and a second, N-terminal histidine residue is colored magenta. Side chains of both labelled residues point in towards a predicted channel.

Figure 5-12: Homology-based model of CER2-LIKE2 tertiary structure

The N-terminal 100 amino acids are colored blue, the histidine of the predicted HXXXD catalytic motif is colored orange, and a second, N-terminal histidine residue is colored magenta. Side chains of both labelled histidines point in towards a predicted channel.

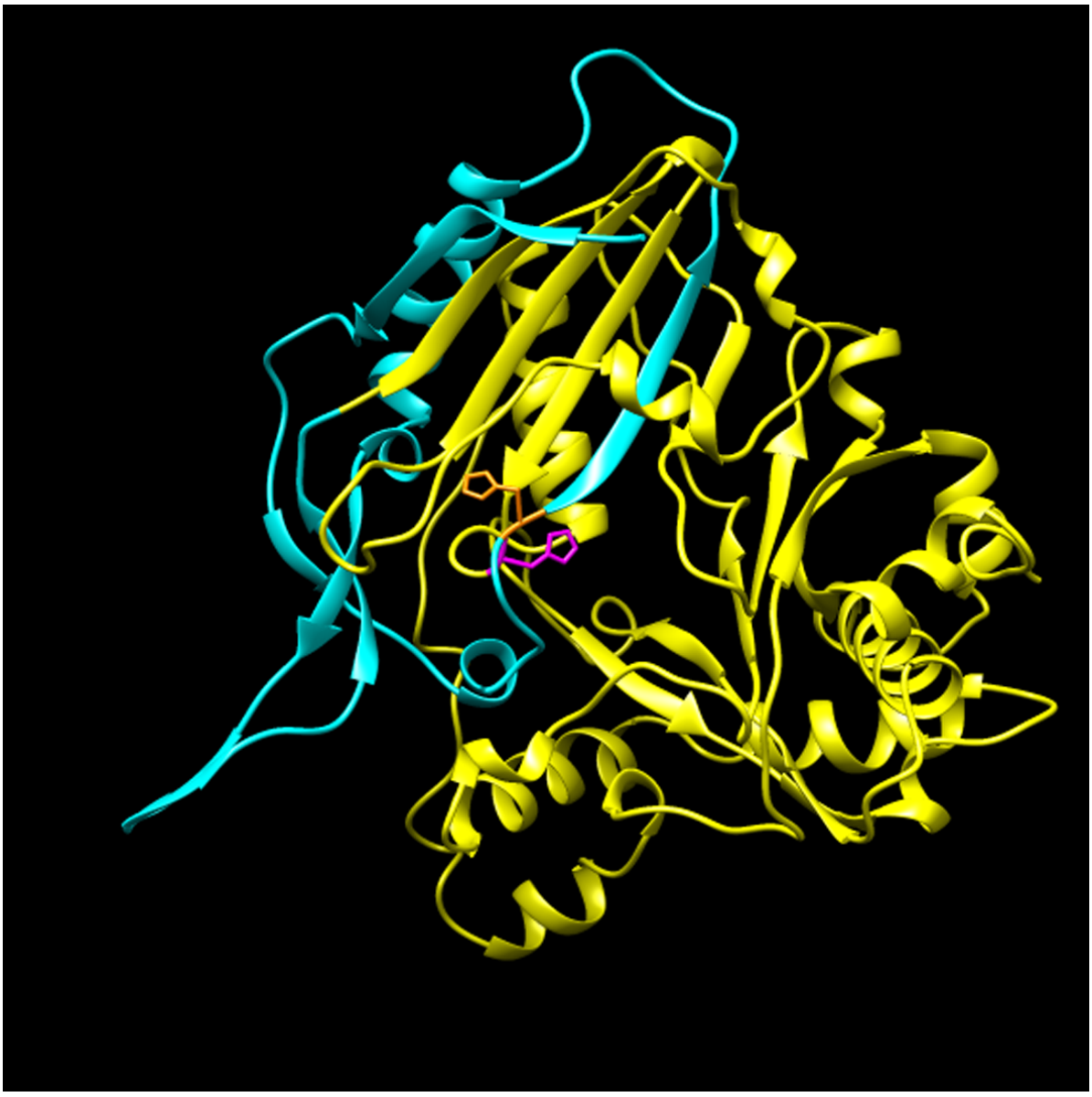

Figure 5-13: Homology-based model of CER2-LIKE3 tertiary structure

The N-terminal 100 amino acids are colored blue, the histidine of the predicted HXXXD catalytic motif is colored orange, and a second, N-terminal histidine residue is colored magenta. Side chains of both labelled histidines point in towards a predicted channel.

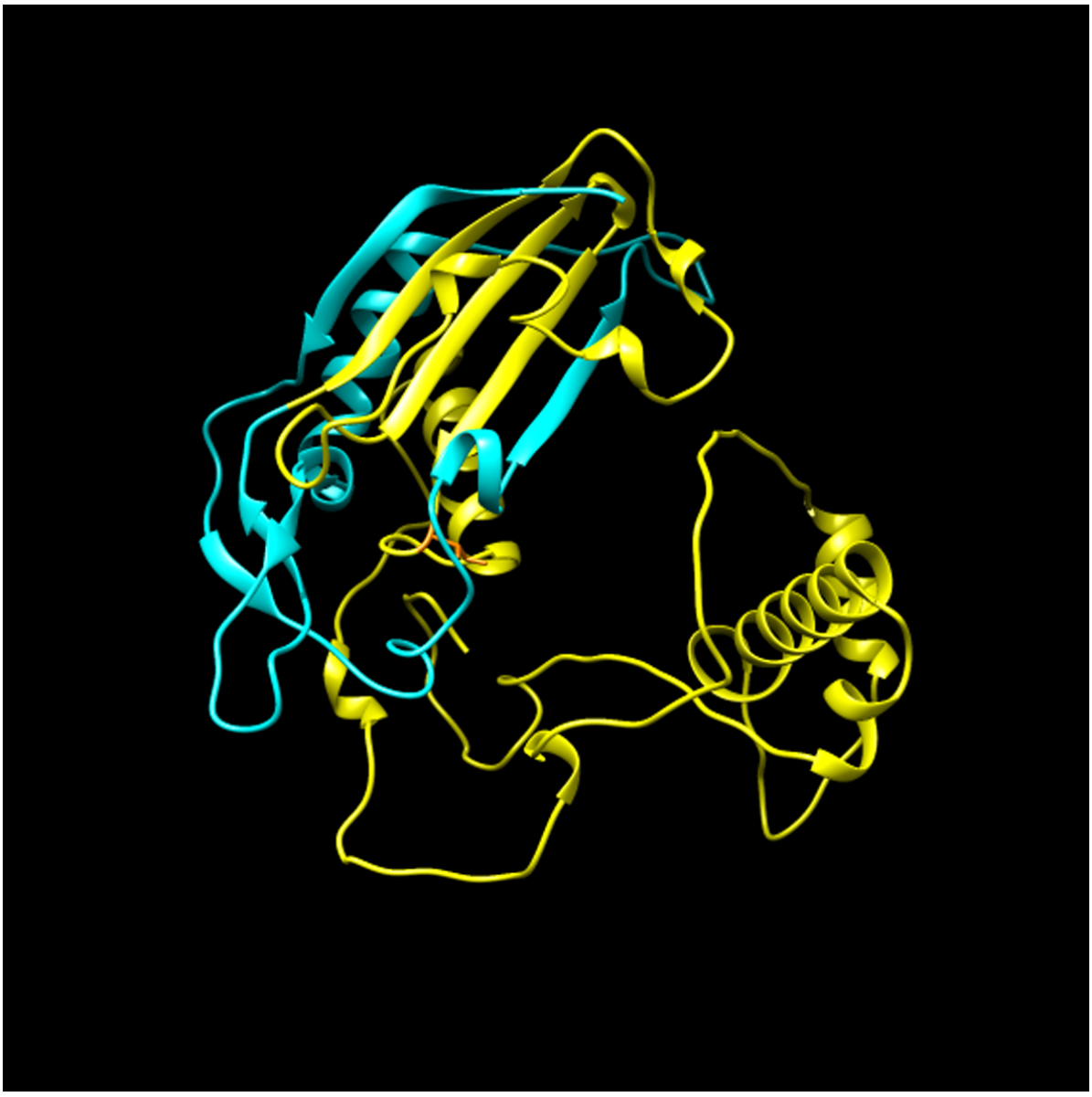

Figure 5-14: Homology-based model of CER2-LIKE4 tertiary structure

The N-terminal 100 amino acids are colored blue, the asparagine which substitutes for histidine in the predicted HXXXD catalytic motif is colored orange.

5.2.6 CER2-LIKEs do not require a second histidine in the substrate-binding pocket for function

Site-directed mutagenesis was used to establish whether the N-terminal H38 of CER2 is required for its function in VLCFA elongation. H38 was replaced in the CER2 coding sequence with an alanine (H38A) to abolish any catalytic activity. I also attempted to generate a gain-of-function mutant allele of CER2-LIKE4 by inserting a short peptide sequence from CER2 that includes H38, and the surrounding fragment of the N-terminal sequence that protrudes into the channel of CER2. The sequence GIFRRTV of CER2-LIKE4 was replaced by LHYV from CER2 by overlap extension mutagenesis. The gain-of-function experiment was undertaken with some skepticism, as the predicted structure of CER2-LIKE4 is very obviously unlike that of other CER2-LIKEs. There are many possible reasons beyond the presence or absence of putative catalytic residues why CER2-LIKE4 might not contribute to elongation. The mutant alleles were cloned into p42X yeast expression vectors. The mutant alleles, and unmodified controls, were then co-transformed with a CER6 expression construct into yeast.

The H38A allele of CER2 retained its activity in a yeast fatty acid elongation assay. Further, there was no gain-of-function for the mutagenized CER2-LIKE4 protein (Figure 5-15). I conclude that, like the HXXXD histidine, the N-terminal histidine of CER2 is not required for its activity in VLCFA elongation. This experiment strongly suggests that the role of CER2, and CER2-LIKEs, does not involve acyl transfer activity.

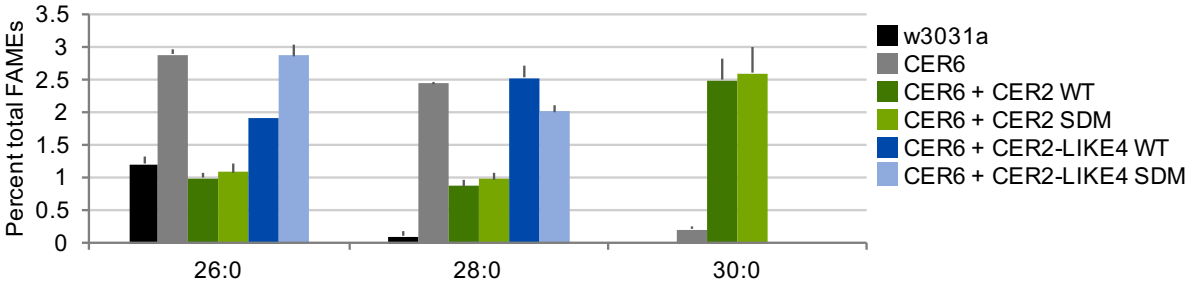

Figure 5-15: Elongation assay of mutagenized CER2-LIKEs with CER6 in *Saccharomyces*

The H38 residue does not affect CER2 activity in VLCFA elongation.

5.3 Discussion

5.3.1 CER2 physically interacts with the fatty acid elongase complex

The phenotypes of Arabidopsis *cer2-like* mutants indicate that this gene family is necessary for the elongation of VLCFA precursors of cuticular waxes. That CER2-LIKEs and CER6 function together in yeast to produce 30-carbon VLCFAs (and longer) demonstrates that their combined activity is sufficient for VLCFA elongation. How CER2-LIKEs affect elongation is not clear, but given that condensing enzymes determine the substrate specificity of the fatty acid elongase, and that CER2 requires CER6 for activity in yeast, physical interaction between the two proteins is likely. Interaction would be necessary if CER2-LIKEs were to somehow alter the substrate binding capacity of CER6, or to feed substrate to CER6. Here, physical interaction between CER6 and CER2 was demonstrated using three experimental approaches.

A split luciferase assay was used to test CER2 interactions with all four core components of the fatty acid elongase. I paired CER2 with CER6, and the three generalist components of the elongase: ketoacyl-CoA reductase 1 (KCR1), hydroxyacyl-CoA dehydratase (PAS2), and enoyl-CoA reductase (CER10). CER2 interacted with all of these proteins, suggesting that CER2 is in close physical proximity to the entire elongase complex. Notably, a positive result in the split-luciferase assay does not indicate a direct protein-protein interaction, as the two halves of luciferase could reconstitute the functional enzyme if the proteins to which they are tagged are simply in close proximity.

CER2-CER6 interactions were next examined by co-immunoprecipitation of the ectopically-expressed and epitope-tagged proteins from yeast. The epitope-tagged proteins were functional in an elongation assay. While solubilization and precipitation of CER6 was a constant challenge, CER2 did consistently co-precipitate with CER6. It is possible that CER6-CER2 interaction is mediated by a third interacting partner. However, in that case, highly similar orthologs of such a protein would need to be present in Arabidopsis and in yeast. This seems improbable given that CER2-LIKEs are not found in yeast. Thus, CER2-CER6 interaction is likely direct.

Finally, to determine whether physical interaction between CER2 and CER6 is the basis for CER2 localization to the ER, localization patterns of CER2-GFP in the presence and absence of CER6 protein were compared. Introduction of CER2-GFP into *cer2* complemented the mutant phenotype, and resulted in a distinct, tight, web-like pattern of GFP fluorescence characteristic of ER localization. In contrast, CER2-GFP in the *cer2 ew2* double mutant

background had a more diffuse pattern of fluorescence that strongly resembled free GFP fluorescence patterns in the cytosol of stem epidermal cells. This result demonstrates that CER6 is required for CER2 association with the ER.

5.3.2 CER2-LIKEs are not acyltransferases

The presence of a conserved HXXXD motif is nearly ubiquitous among BAHD acyltransferases, and there is robust evidence that the histidine residue in this motif is essential for acyl transfer activity. Site-directed mutagenesis of the predicted catalytic histidine residues of anthocyanin malonyltransferase of *Salvia splendens* (Suzuki et al., 2003), vinorine synthase of *Rauvolfia serpentina* (Bayer et al., 2004), hydroxycinnamoyltransferase of *Sorghum bicolor* (Walker et al. 2013), and hydroxycinnamoyltransferase of *Coffea canefora* (Lallemand et al., 2012) have all demonstrated that this residue is essential for metabolic function. The only exception to this rule that I am aware of is the baccatin III:3-amino-3-phenylpropanoyltransferase (BAPT) enzyme from *Taxus*, which is required for the synthesis of taxol. In this protein, the catalytic histidine is substituted by a glycine. An amine group beta to the CoA of the acyl donor has been suggested to functionally replace the histidine and deprotonate the hydroxyl group of the acyl acceptor to create a nucleophile (Walker et al., 2002).

Histidine 166 of the CER2 amino acid sequence was predicted to be a catalytic residue based on alignment to BAHD acyltransferase protein sequences. Structural models of CER2 also placed H166 in a similar position to that described for characterized BAHDs. Site-directed mutagenesis converting the H166 of CER2 to an alanine or an asparagine revealed that, just like CER2-LIKE1, CER2 does not require the HXXXD sequence for activity. Therefore, CER2 and the CER2-LIKEs represent a clade with biochemical functions distinct from those of characterized BAHD family members. Arguably, they may not be acyltransferases at all.

There are no histidine residues neighboring H166 in the CER2 amino acid sequence – the closest histidine upstream of H166 is 32 amino acids away, and the nearest downstream histidine is 22 amino acids away. However, tertiary structure models of CER2, CER2-LIKE1, CER2-LIKE2, and CER2-LIKE3 all suggested that a histidine residue from the N-terminus of each sequence is positioned in very close physical proximity to the HXXXD histidine, within channels running through the core of each protein. The only CER2-LIKE that lacks this residue is CER2-LIKE4, which does not appear to enhance elongation. This second, N-terminal histidine presented a pressing reason to doubt my previous conclusion that CER2-LIKEs entirely lack acyl transfer activity.

I mutagenized the N-terminal histidine of CER2 cDNA, H38, and substituted it with an alanine. I also swapped the short amino acid sequence from CER2 that contains H38, LHYV, into CER2-LIKE4, removing the sequence GIFRRTV. The exact regions used for this sequence swap were selected based on superposition of the structural models of CER2 and CER2-LIKE4. Both mutagenized CER2 (H38A) and CER2-LIKE4 (GIFRRTV>LHYV) retained the activity of their wild-type sequences when co-expressed in yeast with the CER6 condensing enzyme. Therefore, neither H166 nor H38 are required for CER2 function in elongation.

Remarkably, there is a precedent for an N-terminal histidine residue (H35) situated in close physical proximity to a true, mid-chain catalytic histidine (H153), in the BAHD hydroxycinnamoyltransferase from *Coffea canefora* (robusta coffee) (CcHCT) (Lallemand et al., 2012). Analysis of the crystal structure of CcHCT revealed pi-stacking interactions between the imidazole rings of the two histidine residues, which prompted the authors of this study to suggest that the N-terminal histidine served to help orient the catalytic histidine for catalysis. This hypothesis is supported by site-directed mutagenesis: mutagenesis of H153 abolished CcHCT activity, and mutagenesis of H35 reduced activity. In light of this I infer that the N-terminal H38 of CER2 does not substitute for the function formerly ascribed to H166, but that it is another remnant of ancestral BAHD function.

The only evidence remaining that CER2-LIKEs are BAHD acyltransferases is their homology to this protein family. However, examination of the most conserved features of BAHD sequences puts this classification in question. CER2-LIKEs entirely lack the DFGWG motif present at the C-terminus of most BAHDs. The mid-peptide HXXXD motif is present in some, but not all, CER2-LIKEs, but I have shown with site-directed mutagenesis that this motif is not required for CER2-LIKE function. I examined models of CER2-LIKE structure for other histidine residues that might function as base catalysts for an acyl transfer reaction, and identified H38. Because site-directed mutagenesis demonstrated that this residue is also not required for function, I am left without any evidence in support of the notion that CER2-LIKEs are acyltransferases. I conclude that while CER2-LIKEs are clearly related to the BAHD acyltransferase family, the CER2-LIKE clade has evolved a new function distinct from characterized members of this diverse protein family.

5.3.3 CER2-LIKE structures do not suggest a catalytic function

The CER2-LIKE sequence chimeras generated using CER2-LIKE1 and CER2-LIKE2 revealed that the product specificity of elongation is determined by the N-terminus of these two CER2-LIKE proteins. This fragment could be reduced to 100 amino acids without substantially

altering the specificity or efficacy of CER2-LIKE1/CER2-LIKE2 function. However, the truncated N-terminal fragment of CER2-LIKE2 was not sufficient to maintain function, nor was it functional when swapped onto two other proteins, the BAHD ASFT or CER2-LIKE3, which both have lower homology to CER2-LIKE2 than does CER2-LIKE1. Perhaps the N-terminal peptide fragment requires the structure of the remainder of the protein to support its function.

Structural models of all five CER2-LIKE proteins except CER2-LIKE4 were very similar. Most of the N-terminal peptide was positioned on the exterior surfaces of the protein, but a loop of each N-terminal fragment extended into the channel. These models cannot provide conclusive information about the biochemical function of CER2-LIKEs, but rather suggest that either an activity involving binding of a ligand, or activity mediated by the surface of the protein, could be the basis of CER2-LIKE function in very-long-chain fatty acid elongation.

5.3.4 Models of paired CER6-CER2 activity

At present, how CER2-LIKEs contribute to elongation is unclear. Several models can be proposed, however, based on the results of this chapter and prior characterization of CER2-LIKEs (Figure 5-16). In addition to suggesting biochemical functions for CER2-LIKEs, I have tried to account for two related, outstanding questions regarding the metabolism of cuticular wax precursors. First, why do plant KCSs not produce acyl-CoAs longer than 28 carbons, and why are differences in KCS expression and activity alone insufficient to determine the upper limit of elongation? Second, how does an epidermal cell accommodate the massive quantities of VLC-acyl-CoAs required to support cuticular wax biosynthesis?

5.3.4.1 Providing a physical extension of the CER6 acyl-CoA binding pocket

Acyl-CoA substrate specificity of plant KCS enzymes has primarily been investigated using molecular genetic approaches. Domains affecting specificity have been identified in domain swaps between orthologous genes (Blacklock and Jaworski, 2002), and residues that affect substrate specificity have been found by QTL mapping in wild accessions (Jasinski et al., 2014). The structure of acyl-CoA binding pockets of KCSs have only been described using homology-based models (Joubès et al., 2008). Therefore, while relative size predictions can be compared between KCSs, the absolute depths of substrate binding pockets are unknown. It is not clear whether the substrate-binding pocket of CER6 can support binding of 26-, 28-, 30-, or 32- carbon acyl-CoAs. In this first model of CER2-LIKE activity, I propose that CER6 alone can only accept acyl-CoA substrates up to 26 carbons in length, based on the fact that CER6 only generates 28-carbon product when expressed alone in yeast cells.

Structural models predict channels in all CER2-LIKEs except CER2-LIKE4. This is not surprising given that the models were generated based on crystal structures of BAHDs. Since CER2-LIKEs are derived from BAHD acyltransferases that bind acyl-CoAs, it does seem reasonable that these channels could exist within CER2-LIKEs, and that CER2-LIKEs could bind acyl-CoA substrates. Assuming that CER2-LIKEs have indeed retained the capacity to bind acyl-CoA groups, it becomes a possibility that CER2-LIKEs could serve as a physical extension of the substrate-binding pocket of KCSs such as CER6. CER2-LIKEs could thereby determine the upper limit of the length of acyl-CoA that CER6 accepts for condensation with malonyl-CoA (Figure 5-16A). This model depends heavily on direct CER2-LIKE-CER6 interaction, which is supported by CoIP, split-luciferase, and CER2-GFP localization data. Structural determination of CER2, CER6, and mapping of the interacting domains of both proteins will be required to test this hypothesis.

5.3.4.2 Manipulation of CER6 structure to allow it to bind longer-chain substrates

Again, assuming that the size of the CER6 substrate-binding pocket limits the chain length of VLC-acyl-CoA it can accept for condensation, CER2-LIKEs could serve as allosteric modifiers of CER6 specificity. CER2-LIKE binding could alter the tertiary structure of CER6 in such a way as to reshape or expand the size of the substrate-binding pocket. Different CER2-LIKEs would interact in subtly different ways with CER6 to account for the unique product specificities of CER2-LIKEs (Figure 5-16B). This model does not require that CER2-LIKEs bind acyl-CoAs. However, it remains a possibility that VLC-acyl-CoAs or malonyl-CoA could be bound by CER2-LIKEs and affect protein structure or activity. This model requires support in the form of structural determination of CER6 alone and in the presence of CER2.

5.3.4.3 Maintaining a pool of VLC-CoA substrate for CER6

Acyl-CoAs are amphipathic molecules that partition into lipid membranes (Jolly et al., 1997; Gossett et al., 1996), and the affinity of acyl-CoAs for membranes increases with increasing chain length (Boylan and Hamilton, 1992). Given that greater than 95% of long-chain acyl-CoAs partition into microsomes (Jolly et al., 1997), I anticipate that 28-, 30-, and 32-carbon very-long-chain acyl-CoA precursors of cuticular wax biosynthesis would partition almost entirely into lipid membranes.

The structure of the fatty acid elongase is obscure; crystal structures are not available for any of the core elongase components, and the quaternary structure and stoichiometry of the complex is a complete mystery. It is not known how substrate is received and transferred

between elongase components within and between elongation cycles. However, it seems unlikely that VLC-acyl-CoA substrate is provided to plant KCSs directly from cell membranes. Cuticular lipids constitute roughly 50% of the acyl-lipid output of stem epidermal cells (Suh et al., 2005), and, as shown in Figure 4-7, the 28-, 30- and 32- carbon acyl-CoA precursors of cuticular waxes make up nearly 20% of the acyl-CoA pool of whole rosette leaves. If all of the saturated, very-long-chain acyl-CoA precursors of cuticular wax were integrated in ER membranes, concentrated around the elongase, I would anticipate that the cohesion and stability of the membrane would be compromised.

Acyl-CoA binding proteins (ACBPs) play a role in lipid metabolism by solubilizing acyl-CoAs, thereby making them available for sub-cellular transport and lipid synthesis, and preventing hydrolysis of the CoA group. In Arabidopsis, there are six characterized ACBPs, which have different physiological roles and binding affinities (Xiao and Chye, 2011). Notably, ACBP1 has been found to bind VLC-acyl-CoAs up to 26 carbons in length, but binds these with lower affinity than long-chain acyl-CoAs (Xue and Xia et al., 2014). ACBP1 has not been tested with substrates longer than 26 carbons. This unknown is not for lack of interest; longer VLC-acyl-CoA substrates are effectively insoluble in aqueous media, and are therefore very difficult to work with *in vitro*. Nevertheless, the low affinity of ACBPs for VLC-acyl-CoAs in general suggests that other proteins might be required to make these substrates soluble in the cell.

If CER2-LIKE proteins do bind acyl-CoAs as suggested, they might serve as specialized VLC-acyl-CoA binding proteins that solubilize substrate for CER6 in the cytosol. Based on the fact that CER2 interacts with CER6, VLC-acyl-CoA binding by CER2-LIKEs could also serve to concentrate substrate around the fatty acid elongase complex. In this model, specificity of CER2-LIKEs for chain lengths of acyl-CoAs would determine what chain lengths of substrate would be available for use by CER6 (Figure 5-16C). Unlike the previous two models presented, this one implies that CER6 constitutively accepts chain-lengths of acyl-CoAs up to 32 carbons, but is limited by the availability of these VLC-acyl-CoAs in the cytosol. Investigation of the effect of *CER2-LIKEs* on the acyl-CoA pool, the capacity of CER2-LIKEs and CER6 to bind acyl-CoAs, and distribution of acyl-CoAs in different sub-cellular fractions, will be essential to further explore this hypothesis.

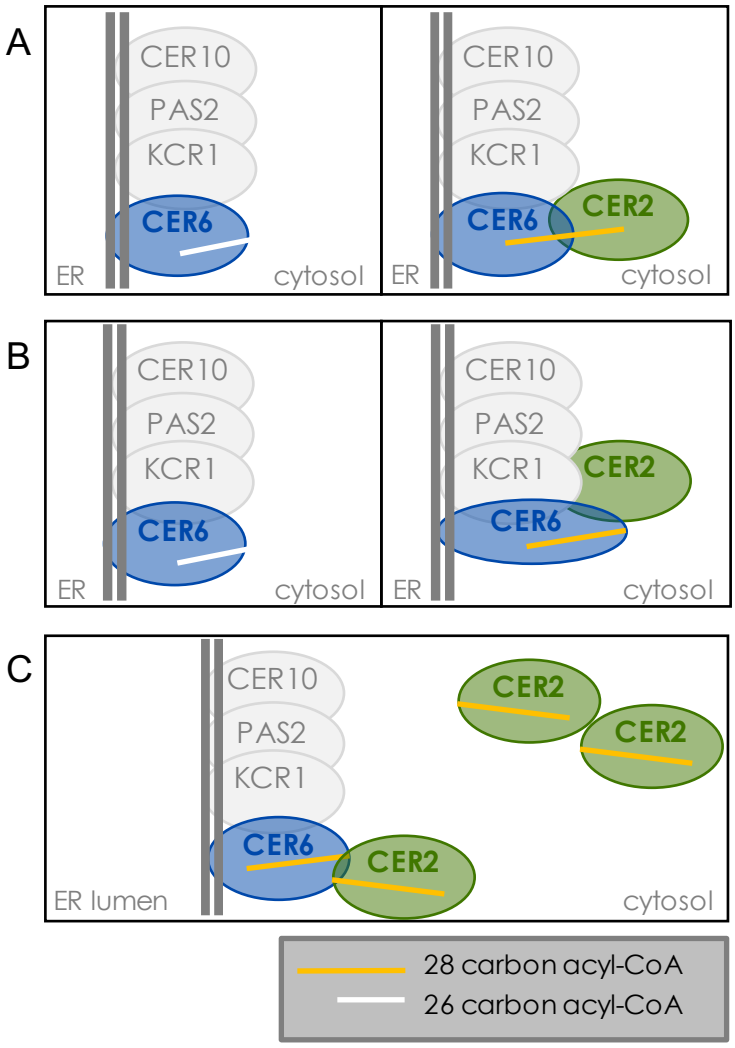

Figure 5-16: Models of paired CER2-CER6 activity

(A) Active site extension. A hypothetical acyl-CoA binding site in CER2 could physically extend the substrate-binding pocket of CER6. (B) Allosteric modulation. Protein-protein interaction between CER2 and CER6 could modify the structure of the substrate-binding pocket of CER6, enabling it to accept longer acyl chains. (C) Substrate solubilization and concentration. CER2 could bind, solubilize, and concentrate acyl-CoAs around the fatty acid elongase.

Chapter 6: Conclusions

6.1 Major findings of this work

6.1.1 Perspective: why length matters

Fatty acid elongation is a cornerstone in our model of cuticular wax metabolism. While wax composition varies immensely among individual plant species, the exceptional length of cuticular waxes is a common feature of these lipids in many flowering plants. Elongation of fatty acids past 26 carbons is the committed step in cuticular wax synthesis in Arabidopsis, with shorter chain lengths of VLCFAs shared among wax, suberin, seed oil, and sphingolipid synthetic pathways. Up-regulation of elongation beyond 26 carbons in young shoot epidermal cells is necessary to support the assembly of an effective cuticular barrier, and to fuel increased wax production in response to environmental stresses such as cold, drought, and high light. At the same time, elongation up to 26 carbons must be precisely coordinated to ensure sufficient VLCFA substrate is retained for sphingolipid metabolism, without which the plant will die.

Within the range of VLCFA chain lengths used to make cuticular waxes, some are more readily taken up by either the acyl reduction or alkane-synthetic pathway. Current work on FARs (summarized in Rowland and Domergue, 2012) and CER1 homologs (unpublished results reported at the 2016 International Symposium on Plant Lipids and the 2015 Plant Apoplastic Diffusion Barriers Meeting by Dr. Jérôme Joubès) indicate that enzymes from each of these families have their own substrate chain-length specificities. Consequently, the chain length profile of the pool of VLCFA wax precursors will affect substrate partitioning between the two pathways. It remains unclear what specific properties of the cuticle may be attributed to different wax functional groups. It is also unknown how specific chain lengths of waxes contribute to cuticle structure and function, independent of their downstream modification. However, the phenotype of the *CER6pro::CER2-LIKE1* over-expression line is evidence that changes in chain length profile alone are sufficient to alter cuticle structure.

Considering how profoundly chain length affects substrate channelling into cuticular wax biosynthesis, partitioning of substrate between wax modification pathways, and the physical properties of the plant cuticle, understanding how the plant cell produces and regulates the metabolism of these exceptionally long acyl-CoAs is key to understanding cuticular wax biosynthesis. Despite extensive work dissecting the elongation of wax precursors in Arabidopsis, glaring deficiencies in our understanding of this process remain. For example, the biochemical functions of CER2-LIKEs remain unknown. It is also unclear why the

elongation of VLCFAs by KCSs cannot exceed 28 carbons. Further, it's not apparent how plant cells can accumulate the large quantities of VLC-acyl-CoAs required to produce waxes. In this thesis, I have characterized the CER2-LIKE proteins from Arabidopsis in an attempt to determine their biochemical function and address some of these other pressing questions concerning fatty acid elongation.

6.1.2 Summary: what we've learned about CER2-LIKEs

Previous characterization of several *cer2* mutant alleles revealed that *CER2* is required for the production of cuticular waxes longer than 28 carbons (McNevin et al., 1993). The *CER2* gene was cloned by position and found to encode a protein with homology to BAHD acyltransferases (Xia et al., 1996).

Similar to condensing enzymes, CER2 activity can be assayed in yeast (Chapter 3). When co-expressed with the CER6 condensing enzyme that elongates VLCFAs to 28 carbons, CER2 increases the chain-length specificity of elongation to 30 carbons. It is clear that CER2 cannot function independently to elongate fatty acids from 28 to 30 carbons, as CER2 has no activity when co-expressed with another condensing enzyme that produces 28-carbon VLCFAs, LfKCS45. This simple experiment demonstrates that CER2 and CER6 are necessary and sufficient to produce 30-carbon VLCFAs, which are essential to cuticular wax biosynthesis. Further, it reveals that CER6 has a property lacking from LfKCS45 that enables it to function with CER2.

There are five *CER2-LIKE* genes in Arabidopsis, and all of them affect elongation (Chapter 4). In yeast, each CER2-LIKE has a unique effect on the product specificity of elongation, and affects elongation only when paired with the same specific condensing enzymes. Analysis of *cer2-like* mutant phenotypes show that in the plant, CER2-LIKEs are required to produce the bulk of VLCFA precursors of cuticular lipids. Further, the unique substrate specificities of different CER2-LIKEs fine-tune elongation to determine the precise chain-length profile of cuticular waxes and pollen coat lipids. Condensing enzymes are absolutely required to produce VLCFAs and until now their activity and expression were thought to control the substrate specificity of elongation. The contribution of CER2-LIKEs to substrate specificity demonstrated here does not contradict this model, but introduces another layer of complexity to our understanding of elongation and its regulation.

Though biochemical activities of CER2-LIKEs remain unknown, experiments described in this thesis have provided clues about their function (Chapter 5). First, while CER2-LIKEs are homologous to BAHD acyltransferases, site-directed mutagenesis shows that CER2 cannot

possibly use the same mechanism described for other characterized BAHDs. *CER2-LIKE*s form a unique clade within the BAHD family that modify the substrate specificity of elongation by an unknown mechanism, which is unlikely to involve acyl transfer. Second, the split-luciferase assay, co-immunoprecipitation, and localization patterns of CER2-GFP demonstrate that CER2 and CER6 physically interact. This protein-protein interaction in and of itself neither proves nor disproves anything about CER2 function. However, interaction between these two proteins is requisite support for all three of the CER2 activity models proposed (Figure 5-16).

6.2 Future directions

I investigated the roles of CER2-LIKEs in an attempt to better understand how plants synthesize and regulate the production of the VLC-acyl-CoA precursors of waxes, but my efforts fell short of elucidating their biochemical function. Models for paired CER2-CER6 activity were suggested in Chapter 5, along with experimental approaches that could be taken to test them. Additionally, in Chapter 4, next steps to explore the physiological function of the anomalous CER2-LIKE4 were proposed. As these immediate steps were discussed in previous chapters, in the final section of this thesis, I will focus on related questions that could be pursued in future research.

6.2.1 The origin of *CER2-LIKE* genes

6.2.1.1 BAHD acyltransferases

The BAHD acyltransferase family is diverse; BAHDs have a broad range of substrate specificities, and there is very low common sequence identity among these proteins. This breadth of form reflects the diversity of specialized metabolic pathways that BAHDs are associated with. Genes involved in specialized metabolism more readily adapt under selective pressure than genes associated with primary metabolic pathways, as they can neofunctionalize with or without prior gene duplication (Pichersky and Lewinsohn, 2011; Pichersky and Gang, 2000). Perhaps it is not entirely surprising then that CER2-LIKEs have diverged so profoundly from their BAHD ancestors as to lose acyl transfer activity, and to acquire an entirely new function. In fact, another example of BAHDs losing their catalytic function was recently published.

Two hydroxycinnamoyltransferases (HCTs) from maize have been reported to have functions in plant defence, independent of acyl transfer activity (Wang et al., 2015). Both proteins, HCT1806 and HCT4918, interact with and down-regulate the activity of a

constitutively-active positive regulator of the hypersensitive response, Rp1-D21. Site-directed mutagenesis of both HCTs revealed that their predicted, catalytic histidine residues are not required for their negative regulation of the hypersensitive response (Wang et al., 2015). The authors of this study suggested that, as phenylpropanoid metabolism is sometimes up-regulated in response to pathogen attack, some HCT proteins may be targets of pathogen effectors. In a healthy plant, HCT1806 and HCT4918 would interact with and disable Rp1-D21 activity by default; upon infection, HCT1806 and HCT4918 would serve as decoys, in that their modification by pathogen effectors would cause them to dissociate from Rp1-D21, and thereby enable the hypersensitive response (Wang et al., 2015; Wang et al., 2016).

While this model of HCT function is distinct from my models for CER2-LIKE function, both are examples of loss of acyl transfer function within the BAHD family. There may be other instances of BAHDs losing their acyl transfer function that have yet to be characterized. It will be interesting to investigate how these divergent clades of BAHDs arose from true BAHD acyltransferases, and what their ancestral functions were.

6.2.1.2 Metabolic gene clusters

The activity of CER2-LIKEs and other genes involved in cuticular wax metabolism exist in a grey area between primary and specialized metabolic processes. Specialized metabolic pathways have historically been investigated in non-model plants with no sequenced genome available. Hence, the identification and characterization of genes involved in these processes has largely relied on transcriptomic data. As genomic data becomes available for an increasing number of species, it is becoming apparent that genes required for the synthesis of specialized metabolites are often arranged in clusters reminiscent of prokaryotic operons – more frequently than they are found randomly dispersed throughout the genome (Osbourn and Field, 2009; Nützmann and Osbourn, 2014). This emerging aspect of metabolic evolution will be particularly exciting to explore in the context of cuticular wax metabolism. While there is no evidence of clustering among genes known to contribute to wax biosynthesis in Arabidopsis, two recent studies identified metabolic gene clusters required for the synthesis of diketone waxes in *Hordeum vulgare* (barley) and *Triticum aestivum* (wheat) (Schneider et al., 2016; Hen-Avivi et al., 2016). It will be interesting to examine whether gene clusters are involved in the synthesis of unique waxes in other organisms, and whether there are mechanisms that regulate the expression of entire clusters.

BAHD acyltransferases have been found in several metabolic gene clusters (Medeema and Osbourn, 2016). If divergent BAHDs such as *CER2-LIKE*s have maintained linkage to

genes from an ancestral cluster, this may shed light on their evolutionary history. *CER2* and *CER2-LIKE4* are both positioned adjacent to CYP450 genes with unknown functions. CYP450s are ubiquitous in plant metabolism, and nearly all plant metabolic gene clusters identified to date include one or more CYP450. Examining the phylogeny of the CYP450s adjacent to *CER2* and *CER2-LIKE4* may help trace the evolution of the *CER2-LIKE* clade.

6.2.1.3 Acyl chain length and cuticle evolution

To date, molecular genetic studies of cuticular wax metabolism have primarily been conducted with model flowering plants such as Arabidopsis, maize, and barley. However, chemical analysis of cuticular wax composition has been carried out in diverse plant phyla. Chemical descriptions of waxes on bryophytes, the extant relatives of early land plants, are cause for further studies of these organisms. While the bulk of wax present in the cuticles of angiosperms is composed of 29-31 carbon components, predominant waxes in bryophytes vary substantially from species to species. In the model moss *Physcomitrella patens* (*P. patens*), the most abundant waxes are primary alcohols and VLCFAs 24, 26, and 28 carbons in length, and wax esters 42-50 carbons in length (dimers from a VLCFA and an alcohol) (Buda et al., 2013). Similar patterns were found across twelve species of the peat bog moss genus, *Sphagnum* (Baas et al., 2000). A study that examined cuticular waxes of both endohydric (*Pogonatum*) and ectohydric (*Andreaea*) mosses had similar results, with 22-28 carbon waxes predominating (Haas, 1982). While wax chain lengths up to 32 carbons could be detected in all of these mosses, shorter chain lengths were consistently more abundant. It is possible that shorter chain lengths of waxes offer a selective advantage to mosses, such as allowing water to be absorbed through shoot tissues, but because the roles of different wax chain lengths are not known, such an advantage is difficult to infer. Another explanation could be that mosses, and perhaps other bryophytes, lack the biosynthetic capacity to efficiently produce waxes of longer chain lengths that predominate in the cuticles of flowering plants.

Molecular genetic investigation of cuticle biosynthetic machinery in bryophytes was not attempted until quite recently. Completion of genome sequencing for *P. patens* (Rensing et al., 2008) has allowed the identification and characterization of an ABC transporter required for cuticular wax deposition in *P. patens* (Buda et al., 2013), and will surely accelerate future work on wax biosynthesis in this species. It will be fascinating to investigate wax metabolism in these extant relatives of the earliest land plants, and to compare the functionality of bryophyte cuticles to the cuticles of vascular plants. The phylogeny of both *KCS*s and *CER2-LIKE*s is of clear interest. In Arabidopsis, the elongation machinery required to make waxes up to 28 carbons in

length does not include CER2-LIKEs, suggesting that mosses might have shorter chain length profiles because they lack a CER2 homolog.

6.2.2 Structure of plant elongase complexes

This thesis has highlighted several unknowns regarding the elongase structure that are relevant to its function. One glaring issue is that the stoichiometry of the elongase components remains unknown. The simplest model is a heterotetramer, with one condensing enzyme and one of each of the generalist enzymes in a single complex. Different elongase heterotetramers could have different condensing enzymes, with substrate passed from one entire complex to another to generate longer and longer acyl chain lengths. Alternatively, multiple condensing enzymes could function with the same suite of generalist components, allowing for elongation of a given fatty acid from start to finish. A sequence of condensing enzymes could be swapped in and out of the complex as longer and longer fatty acids are generated, or multiple condensing enzymes could simultaneously associate with the same complex. Finally, none of these streamlined models is necessarily true; elongases could exist as large aggregations with multiple copies of any or all of their protein components, including condensing enzymes and the generalist enzymes. Determining whether multiple KCS enzymes simultaneously associate with the same elongation complex could be easily studied using molecular genetic assays such as split-luciferase, or co-immunoprecipitations on cells co-expressing multiple, tagged KCSs. Resolving the stoichiometry of the entire fatty acid elongation complex could be achieved by two-dimensional blue native PAGE followed by SDS-PAGE (Swamy et al., 2006).

Regardless of the quaternary structure, there must be a mechanism for transferring acyl-CoAs between components within a given elongase complex, and perhaps among different elongase complexes. As previously discussed, acyl-CoA binding proteins could facilitate transfer of acyl-CoA substrates and intermediates. These proteins could either be archetypal ACBPs, or non-homologous proteins with similar function to ACBPs. Analysis of acyl-CoA profiles of soluble and microsomal cell fractions might help resolve the localization of elongation substrates, products, and intermediates. Additionally, as described in Section 5.3.4.3, further investigation of the roles of ACBPs and CER2-LIKEs in elongation may provide a clear explanation of how metabolites are provided to the elongase complex.

Several genes have been identified in Arabidopsis that resemble elongase components, but which have nebulous functions in VLCFA biosynthesis. These include *KCR2* and *PTPLA*, *ELO*-like *KCS*s, and *PAS1*. The similarities and differences between the ketoacyl-CoA reductases KCR2 and KCR1, and hydroxyacyl-CoA dehydratases PTPLA and PAS2, were

summarized briefly in the introduction to this thesis, and compelling evidence was presented by Morineau et al. (2016) for the existence of dual elongase complexes. While it would appear that the different ketoacyl-CoA reductases and hydroxyacyl-CoA dehydratases make different contributions to VLCFA elongation in different tissues, what function this serves in unclear, given that KCSs alone typically determine substrate specificity.

Similarly, the fact that there are two families of ketoacyl-CoA synthases in Arabidopsis, and presumably in other plants, is puzzling. The *FAE1*-like family that *CER6* belongs to predominates in plants, and so throughout this thesis I've referred to this family simply as *KCS*s. The *FAE1*-like family is homologous to a condensing enzyme discovered in association with seed oil biosynthesis (Kunst et al., 1992; James et al., 1995; Lassner et al., 1996). The *ELO*-like family is homologous to the yeast condensing enzymes responsible for sphingolipid synthesis (Dunn et al., 2004), also characteristic of animal metabolism. While many of the *FAE1*-like *KCS*s from plants have been characterized, the functions of *ELO*-like *KCSs* are almost completely unknown. Obvious approaches to characterizing these genes include analysis of Arabidopsis mutants, and heterologous expression of Arabidopsis *ELO*s in yeast cells. The fact that some *ELO*s have been characterized from a bryophyte (Zank et al., 2002; Eiamsa-ard et al., 2013) suggests that phylogenetic analysis of *ELO* gene distribution and analysis of the contributions of *ELO*s to metabolism in different plant lineages could be insightful.

Finally, *PAS1* is homologous to immunophilins identified in animal systems, has been shown to physically interact with the elongase in the ER, and is required for normal production of VLCFAs and sphingolipids (Roudier et al., 2010). How this gene contributes to elongase function is unknown, but Roudier and coworkers (2010) suggested it might serve as a molecular scaffold for the protein complex.

The fact that so many genes have been discovered that affect VLCFA production, but do not fit into the current model of elongation, suggests that our model needs improvement and that there are very likely other components of the elongation machinery that we are not yet aware of. Many of the genes involved in elongation have been identified based on sequence homology, such as the *KCR*s, which were identified based on homology to the yeast gene, *YBR159*. However, elongation in plants is clearly unique, and homology searches based on other organisms are blind to the intricacies of plant metabolism. Diverse mutant screens have yielded insight into the process of elongation. The screen for *pasticcino* mutants targeted genes involved in cytokinin responses, but yielded the *PAS1* immunophilin, the hydroxyacyl-CoA dehydratase *PAS2*, and the *pas3* mutant allele of *ACETYL-COA CARBOXYLASE* (Faure et al., 1998). Screens for wax-deficient mutants have also led to the identification of components of

the elongase such as *CER2* and *CER10*, the enoyl-CoA reductase of the complex. That elongation defects have been investigated through such different screens underscores the broad influence of VLCFAs on plant health. As the core components of the elongase have now been identified, further suppressor and enhancer mutant screens are possible, again using phenotypes such as cuticular wax load or growth as tools. High-throughput screens for interacting proteins are also possible using proteomics, or yeast-two hybrid systems.

The core components of the plant fatty acid elongation machinery have been identified, characterized, and used to build a model that has served our research community well. This model presents the elongase as a complex of four enzymes with distinct activities. However, there have been many clues that suggest that this model is an oversimplification. The requirement of CER2-LIKE proteins for the synthesis of cuticular wax precursors is one example of an intricacy that refines the activity of the elongase, and strongly influences downstream metabolic pathways. There is no doubt that tracing the evolution of fatty acid elongation in plants, examining the structure of the fatty acid elongase, and screening for genes with peripheral functions in elongation will reveal a much more elaborate process.

References

Aarts, MG, Keijzer, CJ, Stiekema, WJ, and Pereira, A (1995). Molecular characterization of the CER1 gene of Arabidopsis involved in epicuticular wax biosynthesis and pollen fertility. Plant Cell **7**: 2115–2127.

Aarts, MG, Hodge, R, Kalantidis, K, Florack, D, Wilson, ZA, Mulligan, BJ, Stiekema, WJ, Scott, R, Pereira, A (1997) The Arabidopsis MALE STERILITY 2 protein shares similarity with reductases in elongation/condensation complexes. Plant J **12**: 615–623.

Abbadi, A, Brummel, M, Schütt, BS, Slabaugh, MB, Schuch, R, Spener, F (2000) Reaction mechanism of recombinant 3-oxoacyl-(acyl-carrier-protein) synthase III from *Cuphea wrightii* embryo, a fatty acid synthase type II condensing enzyme. Biochem J. **345**:153-160.

Agrawal, VP, Lessire, R, Stumpf, PK (1984) Biosynthesis of very-long-chain fatty acids in microsomes from epidermal cells of *Allium porrum* L. Arch. Biochem. Biophys. **230**:580-1984.

Alonso, JM, et al. (2003) Genome-wide insertional mutagenesis of Arabidopsis thaliana. Science **301**: 653–657.

Asselineau, C, Asselineau, J, Laneelle, G, Laneelle, M-A (2002) The biosynthesis of mycolic acids by Mycobacteria: current and alternative hypotheses. Prog. Lipid Res. **41**: 501-523.

Athenstaedt, K, Daum, G (2005) 1-acyldihydroxyacetone-phosphate reductase (Ayr1p) of the yeast *Saccharomyces cerevisiae* encoded by the open reading frame YIL124w is a major component of lipid particles. J. Biol. Chem. **275**:235–240.

Baas, M, Pancost, R, van Geel, B, Damsté (2000) A comparative study of lipids in *Sphagnum* species. Org. Geochem. **31**:535-541.

Bach, L, Michaelson, L, Haslam, R, Bellec, Y, Gissot, L, Marion, J, Da Costa, M, Boutin, J-P, Miquel, M, Tellier, F, Domergue, F, Markham, JE, Beaudoin, F, Napier, JA, Faure J-D(2008) The very-long-chain hydroxy acyl-CoA dehydratase PASTICCINO2 is essential and limiting for plant development. Proc. Natl. Acad. Sci. USA **105**:14727-14731.

Bayer, A, Ma, X, Stöckigt, J (2004) Acetyltransfer in natural product biosynthesis—functional cloning and molecular analysis of vinorine synthase. Bioorg Med Chem **12**: 2787–2795.

Beaudoin, F, Wu, X, Li, F, Haslam, RP, Markham, JE, Zheng, H, Napier, JA, Kunst, L (2009) Functional characterization of the Arabidopsis β-ketoacyl-Coenzyme A reductase candidates of the fatty acid elongase. Plant Physiol. **150**:1174-1191.

Beaudoin, F, Gable, K, Sayanova, O, Dunn, T, Napier, JA (2002) A *Saccharomyces cerevisiae* gene required for heterologous fatty acid elongase activity encodes a microsomal β-keto-reductase. J. Biol. Chem. **277**:11481-11488.

Bellec, Y, Harrar, Y, Butaeye, C, Darnet, S, Bellini, C, Faure J-D (2002) Pasticcino2 is a protein tyrosine phosphatase-like involved in cell proliferation and differentiation in Arabidopsis. Plant J. **32**:713-722.

Bernard, A, Domergue, F, Pascal, S, Jetter, R, Renne, C, Faure, JD, Haslam, RP, Napier, JA, Lessire, R, Joubès, J (2012) Reconstitution of plant alkane biosynthesis in yeast demonstrates that *Arabidopsis* ECERIFERUM1 and ECERIFERUM3 are core components of a very-long-chain alkane synthesis complex. Plant Cell **24**:3106–3118.

Bessoule, J-J, Lessire, R, Cassagne, C (1989) Partial purification of the acyl-CoA elongase of *Allium porrum* leaves. Arch. Biochem. Biophys. **268**:475-484.

Blacklock, BJ, Jaworski, JG (2002) Studies into factors contributing to substrate specificity of

membrane bound 3-ketoacyl-CoA synthases. Eur. J. Biochem **269**:4789-4798.

Blacklock, BJ, Jaworski, JG (2006) Substrate specificity of Arabidopsis 3-ketoacyl-CoA synthases. Biochem. Biophys. Res. Comm. **346**:583-590.

Boevink, P, Santa Cruz, S, Hawes, C, Harris, N, Oparka, KJ (1996) Virus-mediated delivery of the green fluorescent protein to the endoplasmic reticulum of plant cells. Plant J **10**: 935–941.

Bourdenx, B, Bernard, A, Domergue, F, Pascal, S, Léger, A, Roby, D, Pervent, M, Vile, D, Haslam, RP, Napier, JA, Lessire, R, Joubès, J (2011) Overexpression of Arabidopsis *ECERIFERUM1* promotes wax very-long-chain alkane biosynthesis and influences plant response to biotic and abiotic stresses. Plant Physiol **156**:29–45.

Boylan, JG, Hamilton, JA (1992) Interactions of acyl-coenzyme A with phosphatidylcholine bilayers and serum albumin. Biochemistry. **31**:557-567.

Buda, G, Barnes, WJ, Fich, EA, Park, S, Yeats, TH, Zhao, TH, Zhao, L, Domozych, DS, Rose, JKC (2013) AN ATP binding cassette transporter is required for cuticular wax deposition and desiccation tolerance in the moss *Physcomitrella patens*. Plant Cell. **25**:4000-4013.

Cassagne, C, Lessire, R (1978) Biosynthesis of saturated very long chain fatty acids by purified membrane fractions from leek epidermal cells. Arch. Biochem. Biophys. **191**:146-152.

Cheesbrough, T, Kolattukudy, PE (1984) Alkane biosynthesis by decarbonylation of aldehydes catalyzed by a particulate preparation from *Pisum sativum*. Proc Natl Acad Sci USA **81:**6613–6617.

Chen, H, Zou, Y, Shang, Y, Lin, H, Wang, Y, Cai, R, Tang, X, Zhou, J-M (2008) Firefly luciferase complementation imaging assay for protein-protein interactions in plants. Plant Physiol. **146**:368-376.

Chen, X, Goodwin, SM, Boroff, VL, Liu, X, Jenks, MA (2003). Cloning and characterization of the WAX2 gene of Arabidopsis involved in cuticle membrane and wax production. Plant Cell **15**: 1170–1185.

Choi, H, Ohyama, K, Kim, YY, Jin, JY, Lee, SB, Yamaoka, Y, Muranaka, T, Suh, MC, Fujioka, S, Lee, Y (2014) The role of Arabidopsis ABCG9 and ABCG31 ATP binding cassette transporters in pollen fitness and the deposition of steryl glycosides on the pollen coat. Plant Cell **26**: 310–324.

D'Auria, JC (2006) Acyltransferases in plants: a good time to be BAHD. Curr Opin Plant Biol **9**: 331–340.

Da Costa, M, Bach, L, Landrieu, I, Bellec, Y, Catrice, O, Brown, S, De Veylder, L, Lippens, G, Inzé, D, Faure, J-D (2006) Arabidopsis PASTICCINO2 is an antiphosphatase involved in regulation of cyclin-dependent kinase A, Plant Cell **18**:1426-1437.

Denic, V, Weissman, JS (2007) A molecular caliper mechanism for determining very-long-chain fatty acid length. Cell **130**:663-677.

Dennis, M, Kolattukudy, PE (1992) A cobalt-porphyrin enzyme converts a fatty aldehyde to a hydrocarbon and CO. Proc Natl Acad Sci USA **89:**5306–5310.

Dietrich, CR, Perera, MA, D Yandeau-Nelson, M, Meeley, RB, Nikolau, BJ, Schnable, PS. (2005) Characterization of two GL8 paralogs reveals that the 3-ketoacyl reductase component of fatty acid elongase is essential for maize (Zea mays L.) development. Plant J. **42**: 844–861.

Dunn, TM, Gable, K, Monaghan, E, Bacikova, C (2000) Selection of yeast mutants in sphingolipid metabolism. Methods in Enzymol. **312**:317-330.

Eiamsa-ard, P, Kanjana-Opas A, Cahoon, EB, Chodok, P, Kaewsuwan, S (2013) Two novel Physcomitrella patens fatty acid elongases (ELOs): identification and functional characterization. Appl. Microbiol. Biotechnol. **97**:3485-3497.

Eisner, G, Negruk, V, Hannoufa, A, Lemieux, B (1998) Analysis of *Arabidopsis thaliana* transgenic plants transformed with *CER2* and *CER3* genes in sense and antisense orientations. Theor Appl Genet. **97**: 801-809.

Elleman, CJ, Franklin-Tong, V, Dickinson, HG (1992) Pollination in species with dry stigmas: the nature of the early stigmatic response and the pathway taken by pollen tubes. New Phytol **121**: 413–424.

Faure, JD, Vittorioso, P, Santoni, V, Fraisier, V, Prinsen, E, Barlier, I, Van Onckelen, H, Caboche, M, Bellini, C (1998) The *PASTICCINO* genes of *Arabidopsis thaliana* are involved in the control of cell division and differentiation. Development **125**:909-918.

Fiebig, A, Mayfield, JA, Miley, NL, Chau, S, Fischer, RL, Preuss, D (2000) Alterations in *CER6*, a gene identical to *CUT1*, differentially affect long-chain lipid content on the surface of pollen and stems. Plant Cell **12**:2001-2008.

Franke, R, Höfer, R, Briesen, I, Emsermann, M, Efremova, N, Yephremov, A, Schreiber, L (2009) The DAISY gene from Arabidopsis encodes a fatty acid elongase condensing enzyme involved in the biosynthesis of aliphatic suberin in roots and the chalaza-micropyle region of seeds. Plant J. **57**:80-95.

Gable, K, Garton, S, Napier, JA, Dunn, TM (2004) Functional characterization of the Arabidopsis thaliana orthologue of Tsc13p, the enoyl reductase of the yeast microsomal fatty acid elongating system. J. Exp. Bot. **55**:543–545.

Gehl, C, Kaufholdt, D, Hamisch, D, Bikker, R, Kudla J, Mendel, RR, Hansch, R (2011) Quantitative analysis of dynamic protein-protein interaction *in planta* by a floated-leaf luciferase complementation imaging (FLuCI) assay using Gateway vectors. Plant J. **67**:542-553.

Ghanevati, M, Jaworski, JG (2001) Active-site residues of a plant membrane-bound fatty acid elongase β–ketoacyl-CoA synthase, FAE1 KCS. Biochemica et Biophysica Acta **1530**:77-85.

Ghanevati, M, Jaworski, JG (2002) Engineering and mechanistic studies of the Arabidopsis FAE1 β–ketoacyl-CoA synthase, FAE1 KCS. Eur. J. Biochem. **269**:3531-3539.

Gietz, RD, Woods, RA (2002) Transformation of yeast by lithium acetate/single-stranded carrier DNA/polyethylene glycol method. Methods Enzymol. **350**: 87–96.

Golebiowski, M, Bogus, MI, Paskiewicz, M, Stepnowski, P (2011) Cuticular lipids of insects as potential biofungicides: methods of lipid composition analysis. Anal. Bioanal. Chem. **399**: 3177-3191.

Gossett, RE, Frolov AA, Roths JB, Behnke WD, Kier AB, Schroeder F (1996) Acyl-CoA binding proteins: multiplicity and function. Lipids **31**:895-918.

Gray, JE, Holroyd, GH, van der Lee, FM, Bahrami, AR, Sijmons, PC, Woodward, FI, Schuch W, Hetherington, AM (2000) The HIC signaling pathway links CO_2 to stomatal development. Nature **408**:713-716.

Greer, S, Wen, M, Bird, D, Wu, X, Samuels, L, Kunst, L, Jetter, R (2007) The cytochrome P450 enzyme CYP96A15 is the midchain alkane hydroxylase responsible for formation of secondary alcohols and ketones in stem cuticular wax of Arabidopsis. Plant Physiol. **145**:653-667.

Haas, K (1982) Surface wax of *Andreaea* and *Pogonatum* species. Phytochem **21**:657-659.

Haslam, TM, Kunst, L (2013) Wax analysis of stem and rosette leaves in Arabidopsis thaliana. Bioprotocol **3**:e782/

Han, G, Gable, K, Kohlwein, SD, Beaudoin, F, Napier, JA, Dunn, TM (2002) The *Saccharomyces cerevisiae* YBR159w gene encodes the 3-ketoreductase of the microsomal fatty acid elongase. J. Biol. Chem. **277**:35440-35449.

Hannoufa, A, McNevin, J, Lemieux, B (1993) Epicuticular waxes of *eceriferum* mutants of *Arabidopsis thaliana*. Phytochemistry. **33**:851-855.

Harwood, J (2005) Fatty acid biosynthesis, in: D.J. Murphy (Ed.), Plant Lipids: Biology, Utilization and Manipulation. CRC Press, Boca Raton, pp. 27-56.

Haynes, CA, Allegood, JC, Sims, K, Wang, EW, Sullards, MC, Merrill, AH Jr (2008) Quantitation of fatty acyl-coenzyme As in mammalian cells by liquid chromatography-electrospray ionization tandem mass spectrometry. J Lipid Res **49**: 1113-1125.

Hen-Avivi, S, Savin, O, Racovita, R, Lee, W-S, Adamki, N, Malitsky, S, Almekias-Siegl, E, Levy, M, Vautrin, S, Bergès, H, Friedlander, G, Kartvelishvily, E, Ben-Zvi, G, Alkan, N, Uauy, C, Kanyuka, K, Jetter, R, Distelfeld, A, Aharoni, A (2016) A metabolic gene cluster in the wheat *W1* and the barley *cer-cqu* loci determines β-diketone biosynthesis and glaucousness. Plant Cell. **28**:1440-1460.

Ho, SN, Hunt, HD, Horton, RM, Pullen, JK, Pease, LR (1989) Site-directed mutagenesis by overlap extension using the polymerase chain reaction. Gene **77**: 51–59

Hobbs, DH, Flintham, JE, Hills, MJ (2004) Genetic control of storage oil synthesis in seeds of Arabidopsis. Plant Physiol. **136**:3341-3349.

Hong, B, Ichida, A, Wang, Y, Gens, JS, Pickard, BG, Harper, JF (1999) Identification of a calmodulin-regulated Ca 2+ -ATPase in the endoplasmic reticulum. Plant Physiol. **119**:1165-1176.

Hooker, TS, Millar, AA, Kunst, L (2002) Significance of the expression of the *CER6* condensing enzyme for cuticular wax production in Arabidopsis. Plant Phys. **129**:1568-1580.

James, DW, Dooner, HK (1990) Isolation of EMS-induced mutants in Arabidopsis altered in seed fatty acid composition. Theor. Appl. Genet. **80**:241-245.

James, DW, Lim, E, Keller, J, Plooy, I, Ralston, E, Dooner, HK (1995) Direct tagging of the Arabidopsis *FATTY ACID ELONGATION1* (*FAE1*) gene with the maize transposon Activator. Plant Cell **7**:309-319.

Jasinski, S, Lécureuil, A, Miquel, M, Loudet, O, Raffaele, S, Froissard, M, Guerche, P (2012) Natural variation in seed very long chain fatty acid content is controlled by a new isoform of KCS18 in *Arabidopsis thaliana*. PLoS ONE **7**:e49261.

Jenks, MA, Tuttle, HA, Eigenbrode, SD, Feldmann, KA (1995) Leaf epicuticular waxes of the *eceriferum* mutants in *Arabidopsis*. Plant Physiol **108**:369–377.

Jessen, D, Olbrich, A, Knufer, J, Kruger, A, Hoppert, M, Polle, M, Fulda, M (2011) Combined activity of *LACS1* and *LACS4* is required for proper pollen coat formation in Arabidopsis. Plant J. **68**: 715-726.

Jez, JM, Ferrer, J-L, Bowman, ME, Dixon, RA, Noel, JP (2000) Dissection of malonyl-coenzyme A decarboxylation from polyketide formation in the reaction mechanism of a plant polyketide synthase. Biochemistry. **39**:890-902.

Jolly, CA, Hubbell, T, Behnke, WD, Schroeder, F (1997) Fatty acid binding protein: stimulation of microsomal phosphatidic acid formation. Arch. Biochem. Biophys. **341**:112-121.

Joubès, J, Raffaele, S, Bourdenx, B, Garcia, C, Laroche-Traineau, J, Moreau, P, Domergue, F, Lessire, R (2008) The VLCFA elongase gene family in Arabidopsis thaliana: phylogenetic analysis, 3D modeling and expression profiling. Plant Mol Biol **67**:547-566.

Kapoor, S, Kobayashi, A, Takatsuji, H (2002) Silencing of the tapetum-specific zinc finger gene TAZ1 causes premature degeneration of tapetum and pollen abortion in petunia. Plant Cell **14**: 2353–2367.

Kelley, LA, Sternberg, MJE (2009) Protein structure prediction on the web: a case study using the Phyre server. Nat. Protoc. **4**:363-371.

Kihara, A, Sakuraba, H, Ikeda, M, Denpoh, A, Igarashi, Y (2008) Membrane topology and essential amino acid residues of Phs1, a 3-hydroxyacyl-CoA dehydratase involved in very long-chain fatty acid elongation. J Biol. Chem. **283**: 11199-11209.

Kim, J, Jung, JH, Lee, S-B, Go, YS, Kim, HJ, Cahoon, R, Markham, JE, Cahoon, E, Suh, MC (2013) Arabidopsis 3-ketoacyl-CoA synthase 9 is involved in the synthesis of tetracosanoic acids as precursors of cuticular waxes, suberins, sphingolipids, and phospholipids. Plant Physiol. **162**:567-580.

Koch, K, Ensikat, H-J (2008) The hydrophobic coatings of plant surfaces: Epicuticular wax crystals and their morphologies, crystallinity and molecular self-assembly. Micron. **39**:759-772.

Kohlwein, SD, Eder, S, Oh, CS, Martin, CE, Gable, K, Bacikova, D, Dunn, T (2001) Tsc13p is required for fatty acid elongation and localizes to a novel structure at the nuclear-vacuolar interface in Saccharomyces cerevisiae. Mol. and Cell. Biol. **21**:109-125.

Koornneef, M, Hanhart, CJ, Thiel, F (1989) A genetic and phenotypic description of *Eceriferum* (*cer*) mutants in *Arabidopsis thaliana*. J Heredity. **80**:118-122.

Kosma, DK, Bourdenx, B, Bernard, A, Parsons, EP, Lü, S, Joubès, J, Jenks, MA (2009) The impact of water deficiency on leaf cuticle lipids of Arabidopsis. Plant Physiol. **151**:1918-1929.

Kreuzaler, F, Ragg, H, Heller, W, Tesch, R, Witt, I, Hammer, D, Hahlbrock (1979) Flavanone synthase from *Petroselinum hortense*. Molecular weight, subunit composition, size of messenger RNA, and absence of pantetheinyl residue. Eur. J. Biochem. **99**:89-96.

Kunst, L, Taylor, DC, Underhill, EW (1992) Fatty acid elongation in developing seeds of *Arabidopsis thaliana*. Plant Physiol. Biochem. **30**:425-434.

Kvam, E, Gable, K, Dunn, TM, Goldfarb, DS (2005) Targeting of Tsc13p to nucleus-vacuole junctions: a role for very-long-chain fatty acids in the biogenesis of microautophagic vesicles. Mol. Biol. Cell **16:**3987-3998.

Lai, C, Kunst, L, Jetter, R (2007) Composition of alkyl esters in the cuticular wax on inflorescence stems of *Arabidopsis thaliana cer* mutants. Plant J. **50**:189-196.

Lallemand, LA, Zubieta, C, Lee, SG, Wang, Y, Acajjaoui, S, Timmins, J, McSweeney, S, Jez, JM, McCarthy, JG, McCarthy, AA (2012) A structural basis for the biosynthesis of the major chlorogenic acids found in coffee. Plant Physiol. **160**:249-260.

Larson, TR, Graham, IA (2001) Technical Advance: a novel technique for the sensitive quantification of acyl-CoA esters from plant tissues. Plant J. **25**:115-125.

Lassner, MW, Lardizabal, K, Metz, JG (1996) A jojoba beta-ketoacyl-CoA synthase cDNA complements the canola fatty acid elongation mutant in transgenic plants. Plant Cell **8**:281-292.

Lee, S-B, Jung, S-J, Go, Y-S, Kim, H-U, Kim, J-K, Cho, H-J, Park, OK Suh, M-C (2009) Two Arabidopsis 3-ketoacyl CoA synthase genes, *KCS20* and *KCS2/DAISY*, are functionally redundant in cuticular wax and root suberin biosynthesis, but differentially controlled by osmotic stress. Plant J. **60**:462-475.

Leivar, P, González, VM, Castel, S, Trelease, RN, López-Iglesias, C, Arró, M, Boronat, A, Campos, N, Ferrer, A, Fernàndez-Busquets, X (2005) Subcellular localization of Arabidopsis 3-hydroxy- 3-methylglutaryl- coenzyme A reductase. Plant Physiol. **137**:57-69.

Lemieux, B, Miquel, M, Somerville, C, Browse, J (1990) Mutants of Arabidopsis with alterations in seed lipid fatty acid composition. Theor. Appl. Genet. **80**:234-240.

Leshem, Y, Johnson, C, Wuest, SE, Song, X, Ngo, QA, Grossniklaus, U, Sundaresan, V (2012) Molecular Characterization of the *glauce* Mutant: A Central Cell–Specific Function Is Required for Double Fertilization in *Arabidopsis*. Plant Physiol. **24**:3264-3277.

Lessire, R (a), Juguelin, H, Moreau, P, Cassagne, C (1985) Nature of the reaction product of [1-14C]stearoyl- CoA elongation by etiolated leek seedling microsomes. Arch. Biochem. Biophys. **239**:260-269.

Lessire, R (b), Bessoule, J-J, Cassagne, C (1985) Solubilization of C18-CoA and C20-CoA elongases from *Allium porrum* L. epidermal cell microsomes. FEBS Lett. **187**:314-320.

Li, F, Wu, X, Lam, P, Bird, D, Zheng, H, Samuels, L, Jetter, R, Kunst, L (2008) Identification of the wax ester synthase/acyl-coenzyme A:diacylglycerol acyltransferase WSD1 required for stem wax ester biosynthesis in Arabidopsis. Plant Physiol. **148**:97-107.

Ma, X, Koepke, J, Panjikar, S, Fritzsch, G, Stöckigt, J (2005) Crystal structure of vinorine synthase, the first representative of the BAHD superfamily. J Biol Chem **280**: 13576–13583.

Manjasetty, BA, Yu, X-H, Panjikar, S, Taguchi, G, Chance, MR, Liu, C-J (2012) Structural basis for modification of flavonol and naphthol glucoconjugates by *Nicotiana tabacum*. Planta **236**:781-793.

McNevin, JP, Woodward, W, Hannoufa, A, Feldmann, KA, Lemieux, B (1993) Isolation and characterization of *eceriferum* (*cer*) mutants induced by T-DNA insertions in *Arabidopsis thaliana*. Genome **36**: 610–618.

Medema, MH, Osbourn, A (2016) Computational genomic identification and functional reconstitution of plant natural product biosynthetic pathways. Nat. Prod. Rep. **33**: 951-962.

Millar, A, Clemens, S, Zachgo, S, Giblin, EM, Taylor, DC, Kunst, L (1999) *CUT1*, an Arabidopsis gene required for cuticular wax biosynthesis and pollen fertility, encodes a very-long-chain fatty acid condensing enzyme. Plant Cell **11**:825-838.

Millar, A, Kunst, L (1997) Very-long-chain fatty acid biosynthesis is controlled through the expression and specificity of the condensing enzyme. Plant J. **12**:121-131.

Molina, I, Li-Beisson, Y, Beisson, F, Ohlrogge, JB, Pollard, M (2009) Identification of an Arabidopsis feruloyl-coenzyme A transferase required for suberin synthesis. Plant Physiol. **151**:1317-1328.

Morineau, C, Gissot, L, Bellec, Y, Hematy, K, Tellier, F, Renne, C, Haslam, R, Beaudoin, F, Napier, J, Faure, J-D (2016) Dual fatty acid elongase complex interactions in Arabidopsis. PLoS ONE **11**:e0160631.

Moon, H, Chowrira, G, Rowland, O, Blacklock, BJ, Smith, MA, Kunst, L (2004) A root-specific condensing enzyme from *Lesquerella fendleri* that elongates very-long-chain saturated fatty acids. Plant Mol Biol **56**:917–927.

Mumberg, D, Müller, R, Funk, M (1995) Yeast vectors for the controlled expression of heterologous proteins in different genetic backgrounds. Gene. **156**: 119–122.

Nakagawa, S, Niimura, Y, Gojobori, T, Tanaka, H, Miura, K-I (2007) Diversity of preferred nucleotide sequences around the translation initiation codon in eukaryote genomes. Nuc. Acids Res. **36**:861-871.

Nakagawa, T, Kurose, T, Hino, T, Tanaka, K, Kawamukai, M, Niwa, Y, Toyooka, K, Matsuoka, K, Jinbo, T, Kimura, T (2007) Development of series of gateway binary vectors, pGWBs, for realizing efficient construction of fusion genes for plant transformation. J Biosci Bioeng **104**:34–41.

Negruk, V, Yang, P, Subramanian, M, McNevin, JP, Lemieux, B (1996) Molecular cloning and characterization of the CER2 gene of *Arabidopsis thaliana*. Plant J **9**: 137–145.

Nützmann, H-W, Osbourn, A (2014) Gene clustering in plant specialized metabolism. Curr Opin in Biotech **26**:91-99.

O'Neill, CM, Gill, S, Hobbs, D, Morgan, C, Bancroft, I (2003) Natural variation for seed oil composition

in *Arabidopsis thaliana*. Phytochemistry **64**:1077-1090.

Oh, CS, Toke, DA, Mandala, S, Martin, CE (1997) *ELO2* and *ELO3*, homologues of the *Saccharomyces cerevisiae ELO1* gene, function in fatty acid elongation and are required for sphingolipid formation. J. Biol. Chem. **272**:17376-17384.

Osbourn, A, Field, B (2009) Operons. Cell Mol Life Sci **66**:3755-3775.

Panikashvili, D, Shi, JX, Schreiber, L, Aharoni, A (2009) The Arabidopsis *DCR* encoding a soluble BAHD acyltransferase is required for cutin polyester formation and seed hydration properties. Plant Physiol **151**:1773–1789.

Pappas, A (2014) Sebaceous lipids, in: Pappas, A (ed.) Lipids and skin health. Springer, pp. 127-138.

Pascal, S, Bernard, A, Sorel, M, Pervent, M, Vile, D, Haslam, RP, Napier, JA, Lessire, R, Domergue, F, Joubès, J (2013) The Arabidopsis *cer26* mutant, like the *cer2* mutant, is specifically affected in the very long chain fatty acid elongation process. Plant J **73**: 733–746.

Paul, S, Gable, K, Beaudoin, F, Cahoon, E, Jaworski, J, Napier, JA, Dunn, TM (2006) Members of the Arabidopsis *FAE1*-like 3-ketoacyl-CoA synthase gene family substitute for the Elop proteins of *Saccharomyces cerevisiae*. J. Biol. Chem. **281**:9018- 9029.

Paul, S, Gable, K, Dunn, TM (2007) A six-membrane-spanning topology for yeast and Arabidopsis Tsc13p, the enoyl reductases of the microsomal fatty acid elongating system. J. Biol. Chem. **282**:19237-19246.

Pettersen, EF, Goddard, TD, Huang, CC, Couch, GS, Greenblatt, DM, Meng, EC, Ferrin, TE (2004) UCSF Chimera—a visualization system for exploratory research and analysis. J. Comput. Chem. **25**:1605-1612.

Pfaffl, MW (2001) A new mathematical model for relative quantification in real-time RT-PCR. Nucleic Acids Res. **29**:2002-2007.

Pichersky, E, and Gang, D (2000) Genetics and biochemistry of secondary metabolites in plants: an evolutionary perspective. Trends in Plant Sci. **5**:439-445.

Pichersky, E, and Lewinsohn, E (2011) Convergent evolution in plant specialized metabolism. Annu. Rev. Plant Biol. **62**:549-566.

Preuss, D, Lemieux, B, Yen, G, Davis, RW (1993) A conditional sterile mutation eliminates surface components from Arabidopsis pollen and disrupts cell signaling during fertilization. Genes Dev. **7**:974-985.

Pruitt, RE, Vielle-Calzada, J-P, Ploense, SE, Grossniklaus, U, Lolle, SJ (2000) *FIDDLEHEAD*, a gene required to suppress epidermal cell interactions in Arabidopsis, encodes a putative lipid biosynthetic enzyme. Proc. Natl. Acad. Sci. USA **97**:1311-1316.

Qiu, X, Janson, CA, Konstantinidis, AK, Nwagwu, S, Silverman, C, Smith, WW, Khandekar, S, Lonsdale, J, Abdel-Meguid, SS (1999) Crystal structure of β-ketoacyl-acyl carrier protein synthase III. A key condensing enzyme in bacterial fatty acid biosynthesis J. Biol. Chem. **274**:36465-36471.

Qiu, X, Janson, CA, Smith, WW, Head, M, Lonsdale, J, Konstantinidis, AK (2001) Refined structures of β-ketoacyl-acyl carrier protein synthase III. J. Mol. Biol. **307**:341-356.

Quist, TM, Sokolchik, I, Shi, H, Joly, RJ, Bressan, RA, Maggio, A, Narsimhan, M, Li, X (2009) HOS3, an ELO-like gene, inhibits effects of ABA and implicates a S-1-P/ceramide control system for abiotic stress responses in *Arabidopsis thaliana*. Mol. Plant **2**:138-151.

Rautengarten, C, Ebert, B, Ouellet, M, Nafisi, M, Baidoo, EEK, Benke, P, Stranne, M,

Mukhopadhyay, A, Keasling, JD, Sakuragi, Y, Scheller, HV (2012) Arabidopsis Deficient in Cutin Ferulate encodes a transferase required for feruloylation of v-hydroxy fatty acids in cutin polyester. Plant Physiol **158**: 654–665.

Rensing, SA, et al. (2008) The *Physcomitrella* genome reveals evolutionary insights into the conquest of land by plants. Science **319**:64-69.

Roudier, F, Gissot, L, Beaudoin, F, Haslam, R, Michaelson, L, Marion, J, Molino, D, Lima, A, Bach, L, Morin, H, Tellier, F, Palauqui, JC, Bellec, Y, Renne, C, Miquel, M, Dacosta, M, Vignard, J, Rochat, C, Markham, JE, Moreau, P, Napier, J, Faure, JD (2010) Very-long-chain fatty acids are involved in polar auxin transport and developmental patterning in Arabidopsis. Plant Cell **22**:364-375.

Rowland, O, Domergue, F (2012) Plant fatty acyl reductases: enzymes generating fatty alcohols for protective layers with potential for industrial applications. Plant Sci. **193-194**:28-38.

Rowland, O, Zheng, H, Hepworth, SR, Lam, P, Jetter, R, Kunst, L (2006) *CER4* encodes an alcohol-forming fatty acyl-coenzyme A reductase involved in cuticular wax production in Arabidopsis. Plant Physiol. **142:**866-877.

Samuels, L, Kunst, L, Jetter, R (2008) Sealing plant surfaces: cuticular wax formation by epidermal cells. Annu Rev Plant Biol **59**: 683–707.

Schneider, LM, Adamski, NM, Christensen, CE, Stuart, DB, Vautrin, S, Hansson, M, Uauy, C, von Wettstein-Knowles, P (2016) The Cer-cqu gene cluster determines three key players in a β-diketone synthase polyketide pathway synthesizing aliphatics in epicuticular waxes. J Exp. Bot. **67**:2715-2730.

Schwacke, R, Schneider, A, van der Graaff, E, Fischer, K, Catoni, E, Desimone, M, Frommer, WB, Flügge, UI, Kunze, R (2003) ARAMEMNON, a novel database for Arabidopsis integral membrane proteins, Plant Physiol. **131**:16-26.

Sherman, F (2002) Getting started with yeast. Methods Enzymol **350**: 3–41.

Smyth, DR, Bowman, JL, Meyerowitz, EM (1990) Early flower development in Arabidopsis. Plant Cell **2**: 755–767.

Somerville, CR, Ogren, WL (1982) Isolation of photorespiratory mutants of Arabidopsis. In M Eldman, RB Hallick, NH Chua, eds, Methods in Chloroplast Molecular Biology. Elsevier Science, New York, pp 129-139.

St-Pierre, B, Laflamme, P, Alarco, A-M, De Luca, V (1998) The terminal O-acetyltransferase involved in vindoline biosynthesis defines a new class of proteins responsible for coenzyme A-dependent acyl transfer, Plant J. **14**:703-713.

St. Pierre, B, De Luca, V (2000) Evolution of acyltransferase genes: origin and diversification of the BAHD superfamily of acyltransferases involved in secondary metabolism, in: J.T. Romeo, R. Ibrahim, L. Varin, V. De Luca (Eds.), Recent Advances in Phytochemistry: Evolution of Metabolic Pathways, Elsevier Science Ltd, 34 pp. 285-315.

Swamy, M, Siegers, GM, Minguet, S, Wollscheid, B, Schamel, WWA (2006) Blue native polyacrylamide gel electrophoresis (BN-PAGE) for the identification and analysis of multiprotein complexes. **2006**:p14

Suh, M-C, Samuels, AL, Jetter, R, Kunst, L, Pollard, M, Ohlrogge, J, Beisson, F (2005) Cuticular lipid composition, surface structure, and gene expression in Arabidopsis stem epidermis, Plant Physiol. **139**:1649-1665.

Suzuki, H, Nakayama, T, Nishino, T (2003) Proposed mechanism and functional amino acid residues of malonyl-CoA:anthocyanin 5-Oglucoside-6'"-O-malonyltransferase from flowers of *Salvia splendens*, a

member of the versatile plant acyltransferase family. Biochemistry **42**:1764–1771.

Todd, J, Post-Beittenmiller, D, Jaworski, JG (1999) KCS1 encodes a fatty acid elongase 3-ketoacyl-CoA synthase affecting wax biosynthesis in *Arabidopsis thaliana*. Plant J. **17**:119-130.

Toke, DA, Martin, CE (1996) Isolation and characterization of a gene affecting fatty acid elongation in *Saccharomyces cerevisiae*. J. Biol. Chem. **271**:18413-18422.

Trenkamp, S, Martin, W, Tietjen, K (2004) Specific and differential inhibition of very-long-chain fatty acid elongases from Arabidopsis thaliana by different herbicides. Proc. Natl. Acad. Sci. USA **101**:11903-11908.

Tresch, S, Heilmann, M, Christiansen, N, Looser, R, Grossmann, K (2012) Inhibition of saturated very-long-chain fatty acid biosynthesis by mefluidide and perfluidone, selective inhibitors of 3-ketoacyl-CoA synthases. Phytochemistry **76**:162-171.

Tuominen, LK, Johnson, EV, Tsai, C-J (2011) Differential phylogenetic expansions in BAHD acyltransferases across five angiosperm taxa and evidence of divergent expression among Populus paralogs. BMC Genomics **12**:236.

Unno, H, Ichimaida, F, Suzuki, H, Takahashi, S, Tanaka, Y, Saito, A, Nishino, T, Kusunoki, M, Nakayama, T (2007) Structural and mutational studies of anthocyanin malonyltransferases establish the features of BAHD enzyme catalysis. J Biol Chem **282**: 15812–15822.

Velasco, R, Korfhage, C, Salamini, A, Tacke, E, Schmitz, J, Motto, M, Salamini, F, Döring, H-P (2002) Expression of the glossy2 gene of maize during plant development. Maydica **47**: 71–81.

von Wettstein-Knowles, P (1982) Elongases and epicuticular wax biosynthesis. Physiol. Veg. **20**:797-809.

Walker, AM, Hayes, RP, Youn, B, Vermerris, W, Sattler, SE, Kang, C (2013) Elucidation of the structure and reaction mechanism of sorghum hydroxycinnamoyltransferase and its structural relationship to other coenzyme A-dependent transferases and synthases. Plant Physiol. **162**:640-651.

Walker, K, Fujisaki, S, Long, R, Croteau, R (2002) Molecular cloning and heterologous expression of the C-13 phenylpropanoid side chain-CoA acyltransferase that functions in Taxol biosynthesis. Proc Natl Acad Sci. **99**:12715-12720.

Wattelet-Boyer, V, Brocard, L, Jonsson, K, Esnay, N, Joubès, J, Domergue, F, Mongrand, S, Raikhel, N, Bhalerao, RP, Moreau, P, Boutté, Y (2016) Enrichment of hydroxylated C24- and C26-acyl-chain sphingolipids mediates PIN2 apical sorting at *trans*-Golgi network subdomains. Nat Comm **7**:12788.

Wang, G-F, He, Y, Strauch, R, Olukolu, BA, Nielsen, D, Li, X, Balint-Kurti, PJ (2015) Maize homologs of hydroxycinnamoyltransferase, a key enzyme in lignin biosynthesis, bind the nucleotide binding leucine-rich repeat Rp1 proteins to modulate the defense response. Plant Physiol. **169**:2230-2243.

Wang, G-F, Balint-Kurti, P (2016) Maize homologs of CCoAOMT and HCT, two key enzymes in lignin biosynthesis, form complexes with the NLR Rp1 protein to modulate the defense response. Plant Physiol. **171**:2166-2177.

Wilkins, TA, Smart, LB (1995) Isolation of RNA from plant tissue. In P Krieg, ed, A Laboratory Guide to RNA: Isolation, Analysis, and Synthesis. Wiley-Liss, New York, pp 21-41.

Winter, D, Vinegar, B, Nahal, H, Ammar, R, Wilson, GV, Provart, NJ (2007) An "Electronic Fluorescent Pictograph" browser for exploring and analyzing large-scale biological data sets. PLoS ONE **2**: e718.

Wisman, E, Hartmann, U, Sagasser, M, Baumann, E, Palme, K, Hahlbrock, K, Saedler, H, Weisshaar, B (1998) Knock-out mutants from an *En-1* mutagenized *Arabidopsis thaliana* population generate phenylpropanoid biosynthesis phenotypes. Proc. Natl. Acad. Sci. **95**:12432-12437.

Witkowski, A, Joshi, AK, Lindqvist, Y, Smith, S (1999) Conversion of a β-ketoacyl synthase to a malonyl decarboxylase by replacement of the active-site cysteine with glutamine. Biochemistry **38**:11643-11650.

Xia, Y, Nikolau, BJ, Schnable, PS (1996) Cloning and characterization of CER2, an Arabidopsis gene that affects cuticular wax accumulation. Plant Cell **8**: 1291–1304.

Xia, Y, Nikolau, BJ, Schnable, PS (1997) Developmental and hormonal regulation of the Arabidopsis CER2 gene that codes for a nuclear localized protein required for the normal accumulation of cuticular waxes. Plant Physiol **115**: 925–937

Xiao, S, Chye, M-L (2011) New roles for acyl-CoA-binding proteins (ACBPs) in plant development, stress responses and lipid metabolism. Prog Lipid Res. **50**:141-151.

Xue, Y, Xiao, S, Kim, J, Lung, S-C, Chen, L, Tanner, JA, Suh, MC, Chye, M-L (2014) Arabidopsis membrane-associated acyl-CoA binding protein ACBP1 is involved in stem cuticle formation. J. Exp. Bot. **65**:5473-5483.

Yokoi, S, Tsuchiya, T, Toriyama, K, Hinata, K (1997) Tapetum-specific expression of the Osg6B promoter-b-glucuronidase gene in transgenic rice. Plant Cell Rep **16**: 363–367.

Yu, XH, Gou, JY, Liu, CJ (2009) BAHD superfamily of acyl-CoA dependent acyltransferases in *Populus* and *Arabidopsis*: bioinformatics and gene expression. Plant Mol. Biol. **70**:421-442.

Zank, TK, Zähringer, U, Beckmann, C, Pohnert, G, Boland, W, Holtorf, H, Reski, R, Lerchl, J, Heinz, E (2002) Cloning and functional characterization of an enzyme involved in the elongation of Δ6-polyunsaturated fatty acids from the moss *Physcomitrella patens*. Plant J. **31**:255-268.

Zheng, H, Rowland, O, Kunst, L (2005) Disruptions of the Arabidopsis enoyl-CoA reductase gene reveal an essential role for very-long-chain fatty acid synthesis in cell expansion during plant morphogenesis. Plant Cell **17**:1467-1481.